



UNIVERSITAT  
POLITÈCNICA  
DE VALÈNCIA

CAMPUS D'ALCOI

Comparative study of the prospects of  
hydrogen as an energy source.

TRABAJO FINAL DE GRADO

Korri, Mohammed Amin

Grado en ingeniería mecánica

Alcoy, Julio 2018

Director del proyecto: D. Ruiz Rosales, Santiago





UNIVERSIDAD  
POLITECNICA  
DE VALENCIA

*“Comparative study of the prospects of*





## Abstract

Hydrogen as a fuel has numerous promising features that give it a future as an alternative to hydrocarbons, which see their consumption ever more restrained through regulation of emissions.

On the other hand, ever since the incidents of Fukushima there has been growing concerns for the use of nuclear power, and in Europe for instance the number of nuclear power plants has been decreasing in the past decade. Yet the power demand is steadily increasing in such that the adoption of renewable energies cannot sufficiently supply the demand.

Moreover gas and vapour turbines offer a highly efficient energy conversion of gaseous fuel to electric power or mechanical drive, and the use of hydrogen doesn't suppose major alterations to the design of such appliances.

Therefore this paper explores and analyses the major advantages and drawbacks from adopting such a fuel for energy generation. We will review some of the production and transportation methods that we view as economically and technically viable, as well as discuss some future trends and prospects for a better adoption of hydrogen as a fuel.

Furthermore, we will argue on the thermodynamics of hydrogen adoption on gas turbine cycles; through the exposition of working cycles already introduced in the industry, and later on conduct our own analysis in order to draw conclusions.

Finally, through the report of certain economical models, we will describe the cost of adapting hydrogen as a fuel source for energy production, accounting for the initial inversion cost and what infrastructure; both legislative and urban is in place for such adjustment.







# Table of contents

<b>Abstract.....</b>	<b>3</b>
<b>Table of contents .....</b>	<b>5</b>
<b>1. Background .....</b>	<b>8</b>
<b>2. Methodology.....</b>	<b>9</b>
<b>3. Properties of hydrogen.....</b>	<b>10</b>
3.1. Physical properties.....	12
3.2. Density .....	13
3.3. Specific volume .....	14
3.4. Expansion ratio.....	14
3.5. Chemical properties.....	14
3.6. Hydrogen embrittlement .....	14
3.7. Toxicity.....	15
3.8. Flammability.....	15
3.9. Ignition energy.....	15
3.10. Flame velocity .....	15
3.11. Flame temperature.....	15
3.12. Comparison with other fuels.....	16
<b>4. Hydrogen production.....</b>	<b>17</b>
4.1. Steam methane reforming (SMR) .....	17
4.2. Hydrogen production using nuclear energy .....	19
4.3. Hydrogen production using renewable energies.....	25
4.3.1. WIND POWER .....	25
4.3.2. SOLAR ENERGY .....	26
4.4. Conclusion .....	27
<b>5. Hydrogen distribution and storage.....</b>	<b>27</b>
5.1. Hydrogen transportation .....	27
5.2. Hydrogen storage.....	39
5.2.1. COMPRESSED HYDROGEN .....	41
5.2.2. LIQUID HYDROGEN .....	44
5.2.3. CONCLUSION .....	47
<b>6. Current heat cycle .....</b>	<b>48</b>
6.1. Jericha cycle .....	48
6.2. Zero emission Graz-cycle (rewrite) .....	49
6.3. Regenerative reheat Brayton cycle.....	52
6.4. Conclusion .....	53
<b>7. Thermodynamic analysis.....</b>	<b>54</b>
7.1. Mathematical model.....	58
7.1.1. ADIABATIC FLAME TEMPERATURE.....	58
7.1.2. COMPRESSOR.....	59
7.1.3. COMBUSTION CHAMBER.....	61



7.1.4. TURBINE.....	64
<b>7.2. Results and discussion .....</b>	<b>65</b>
<b>8. Hydrogen safety, standard and regulation .....</b>	<b>70</b>
<b>8.1. Standards and regulation.....</b>	<b>70</b>
<b>8.2. Hydrogen safety.....</b>	<b>71</b>
8.2.1. General consideration and risk control .....	73
8.2.2. Design risks .....	74
8.2.3. Elimination of ignition source.....	76
8.2.4. Detection consideration .....	77
<b>9. Economical analysis.....</b>	<b>78</b>
<b>10. Conclusion .....</b>	<b>86</b>
<b>11. References .....</b>	<b>88</b>
<b>Appendixes .....</b>	<b>95</b>
<b>Appendix A: Curvefit coefficient for thermodynamic properties.....</b>	<b>95</b>
A.1- Curvefit coefficient for fuels specific heat and enthalpy for reference state of zero enthalpy of the elements .....	95
A.2- Curvefit coefficient for thermodynamic properties of (C-H-O-N) systems.....	96
<b>Appendix B: Thermodynamic properties .....</b>	<b>97</b>
B.1- Methane (CH <sub>4</sub> ).....	97
B.2- Carbon monoxide (CO).....	99
B.3- Carbon dioxide (CO <sub>2</sub> ).....	101
B.4- Hydrogen (H <sub>2</sub> ) .....	103
B.5- Water vapour (H <sub>2</sub> O).....	105
B.6- Nitrogen (N <sub>2</sub> ) .....	107
B.7- Nitric oxide (NO).....	109
B.8- Oxygen diatomic (O <sub>2</sub> ) .....	111



# 1. Background

According to the report of the International Energy Outlook (IEO) in 2010 the world net electricity generation projection will increase from 18.8 trillion kilowatt-hours in 2007 to 35.2 trillion kilowatt-hours by 2035.

The increase in world energy prices from 2003 to 2008, combined with international concerns about global warming through greenhouse gas emissions, has led to a renewed interest in alternatives to fossil fuels.

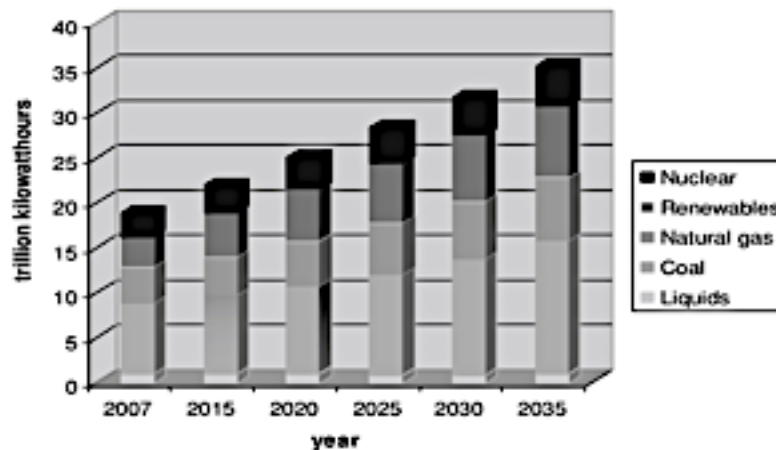


**Fig.1** Forecast of world net electricity generation by fuel, 2007 – 2030, DoE

As we can see in **Figure 1** according to the US Department of Energy (DoE) from 2007 to 2035, world renewable energy use for electricity generation will grow by an average of 3.0% per year, and the renewable share of world electricity generation will increase from 18% in 2007 to 23% by 2035. Whereas coal-fired generation is at a forecast of 2.3% annual increase, though this could be altered substantially, however, by any future legislation that would reduce or limit the growth of greenhouse gas emissions.

Generation from natural gas and nuclear power (which produce low levels of greenhouse gas emissions) according to projections will increase by 2.1 and 2.0% per year, respectively.

So as we can see most of the world's electricity is produced at thermal power plants (TPP), which use traditional fuels, coal, gas and fuel oil, and up to 20% of the world's electricity is produced by hydroelectric power plants (HPP).

Therefore we find that the prevailing infrastructure for electric power generation is at a TPP, which in turn uses gas and steam turbines that in order to comply with the greenhouse gas emissions legislation sees the need for a carbon dioxide extraction and disposal. Obviously the use of hydrogen gas as fuel would negate such needs. Moreover previous studies have presented calculations of thermal efficiencies using a variety of working fluids and gas mixtures – notably hydrogen and nitrogen or syngas– that concluded the achievement of 68% cycle efficiency (Sugisita et al. with the Jericha cycle, Bannister et al. with a novel Rankine cycle to name a few [1]).

## 2. Methodology

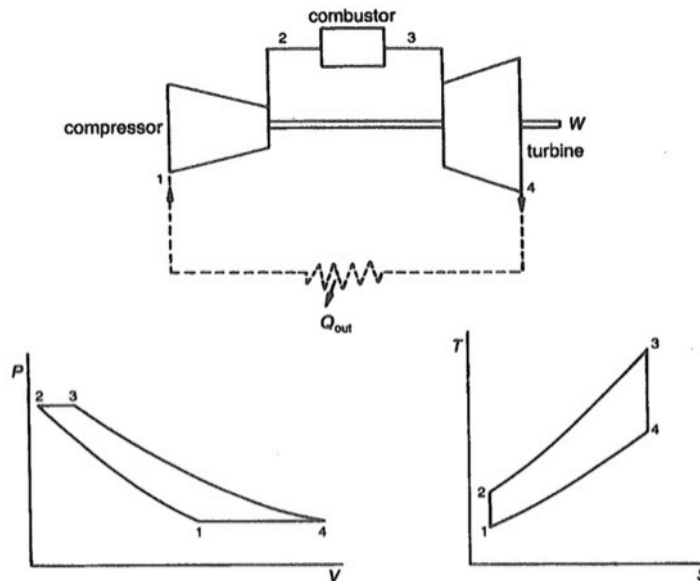


**Fig.2** The air-standard Brayton cycle.

For the completion of this study, two stages have been considered. The first being a literature review of all the research implemented by several entities on the economics and engineering behind a hydrogen based economy, as well as various publications and handbooks describing the mechanisms and concepts needed for a proper understanding of the subject of the matter – sources are cited on the reference chapter. Said review will focus on pertinent information and subsequently discuss in each chapter the status of the data as well as views on the provided solutions.

The second stage is directed towards the integration of an elemental mathematical model, which serves as baseline for relevant calculations on the subject. Furthermore the mathematical model presented in this paper represents a simple idealized Brayton cycle as seen in **Figure 2** under the assumption of elemental bound conditions.

This helps us gain a certain insight to what we've reported on published papers, and later on a baseline for comparison between conventional fuels; that we have chosen to be natural gas, given it's predominant use this past decade for energy generation as well as its low cost.

The third part of this analysis will be the economical breakdown, by transcribing what is currently understood for the adoption of hydrogen as a fuel, and through the assessment of different economical models we will explain the cost of such adoption and discuss the advantages and setbacks proven to be relevant to our study.

Finally, we will conclude by summarizing all what have been said, and by promoting a certain insight to the current technologic and economic challenges that still need to be conquered and by suggesting certain solutions we've seen prevailing in the industry.



### 3. Properties of hydrogen

Hydrogen is a chemical element with the symbol H and atomic number 1. In normal conditions it is colourless and odourless formed by diatomic molecules, H<sub>2</sub>. It is the lightest element on the periodic table and the most abundant chemical substance in the universe.

Hydrogen gas was first artificially produced in the early sixteenth century, via the mixing of metals with acids. English chemist Henry Cavendish was the first to identify the properties of hydrogen after he evolved hydrogen gas by reacting zinc metal with hydrochloric acid, in 1766 [1]. Seven years later, Antoine Lavoisier gave it the name “hydrogen,” which means “water-former” from its property to produce water when combusted [2].

In this subsequent section we will discuss the range of properties inherent to hydrogen. Table. 1 lists the most adequate attributes for our study.

*\*The consecutive paragraphs dive more in depth in their description.*

**Table 1** Physical, Thermal and Chemical properties of hydrogen [3]

Molecular Weight	2.016
Specific Gravity, air = 1	0.070
Specific Volume (m <sup>3</sup> /kg)	12.100
Density of liquid at atmospheric pressure (kg/m <sup>3</sup> )	71.000
Absolute Viscosity (10 <sup>-2</sup> kg m <sup>-1</sup> s <sup>-1</sup> )	0.009
Sound velocity in gas (m/s)	1.315 10 <sup>3</sup>
Specific Heat at constant pressure – cp – (J/kg K)	14.310 10 <sup>3</sup>
Specific Heat Ratio – cp/cv	1.405
Gas constant – R – (J/kg °C)	4.126 10 <sup>3</sup>
Thermal Conductivity (W/m °C)	0.182
Boiling Point - saturation pressure 1 atm - (K)	20.400
Latent Heat of Evaporation at boiling point (J/kg)	4.470 10 <sup>5</sup>
Freezing or Melting Point at 1 atm (K)	14.000
Latent Heat of Fusion (J/kg)	58 10 <sup>3</sup>
Critical Temperature (K)	33
Critical Pressure (bar)	13
Critical Volume (m <sup>3</sup> /kg)	0.033
Heat of combustion (kJ/kg K)	14.4 10 <sup>5</sup>

**Table 1** describes the physical, thermal and chemical properties of hydrogen by bringing light to values of certain concepts essential to the understanding of the behaviour and interactions of the gas. As for **Table 2**, it exhibits the principal values describing the combustion properties of hydrogen.

**Table 2** Combustion properties of hydrogen [3]

Lower heating value (LHV) (kJ/g)	119,93
High heating value (HHV) (kJ/g)	141,86
Flammability limit (% by volume)	4,0 – 75 <sup>a</sup> 4,1 – 94 <sup>b c</sup>
Explosion limit (% by volume)	18,3 – 59 <sup>a</sup> 15 – 90 <sup>b c</sup>
Stoichiometric composition in air (% by volume)	29,53
Minimum energy for ignition in air (mJ)	0,017
Auto-ignition temperature (K)	858 <sup>d</sup>
Auto-ignition temperature with hot air jet (K)	943
Flame temperature in air (K)	2 318
Thermal energy of the flame to the environment (%)	17 – 25
Flame speed in air at normal conditions (m/s)	2,65 – 3,25
Deflagration speed for stoichiometric mixture (m/s)	975
Detonation speed at normal condition (m/s)	1 480 – 2 150
Oxygen limitation index (% by volume)	5,0
Spilled liquid combustion speed (mm/s)	0,5 – 1,1
Explosive energy	
	g TNT/g H <sub>2</sub> ~ 24
	g TNT/kJ H <sub>2</sub> ~ 0,17 <sup>e</sup>
	kg TNT/m <sup>3</sup> at NTP 2,02
	GH <sub>2</sub> g TNT/cm <sup>3</sup> at NEP LH <sub>2</sub> 1,71

<sup>a</sup> Unless otherwise specified, the data source is the reference [3].

<sup>b</sup> These properties are a function of many variables that have to be evaluated to determine their values according to the specific application.

<sup>c</sup> The data source is the reference [4]

<sup>d</sup> Different values have been collected for the range of hydrogen ignition temperatures in air ranging from 773 K to 858 K. This variation may be due to the influence of the different materials used as hydrogen containers in the test apparatus.

<sup>e</sup> Based on HHV

### 3.1. Physical properties

Hydrogen is colourless, odourless, and tasteless and is about 14 times lighter than air, and diffuses faster than any other gas. It has the second lowest boiling point and melting points of all substances; second only to helium, and condenses into a liquid below its boiling point of 20 K and a solid below its melting point of 14 K at atmospheric pressure.

As we can see in our phase diagram in **Figure 3**, hydrogen can be also found in a metallic form under conditions of high pressure and low temperature, in this phase hydrogen behaves as electric conductor. But for the purpose of this study we are interested in the liquid and gaseous forms of hydrogen.

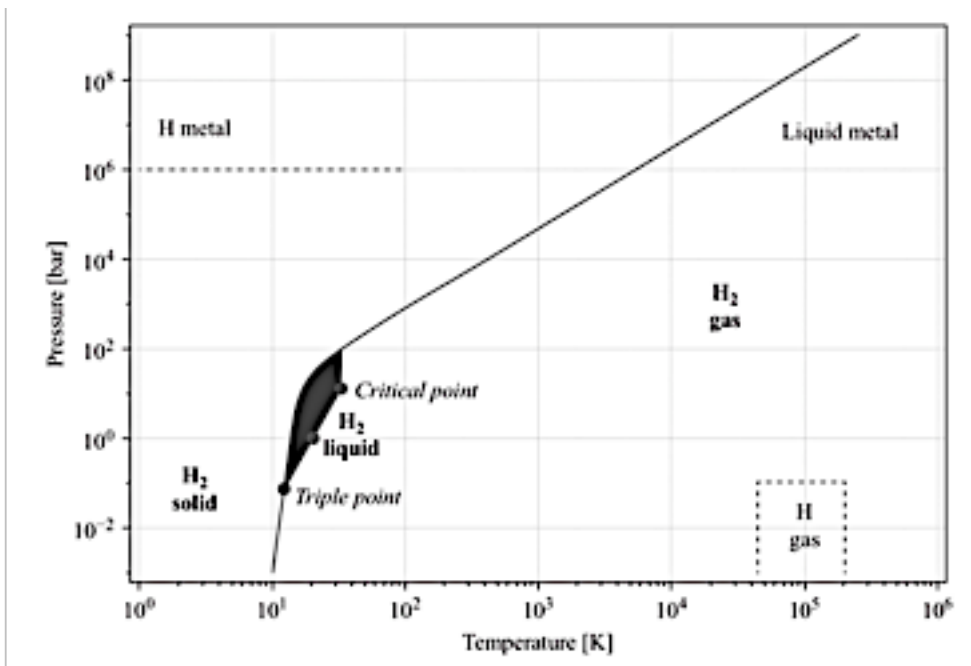


Fig.3 Simple phase diagram for hydrogen

The boiling point of a fuel is a critical parameter since it defines the temperature to which it must be cooled in order to store and use it as a liquid. Liquid fuels take up less storage space than gaseous fuels, and are generally easier to transport and handle. For this reason, fuels that are liquid at atmospheric conditions (such as gasoline, diesel, methanol and ethanol) are particularly convenient. Whereas, fuels that are gases at atmospheric conditions (such as hydrogen and natural gas) are less convenient as they must be stored as a pressurised gas or as a cryogenic liquid.

Hydrogen has also a very low solubility in solvents at ambient conditions. However it is much more pronounced in metals. E.g. palladium dissolves about 1000 times its volume of the gas. The adsorption of hydrogen in steel may cause “hydrogen embrittlement,” which sometimes leads to the failure of equipment.



### 3.2. Density

Density values only have meaning at a specified temperature and pressure since both of these parameters affect the compactness of the molecular arrangement, especially in a gas. The density of a gas is called its vapour density, and the density of a liquid is called its liquid density.

At normal conditions, gaseous hydrogen is about 8 times less dense than methane, while in liquid state it is 6 times less dense than liquid methane and 55 times less dense than gasoline. Moreover, the volume ratio between hydrogen at 1 bar and compressed hydrogen at 700bar is 440. Finally, it is interesting to note that more hydrogen is contained in a given volume of water or gasoline than in pure liquid hydrogen ( $111 \text{ kg/m}^3$ ,  $84 \text{ kg/m}^3$  and  $71 \text{ kg/m}^3$ , respectively).

The density of hydrogen at elevated pressure can be estimated using the principles of thermodynamics. While the behaviour of most gases can be approximated with a high accuracy by the simple equation of state of an ideal gas ( $PV = nRT$ ), that relates the pressure, the volume and the temperature of a given substance, the behaviour of hydrogen deviates significantly from the predictions of the ideal gas model. The resulting deviation from the ideal gas law is always in the form of expansion – the gas occupies more space than the ideal gas law predicts. One of the simplest ways of correcting for this additional compression is through the addition of a compressibility factor; designated by the symbol  $Z$ . Compressibility factors are derived from data obtained through experimentation and depend on temperature, pressure and the nature of the gas. The  $Z$  factor is then used as a multiplier to adjust the ideal gas law to fit actual gas behaviour as follows:  $PV = nZRT$  [5]

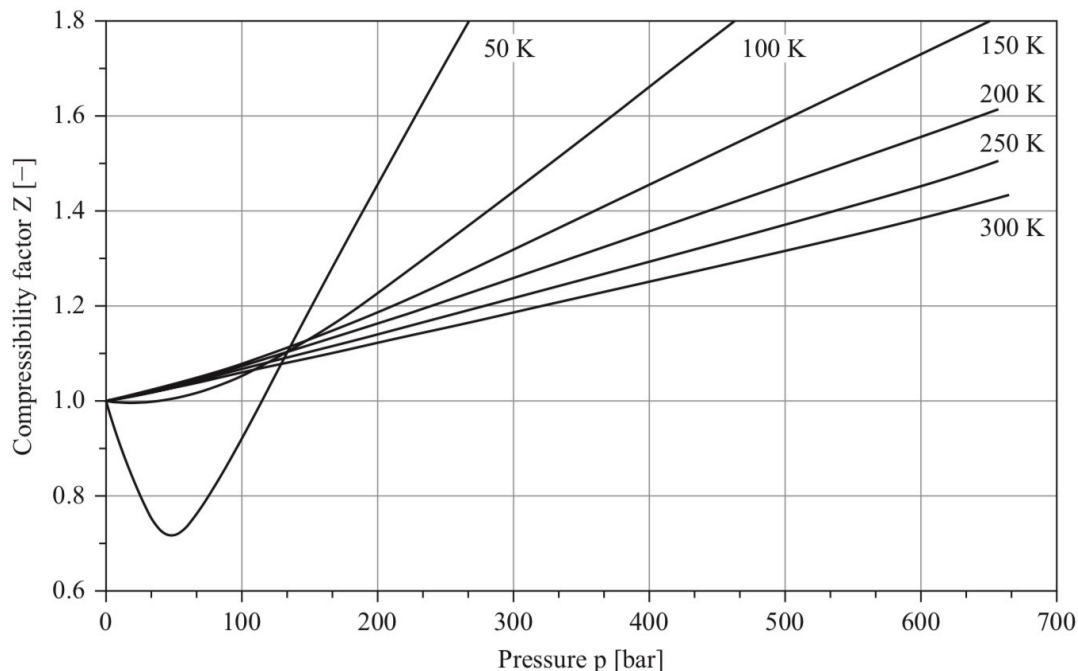


**Fig. 4** Compressibility factor of hydrogen [5]



By reducing the pressure  $P$  to the critical pressure  $P_{cr}$  and the temperature  $T$  to the critical temperature  $T_{cr}$ , a generalised compressibility factor for all gases, can be drawn as a function of  $P_r = \frac{P}{P_{CR}}$  and  $T_r = \frac{T}{T_{CR}}$ . The value of compressibility factor  $Z$  for hydrogen at high pressures and low temperatures in Figure 4 shows that, at ambient temperature, a value of 1.2 is reached at 300bar, and at low temperatures even earlier. This means that a calculation of the hydrogen mass in a container from a measurement of temperature and pressure using the ideal gas equation will result in a mass 20% greater than in reality.

### **3.3. Specific volume**

The Specific volume is the inverse of density and expresses the amount of volume per unit mass. Thus, the specific volume of hydrogen gas is 11.9 m<sup>3</sup>/kg at 293K and 1atm, and the specific volume of liquid hydrogen is 0.014 m<sup>3</sup>/kg at 20K and 1atm.

### **3.4. Expansion ratio**

The difference in volume between liquid and gaseous hydrogen can easily be appreciated by considering its expansion ratio. Expansion ratio is the ratio of the volume at which a gas or liquid is stored compared to the volume of the gas or liquid at atmospheric pressure and temperature. Hydrogen's expansion ratio is 1:851.

### **3.5. Chemical properties**

At normal temperatures, hydrogen is relatively nonreactive unless it has been activated in some manner. Rather, the hydrogen atom is chemically very reactive, and that is the reason it is not found chemically free in nature. In fact, very high temperatures are needed to dissociate molecular hydrogen into atomic hydrogen. For example, even at 5000 K, about 5% of the hydrogen remains undissociated. Therefore, in order to obtain hydrogen from natural compounds, energy is needed.

### **3.6. Hydrogen embrittlement**

Hydrogen embrittlement can lead to leakage or catastrophic failures in metal and non-metallic components. The mechanisms that cause hydrogen embrittlement effects are not well defined. Factors known to influence the rate and severity of hydrogen embrittlement include hydrogen concentration, hydrogen pressure, temperature, hydrogen purity, type of impurity, stress level, stress rate, metal composition, metal tensile strength, grain size, microstructure and heat treatment history. Moisture content in the hydrogen gas may lead to metal embrittlement through the acceleration of the formation of fatigue cracks.



### **3.7. Toxicity**

Hydrogen is non-toxic but can act as a simple asphyxiant by displacing the oxygen in the air in the case of a leak.

### **3.8. Flammability**

Hydrogen has a wide flammability range in comparison with nearly all other fuels (4-74% against 1.4-7.6% volume in air for gasoline), it is also a function of concentration level. As a result, this first leads to obvious concerns over the safe handling of hydrogen, but it also implies that hydrogen can be combusted over a wide range of fuel-air mixtures, which depend on the ignition energy, temperature, pressure, presence of diluents, and size and configuration of the equipment, facility, or apparatus. Such a mixture may be diluted with either of its constituents until its concentration shifts below the lower flammability limit or above the upper flammability limit. A significant advantage of this is that hydrogen can run on a lean mixture. A lean mixture is one in which the amount of fuel is less than the theoretical, stoichiometric or chemically ideal amount needed for combustion with a given amount of air.

Additionally, the final combustion temperature is generally lower with a low-visibility flame, reducing the amount of pollutants, such as nitrogen oxides, emitted in the exhaust.

### **3.9. Ignition energy**

Hydrogen has very low ignition energy when its concentration is in the flammability range. The amount of energy needed to ignite hydrogen is about one order of magnitude less than that required for gasoline or methane (0.02 mJ as compared to 0.24 mJ for gasoline and 0.28 mJ for methane). Unfortunately, the low ignition energy means that hot gases can serve as sources of ignition, creating problems of premature ignition and flashback. The wide flammability range of hydrogen means that almost any mixture can be ignited by a hot spot.

### **3.10. Flame velocity**

Hydrogen has a high flame velocity at stoichiometric ratios. Under these conditions, the hydrogen flame speed is nearly an order of magnitude higher (faster) than that of other gases (1.85 m/s against 0.42 m/s for gasoline vapour and 0.38 m/s for methane).

### **3.11. Flame temperature**

The hydrogen/air flame is hotter than methane/air flame and cooler than gasoline at stoichiometric conditions (2480K compared to 2190K for methane and 2580K for gasoline).

### 3.12. Comparison with other fuels

Now that we've defined all the concepts linked to the behaviour of hydrogen as a combustible, we shall compare it to other conventional fuels.

**Table 3.1** Property of conventional and alternative fuels [6]

Property	Gasoline	No. 2 Diesel	Methanol	Ethanol	Propane	CNG	Hydrogen
Chemical formula	C <sub>4</sub> -C <sub>12</sub>	C <sub>9</sub> -C <sub>25</sub>	CH <sub>3</sub> OH	C <sub>2</sub> H <sub>5</sub> OH	C <sub>3</sub> H <sub>8</sub>	CH <sub>4</sub>	H <sub>2</sub>
Physical state	Liquid	Liquid	Liquid	Liquid	Compressed gas	Compressed gas	Compressed gas or liquid
Molecular weight	100-105	200-300	32	46	44	16	2
Composition (wt%)							
Carbon	85-88	84-87	39.5	52.2	82	75	0
Hydrogen	12-15	13-16	12.6	13.1	18	25	100
Oxygen	0	0	49.9	34.7	NA	NA	0
Specific gravity (15.5°C/15.5°C)	0.72-0.78	0.81-0.89	0.796	0.796	0.504	0.424	0.07
Boiling temperature (°C)	27-225	190-345	68	78	-42	-161	-252
Freezing temperature (°C)	-40	-34	-97.5	-114	-187.5	-183	-260
Reid vapor pressure (psi)	8-15	0.2	4.6	2.3	208	2400	NA

**Table 3.2** LHV energy densities of fuels [7]

Fuel	Energy Density (MJ/m <sup>3</sup> at 1 atm., 15°C)	Energy Density (MJ/m <sup>3</sup> at 200 atm., 15°C)	Energy Density (MJ/m <sup>3</sup> at 690 atm., 15°C)	Energy Density (MJ/m <sup>3</sup> of Liquid)	Gravimetric Energy Density (MJ/kg)
Hydrogen	10.0	1,825	4,500	8,491	140.4
Methane	32.6	6,860		20,920	43.6
Propane	86.7			23,488	28.3
Gasoline				31,150	48.6
Diesel				31,435	33.8
Methanol				15,800	20.1

**Table 3.3** Comparison of hydrogen with other fuels [7]

Fuel	LHV (MJ/kg)	HHV (MJ/kg)	Stoichiometric		Flame Temperature (°C)	Min. Ignition Energy (MJ)	AutoIgnition Temperature (°C)
			Air/Fuel Ratio (kg)	Combustible Range (%)			
Methane	50.0	55.5	17.2	5-15	1914	0.30	540-630
Propane	45.6	50.3	15.6	2.1-9.5	1925	0.30	450
Octane	47.9	51.1	15.1	0.95-6.0	1980	0.26	415
Methanol	18.0	22.7	6.5	6.7-36.0	1870	0.14	460
Hydrogen	119.9	141.6	34.3	4.0-75.0	2207	0.017	585
Gasoline	44.5	47.3	14.6	1.3-7.1	2307	0.29	260-460
Diesel	42.5	44.8	14.5	0.6-5.5	2327		180-320

As we may notice from **Table 3.1 – 3.3**, hydrogen is the most energy dense in terms of heating value, though its lower density compared to other fuels limits to great extent its actual energy density at normal conditions.

## 4. Hydrogen production

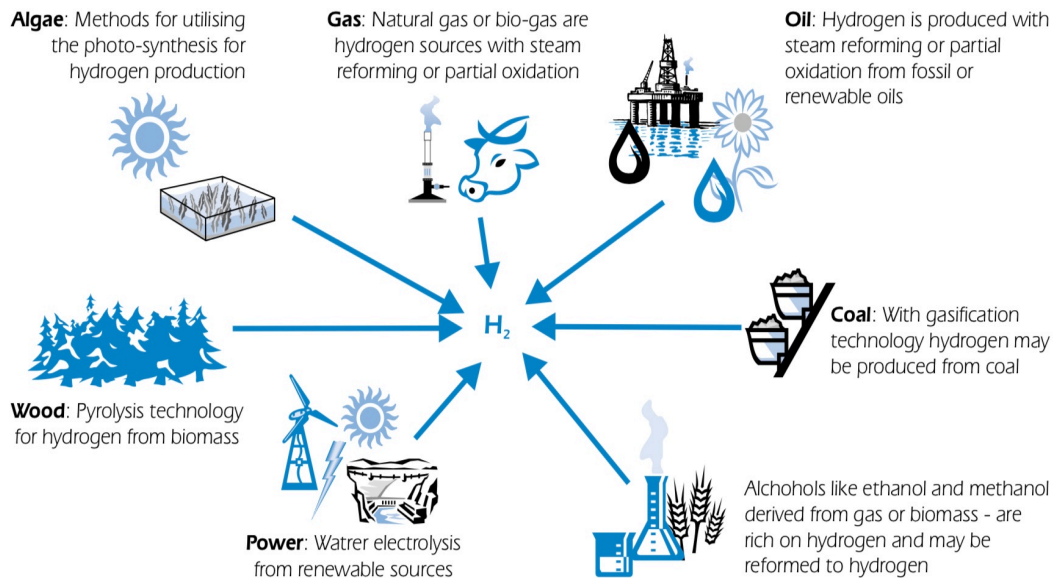


**Fig.5** Diagram of diverse hydrogen sources from the *International Energy Agency* “Hydrogen–production and storage”

As evident through Figure 5 hydrogen is produced from distinct industries; mostly as a byproduct of petroleum, metallurgical, pharmaceutical, electronic, and food industries. Currently, the largest consumers of industrial hydrogen are ammonia synthesis facilities (62.4%), oil refineries (24.3%), and methanol production plants (8.7%).

As seen in the research of the US DoE the overall challenge to hydrogen production is cost. For cost-competitiveness hydrogen must be comparable to conventional fuels and technologies. In order to reach such goals of competitiveness, the dispense price of hydrogen needs to be less than \$4/gasoline gallon equivalent, or the amount of fuel that has the same amount of energy as a gallon of gasoline – one kilogram of hydrogen is roughly equivalent to 3.8 litres of gasoline –.

Therefore for the purpose of this study it would be interesting to investigate processes that are cost effective as well as environmental friendly.

### 4.1. Steam methane reforming (SMR)

Given that Natural gas contains methane ( $CH_4$ ) as well as other gases including heavier hydrocarbons, acid gases –Hydrogen sulphide ( $H_2S$ ), carbon dioxide ( $CO_2$ )...–, water vapour and Nitrogen ( $N_2$ ). One of the first stages of the steam methane reforming (SMR) is the desulfurization of natural gas (NG).

The desulfurization process is accomplished through the conversion of Sulphur–organic compounds; e.g. thiols ( $R-SH$ ) that are first converted into Hydrogen sulphide ( $H_2S$ ) by catalytic hydrogenation reaction at 643K.

This is followed by H<sub>2</sub>S scrubbing by a ZnO bed (at 613K – 663K) according to the following reaction:



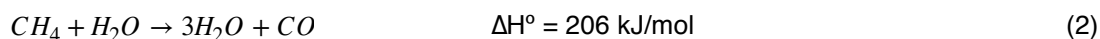
*\*In some cases, traces of halides (e.g., chlorides) are also present in the natural gas feedstock, and an alumina guard bed removes these.*

After this stage, the natural gas is fed to a second catalytic reforming unit where it reacts with steam to produce synthesis gas.

Depending on the concentration of heavier hydrocarbons in natural gas, there may be an additional step, called pre-reforming, which is designed to remove those heavier compounds. The pre-reforming process converts heavier hydrocarbons in the feed to CH<sub>4</sub>, CO<sub>x</sub>, and H<sub>2</sub> in an adiabatic reactor at 573K – 798K using a mixture of alumina<sup>a</sup> with high levels of nickel<sup>b</sup> for catalyst.

Thus far permitting the manufacturer to use a wide variety of feedstocks and allowing for the reduction of the unit’s overall steam/carbon ratio (due to a lesser coke formation) and therefore increasing the plant’s efficiency.

Subsequently the pretreated natural gas feedstock is mixed with steam at pressures of 2.6MPa. The resulting mixture is preheated to 773K and introduced to the catalytic reforming reactor in which, the steam/methane mixture is passed through externally heated reformer tubes filled with nickel catalyst, where it is converted to carbon monoxide (CO) and hydrogen (H<sub>2</sub>) at 1123K – 1173K according to the following equation:



The reaction is highly endothermic and favoured by low pressures. However, in most industrial application, hydrogen is processed at pressures of at least 2.0MPa, therefore, the reformers are operated at elevated pressures (usually, 2.0 – 2.6MPa). High pressures allow for a more compact reactor design, thus increasing the reactor throughput and reducing the cost of materials. According to the stoichiometry in reaction (2), the molar ratio of steam to methane is H<sub>2</sub>O:CH<sub>4</sub> = 1:1, however, in practice: an excess of steam (commonly, steam/methane ratio of 2.5:3) is used to prevent carbon (*coke*) deposition on the catalyst surface. In order to supply heat for the endothermic steam methane reforming reaction, the catalyst is loaded into a bundle of reactor tubes made out of heat-resistant nickel alloy. These catalyst-containing tubes are placed inside a furnace box with multiple burners mounted along the inside walls. The typical inlet temperatures are 723K – 923K, with the product gas leaving the reformer at 973K – 1223K.

Ensuing reaction (2) the gaseous mixture containing H<sub>2</sub>, CO, and steam (and usually about 4% of unconverted methane) leaves the reformer at about 1073K – 1173K. It is then cooled rapidly to about 623K (thereby generating steam) and is fed to the water gas shift reactors, where CO reacts with steam over a catalyst bed producing H<sub>2</sub> and CO<sub>2</sub>:



<sup>a</sup> Aluminium oxide Al<sub>2</sub>O<sub>3</sub> highly porous adsorbent for catalyst with high surface area

<sup>b</sup> Ni-based catalysts prepared using sol gel made γ-alumina support have higher hydrogen selectivity





Finally the H<sub>2</sub> is separated from CO<sub>2</sub> and purified.

As mentioned earlier, the driving factor of the eligibility of a process over another in this study is its cost effectiveness as well as its sustainability factor.

For this process the efficiency is defined as the ratio between the total energy produced and consumed as follows:

$$\eta = \frac{E_{H_2} + E_{Steam, 4.8 MPa}}{E_{NG} + electricity + E_{steam, 2.6 MPa}} \quad (4)$$

Where  $\eta$  is the energy efficiency,  $E_{H_2}$  equivalent to the energy supplied by H<sub>2</sub>,  $E_{steam, 4.8 MPa}$  the 4.8 MPa steam energy (exported),  $E_{NG}$  the NG energy, and  $E_{steam, 2.6 MPa}$  the 2.6 MPa steam (required).

According to Scholz [8] it is found that for a given hydrogen plant operating under normal conditions with the capacity of the order of  $1.5 \times 10^6$  m<sup>3</sup>/Day, the overall efficiency is 81.2%. And taking into account as cited by Li Kaiwen [9] the affordable transportation of natural gas given through its maturity we are looking at costs of production of 2.48\$ – 3.17\$/kg H<sub>2</sub>

*\*Though production from coal by gasification process is more economically feasible, but due to its environmental impacts and high CO<sub>2</sub> emission, it will not be taken into account.*

Lastly as stated by scholz, normal CO<sub>2</sub> emissions are estimated to be at around 0.44m<sup>3</sup> CO<sub>2</sub>/m<sup>3</sup>H<sub>2</sub>, which translates to an emission capacity under normal conditions of  $6.6 \times 10^5$  m<sup>3</sup>/Day which though far from ideal is at an acceptable level.

In order to reach an ideal solution in the near-to medium term, the use of nuclear reactors, sequestration of CO<sub>2</sub> in steam methane reforming plants, as well as renewable energies such as solar power and wind could be implemented.

## 4.2. Hydrogen production using nuclear energy

There are several ways in which Hydrogen could be produced through the use of nuclear power:

1. Nuclear heated steam reforming of natural gas
2. Electrolysis of water using nuclear power
3. High Temperature Electrolysis.
4. Thermochemical splitting.

Since the topic of steam reforming of natural gas has already been delved into in the section prior, and considering that high temperature electrolysis is less demanding of electricity than the conventional water electrolysis – a point that we shall prove further in this section\* – we can therefore focus this part of the study at the process of high temperature electrolysis neglecting thermochemical splitting of water in an iodine–sulphur medium as further research is needed on the subject and major issues are still noted.

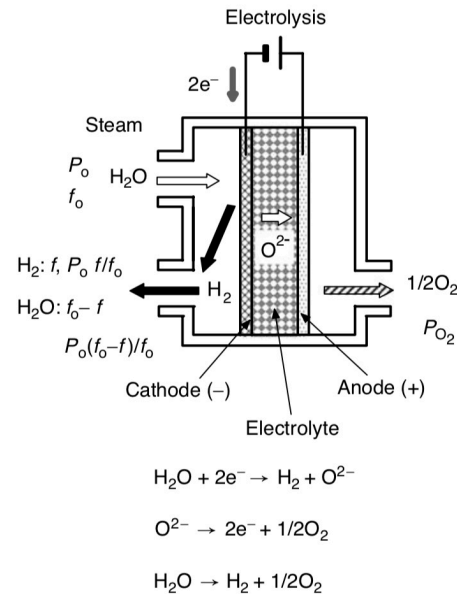


**Fig.6** Principle of high temperature electrolysis on steam

The process of high temperature electrolysis (HTE) is a reverse oxidation. At the cathode – usually a thin porous layer on the electrolyte – steam is dissociated with hydrogen molecules ( $H_2$ ) forming on the cathode surface:



The electrolyte being an ionic conductor allows for the migration of the oxygen molecule through vacancies in its lattice

Oxygen molecules then form on the anode surface with the release of electrons:



The products, hydrogen and oxygen, are separated by the gas-tight electrolyte. Reactions on the two electrodes are summed up as:



\*Theoretical energy demand ( $\Delta H$ ) for water and steam decomposition is the sum of the Gibbs energy ( $\Delta G$ ) and the heat energy ( $T\Delta S$ ).

$$\Delta H = \Delta G + T\Delta S \quad (4)$$

$$\Delta G = \Delta G_0 + RT \cdot \ln \left( \frac{\alpha_{H_2} \alpha_{O_2}^{1/2}}{\alpha_{H_2O}} \right) \quad (5)$$



$\Delta G_0$  is the standard Gibbs free energy change (per mole) at a temperature of T, with R being the gas constant, and  $\alpha_{H_2}$ ,  $\alpha_{O_2}$ , and  $\alpha_{H_2O}$  the activities of  $H_2$ ,  $O_2$ , and  $H_2O$  in the cell, with  $\alpha = \gamma \cdot \frac{p}{p^\ominus}$  for gas, where  $\gamma$  is the activity coefficient (a constant number based on what the substance is, what the solvent is and other factors),  $p$  the partial pressure and  $p^\ominus$  the standard state pressure for the gas.

Knowing that  $E = \frac{\Delta G}{2F}$  and that  $E_0 = \frac{\Delta G_0}{2F}$  with F being the faraday constant and  $E_0$  the standard electromotive force. We can then substitute in (5) to get the following equation:

$$E = E_0 + \left(\frac{RT}{2F}\right) \cdot \ln\left(\frac{\alpha_{H_2} \alpha_{O_2}^{\frac{1}{2}}}{\alpha_{H_2O}}\right) \quad (6)$$

As the equation (5), bears resemblance to the Nernst equation. Activities of reactants and products can be expressed as partial pressures as the reaction takes place in a gas phase. The over-voltage,  $\eta$ , is caused mainly by shortage of steam concentration at the cathode and electrical resistance.

$$E = E_0 + \left(\frac{RT}{2F}\right) \cdot \ln\left(\frac{p_{H_2} p_{O_2}^{\frac{1}{2}}}{p_{H_2O}}\right) + \eta \quad (7)$$

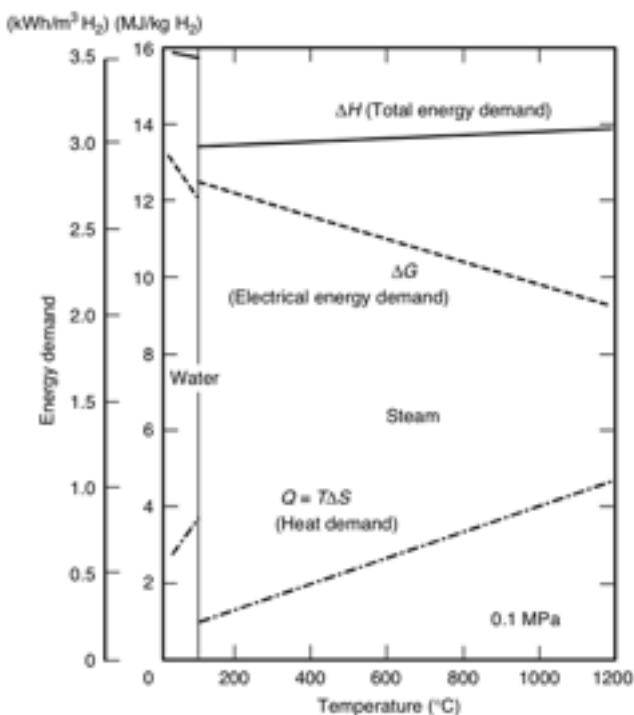


**Fig.7** Energy to temperature plot for water electrolysis

Considering the fact that  $E - \eta$  is the value of the open circuit voltage in the cell and that the steam of molar flow rate,  $f_0$ , and pressure,  $P_0$ , is reduced to hydrogen gas of flow rate,  $f - f_0$ , and partial pressure,  $P_0(f_0 - f)/f_0$ , in the cathode compartment:  $(f_0 - f)/f_0$  is a conversion ratio from steam

to  $H_2$ . The partial pressure of  $O_2$ ,  $P_{O_2}$ , is assumed to be unity. Using the steam conversion ratio,  $X = (f_0 - f)/f_0$ , Equation 6 can be written as follows:

$$E - \eta = E_0 + \left(\frac{RT}{2F}\right) \cdot \ln \frac{X}{1-X} \quad (8)$$

From (8) we can then extrapolate to the following plot in order to clarify the energy needs for electrolysis.

As seen in figure 7 although the total energy supplied increases along with higher temperatures, the electrical demand decreases ( $\Delta G$ ).

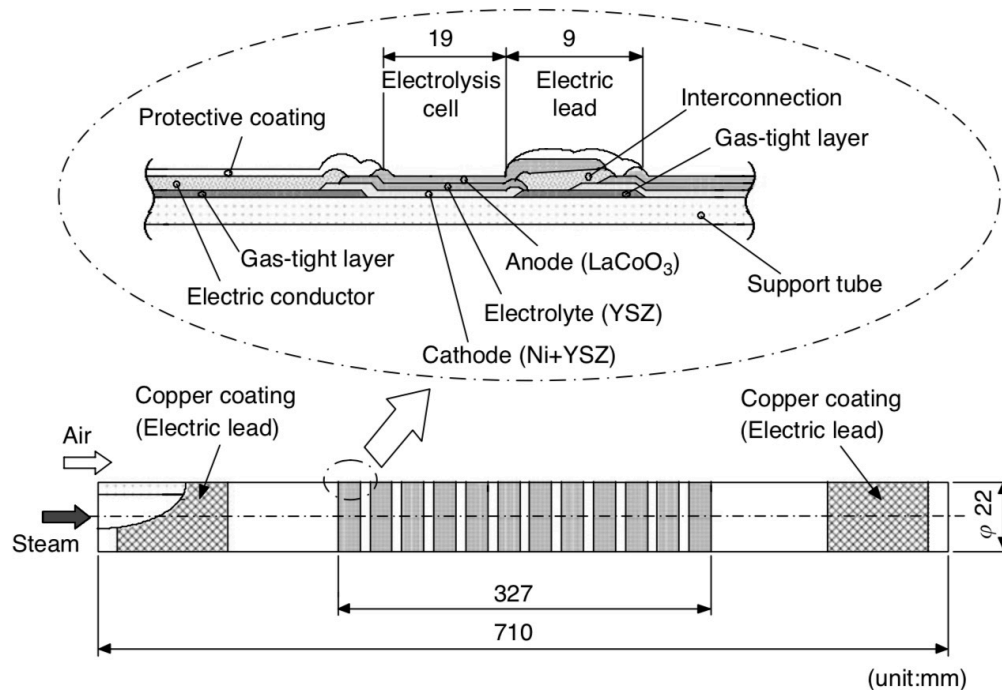


**Fig.8** Schematics of an electrolysis tube [10]

Utilising the research of Nagata [10] we can find an experimental application of this process through tubular cells. In this application the electrolysis tube is composed of 12 electrolysis cells; which we can see the schematic view of in **Figure 8**, of 19mm in length, the length of which was determined so as to keep the current density uniform.

These cells were connected in series with the electrolyte layer made of  $YSZ^a$  and sandwiched between the porous cathode and anode layers: nickel-cermet (Ni + YSZ) for the cathode and  $LaCoO_3$  for the anode.

At the ends of the electrolysis tube, platinum (Pt) wires working as electric leads were welded on copper-coated layers. These layers were connected to thin plies of electric conductors. Thin alumina gas-tight sheets and YSZ protective layers coated the outside of the electrolysis tube,

<sup>a</sup> Yttria-stabilized zirconia (YSZ) is a ceramic in which the crystal structure of zirconium dioxide is made stable at room temperature by an addition of yttrium oxide.

except the cells and the copper coatings. These layers were formed on a porous CSZ tube (support tube) of 22 mm in outer diameter, 3 mm in thickness, and about 38% of porosity, by using the plasma spraying. The thickness of each layer was in the range from 0.1 to 0.25 mm. The total length of the electrolysis tube was 710 mm. **Figure 9** provides an image of the final product.

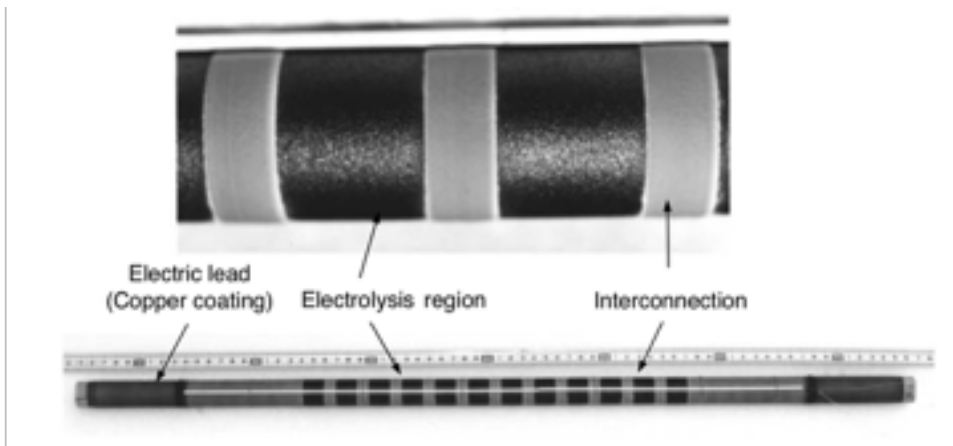


**Fig.9** Outer view of a tubular electrolysis cell

The experiments were carried out at the temperatures of 1123K, 1173K, and 1223K under the absolute pressure of 0.11MPa. Steam was supplied with argon carrier gas at a rate of about 0.32 g/min. The heating and cooling rates were set to be less than 20°C/h during start-up and shut-down in order to avoid generating high interfacial stress from differential thermal expansion among the electrolysis tube components otherwise occurring under rapid heating or cooling.

Before applying the electrolysis voltage, the cathode material, nickel-cermet, was chemically reduced with hydrogen mixed with argon carrier gas for 1 h at least.

**Table 4** Production rate of hydrogen under different condition

Temperature (K)	Voltage (V)	Intensity (A)	Production Rate (l/h)
1123	15.7	1.42	3.8
1173	16.3	1.38	4.3
1223	15.6	1.72	6.9

The over-voltage increases with the hydrogen production rate. The Faraday efficiency at 1223K and in a range of 0.74 to 0.85 V applied voltage with more than 6 W applied power, which results in current density of more than 45 mA/cm<sup>2</sup>, is estimated to range from 0.27 to 0.56.

When connected to the reactor, the HTE operating temperature will be up to 1173K. It is necessary to use other solid-oxide electrolytes working below that temperature and having considerably higher oxygen ion conductivity than that of YSZ. One candidate is Ytterbium (Yb<sub>2</sub>O<sub>3</sub>) – stabilised ZrO<sub>2</sub> (YbSZ). It is also necessary to enhance the hydraulics of the steam supply to the interface between the electrolysis and the electrode, which might be realised by decreasing the fuel electrode layer thickness and by increasing its porosity.

After the experiments, it was observed that large parts of the anode layers had been separated from the electrolyte layers, although the electrolysis tube had served for one thermal cycle only. This indicates that the durability of the cell against thermal cycles, especially the durability of the anode layer, is one of the key issues of HTE. It could be met by raising the bonding force and keeping high residual compression stress of the anode layer to the electrolyte layer against large differential thermal expansion of these layers considering the relevant service conditions. In conclusion as specified by **Table 4** the rates of production do line up with what is predicted by theory. As the temperature advances the rates of production do increment significantly. If scaled up properly the tubular electrolysis cell could offer a better alternative to regular electrolysis, thus offering an improvement on energy consumption and diminishing the overall environmental impact.

### 4.3. Hydrogen production using renewable energies

The production of hydrogen through renewable energy is an interesting aspect, as this solution could offer a chemical battery in form of fuel to store energy in case of lack of natural resources such as wind or sun. The whole process behind the production of hydrogen through renewable energy utilize the water electrolysis method, but with the electricity being provided by a renewable energy source. In this paragraph we will summarize the most widely spread technics for solar renewable and wind as they the prevalent methods of harnessing renewable energy.

*\*In the case of solar energy we've chosen to skip the photosynthesis process, as it is highly technical and still under developed at the current moment.*

#### 4.3.1. WIND POWER

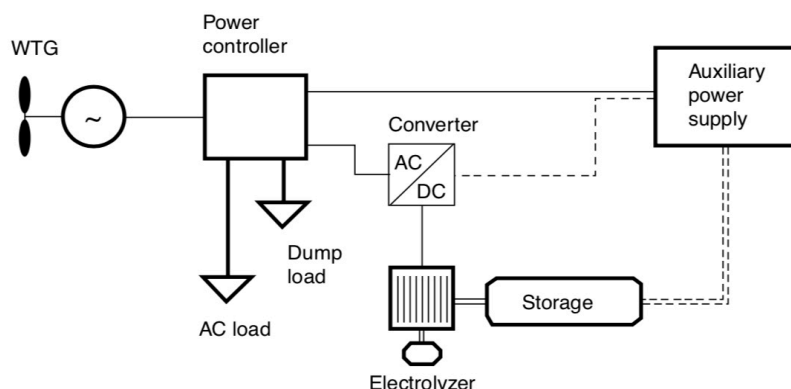


**Fig.10** Schematics of a stand-alone wind-hydrogen power system

There is a particular manner on how to apply an electrolyzing hydrogen production unit for each wind energy system category. The most common being the stand-alone wind energy system combined with an electrolyser. This electrolyser is connected in the place of the battery cluster.

The electrolyser unit can be either a PEM<sup>a</sup> or an alkaline type where there is a constant feed with water. The produced hydrogen is usually stored in a tank at the output pressure of the electrolyser or compressed at a higher pressure by a gas compressor.

For energy security reasons, the presence of an auxiliary power supply unit is necessary. This unit can be preferably either a hydrogen internal combustion engine or a fuel cell of corresponding capacity to meet at least the minimum needs of the system. **Figure 10** shows a stand-alone wind-hydrogen system that is autonomous. The dashed line in some parts of it implies that these connections may not exist as well. The DC/AC converter/controller should have the capability to operate vice versa and power up the lines through the power controller.

Alternatively, the auxiliary power device can be diesel engine, which can be obtained in various sizes and specifications. It is presumed that in a stand-alone system the requirements for power quality are not the same as that for a grid-connected consumer [11].

The determination of the size of the hydrogen equipment for these stations is very important to decrease the total cost and the amount of the dumped load due to technical constraints [12]. This determination can be achieved by simulating the operation of the whole system based on real wind data of the site and considering all the possible energy losses that might occur.

Hydrogen production from wind energy has not been implemented in large-scale yet. The main reason for this, apart from the high cost, is that the present commercially available electrolyzes are designed to operate at lower capacities. An increase in the size of an electrolyser is achieved by connecting electrolysis stacks in series.

### 4.3.2. SOLAR ENERGY

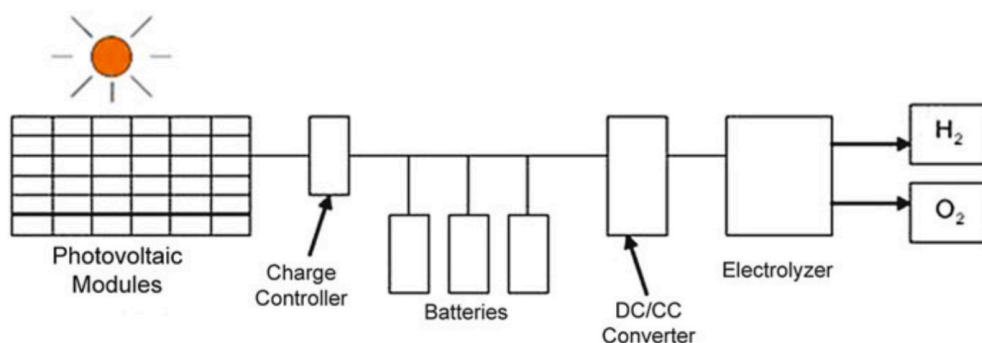


**Fig.11** Conventional solar hydrogen production system [13]

As we see in **Figure 11** solar energy can be used, just as discussed previously to furnish the power necessary for water electrolysis. According to Gibson and Kelly [13] photovoltaic modules are connected to charge controllers and DC/CC converters, which allow the batteries to be fully

<sup>a</sup> Proton exchange membrane is the electrolysis of water in a cell equipped with a solid polymer electrolyte that is responsible for the conduction of protons, separation of product gases, and electrical insulation of the electrodes.



charged and prevent over-discharging; these converters are needed to supply the typical voltage characteristic of an electrolyser.

When a photovoltaic panel is connected to any equipment, voltage drops below open-circuit due to the internal resistance of the module and equipment. The DC voltage applied to the electrolysis system is limited by the output of the panel circuit, and the voltage and current of the electrolysis process are limited by the operating characteristics of the electrolyser, hence the need for a DC/DC converter [13].

Furthermore, the low efficiency of photovoltaic panels (peak efficiency circa 14% for monocrystallin silicon) renders the electrolysis process very tedious and unpractical. Other methods are being developed such as photo-electrochemical processes. These processes rely on the interexchange of electrons through excitement of light; such donors can be semi-conductors or certain types of oxides, i.e. Titanium oxide or Strontium oxide.

#### **4.4. Conclusion**

Natural gas reforming, coal gasification and water electrolysis are proven technologies for hydrogen production today and are applied at an industrial scale all over the world. These are also the most likely hydrogen production technologies to be employed until 2030 and beyond.

And it is clear, that the production of hydrogen from more renewable sources (such as wind and solar) is a goal to strive for, yet the economics of such production methods renders the adoption of renewable for energy conversation a rather costly aspect of hydrogen production. Therefore it is apparent that till the near future SMR, and coal gasification are the best production methods for hydrogen, this if equipped with carbon captures plants could be a good starting point for fossil fuel independence.

## **5. Hydrogen distribution and storage**

The most problematic aspects of hydrogen storage and distribution systems are the rather low density of hydrogen, the failures enabled by the degradation of the material, and the high energy cost of transportation and storage. Consequently, the most important technical and economic facets to meet are the safety considerations for the proper depositary and shipment of the product, alongside the maintenance and reliability of the process, as well as the adaptability of current supply infrastructure and the cost of integration of new ones. This chapter will be divided in two sections: distribution and storage, each will review the most likely solutions that take in consideration the issues cited prior.

### **5.1. Hydrogen transportation**

There are several methods of transportation; continuous transportation, and batch transportation. A continuous transportation revolves around continuously delivering hydrogen, i.e. pipelines, whereas batch transportation would load vessels containing hydrogen in different states (liquid,

pressurised or metal hybrid) onto mobile units.

However each method needs its own exclusive pressurised or insulated equipment, thus rendering the price high. Hence, the production rate is confined to the on-going demand therefore restraining to great extent the distances of transportability of hydrogen to an area close to the production facility or to small-scale hydrogen sales for highly advanced usage.



**Fig. 11.1** Geographical distribution of industrial Hydrogen production facilities in Europe – Roads2HyCom (2007)

*\* Given the similarity between the batch transportation and the storage methods through the use of carrying vessels we shall dedicate a considerable part of this section to the continuous transportation method.*





Fig. 11.2 Hydrogen pipeline network in north-western Europe – Roads2HyCom (2007)

For half a century pipelines have been used to transport hydrogen and, today, there are about 16.000km of hydrogen pipelines around the world that supply hydrogen to refineries and chemical plants; for instance dense networks exist between Belgium, France and the Netherlands, as seen in figure 10.2. Existing hydrogen pipelines are about 100–300 mm in diameter and usually operate at a pressure of 10–30 bar, but pressures up to 100bar can also be used according to the International Energy Agency.

For transporting hydrogen by pipeline, three principal options exist:

1. Build new, dedicated hydrogen distribution networks
2. Adapt existing natural gas pipelines for hydrogen transport (if possible)
3. Blend hydrogen with natural gas up to a certain extent and either separate the two at the delivery point, or use the mixture, e.g., in stationary combustion applications

Consecutively we shall address the formulas involved in the calculations of the comportment of the gas inside a pipe. As we can approximate the behaviour of hydrogen to that of natural gas in a pipeline, we shall then base our proceedings on the recommendations of the U.S bureau of mines, and the American gas association (AGA).

The pressure drop occurring in the pipe due to friction when transporting hydrogen (or any other gas) depends on the pipe diameter, the gas throughput, the surface properties of the pipe material, the pressure level in the pipe and the density of the gas. Generally, the pressure drop needs to be compensated by recompression every 200–300 km.

Taking into account Bernoulli's equation for gas flow we can then derivate the pressure drop from the following equation:

$$P_{in} - P_{out} = Z_{out} - Z_{in} + \frac{V_{out}^2}{2g} - \frac{V_{in}^2}{2g} + h_f - H_p \quad (1)$$

h, Total frictional pressure loss





H<sub>b</sub> Head added to the fluid by a compressor at the inlet point

The General Flow equation, also called the Fundamental Flow equation, for the steady-state isothermal flow in a gas pipeline is the basic equation for relating the pressure drop with flow rate.

$$Q = 5.747 \times 10^{-4} F \left( \frac{T_b}{P_b} \right) \left[ \frac{(P_1^2 - P_2^2)}{GT_f LZ} \right]^{0.5} D^{2.5} \quad (2)$$

Q Gas flow rate, measured at standard conditions, m<sup>3</sup>/day

F Transmission factor, dimensionless  $F = \frac{2}{\sqrt{f}}$

P<sub>b</sub> Base pressure, kPa

T<sub>b</sub> Base temperature, K (273 + °C)

P<sub>1</sub>, P<sub>2</sub> Upstream and downstream pressures, kPa

G Gas gravity (air = 1.00)

T<sub>f</sub> Average gas flowing temperature, K (273 + °C)

L Pipe segment length, km

Z Gas compressibility factor at the flowing temperature, dimensionless

D Inner pipe diameter, mm

In the General Flow equation, the compressibility factor Z is used. This must be calculated at the gas flowing temperature and average pressure in the pipe segment. Therefore, it is important to first calculate the average pressure in a pipe segment. As a first approximation, we may use an arithmetic average. However, it has been found that a more accurate value of the average gas pressure in a pipe segment is:

$$P_{avg} = \frac{2}{3} \left( \frac{P_1^3 - P_2^3}{P_1^2 - P_2^2} \right) \quad (3)$$

Following the Institute of Gas Technology equation (2) can also be expressed as follows:

$$Q = 1.2822 \times 10^{-3} E \left( \frac{T_b}{P_b} \right) \left( \frac{P_1^2 - P_2^2}{G^{0.8} T_f L_e \mu^{0.2}} \right)^{0.555} D^{2.667} \quad (4)$$

The efficiency (E) usually is added to correct for small amounts of liquid, general debris, weld resistance, valve installations, line bends, and other factors which reduce gas flow rate below the basis rate predicted by the prior equations. The design value of efficiency E in a new clean gas line usually is estimated at 0.92.

Some pipeline companies arbitrarily use a graduated efficiency, such as:

E = 0.85 - adverse (corroded), old, dirty pipe

E = 0.92 - average to good condition, normal pipe design

E = 0.95 - excellent conditions with frequent pigging

E = 1.00 - new straight pipe without bends, seldom used in pipeline design

The amount of energy input to the gas by the compressors is dependent upon the pressure of the gas and flow rate. As the flow rate increases, the pressure also increases and, hence, the power needed will also build up. Since energy is defined as work done by a force, we can state the power required in term of the gas flow rate and the discharge pressure of the compressor station. Nonetheless the compressibility factor and the type of gas compression (adiabatic or polytropic) must be taken into account.

The head developed by the compressor is defined as the amount of energy supplied to the gas per unit mass of gas. Therefore, by multiplying the mass flow rate of gas by the compressor head, we can calculate the total energy supplied to the gas. Dividing this by compressor efficiency, we will get the power required to compress the gas. The equation can be expressed as follows:

$$\Psi = 4.0639 \left( \frac{\gamma}{\gamma - 1} \right) Q T_1 \left( \frac{Z_1 + Z_2}{2} \right) \left( \frac{1}{\eta_a} \right) \left[ \left( \frac{P_2}{P_1} \right)^{\frac{\gamma - 1}{\gamma}} - 1 \right] \quad (6)$$

$\Psi$	Compression Power, kW
$\gamma$	Ratio of specific heats of gas, dimensionless
$Q$	Gas flow rate, m <sup>3</sup> /day
$T_1$	Suction temperature of gas, K
$P_1, P_2$	Suction and discharge pressures, kPa
$Z_1, Z_2$	Compressibility of gas at suction and discharge conditions, dimensionless
$\eta_a$	Compressor adiabatic (isentropic) efficiency, decimal value

Generally the adiabatic efficiency  $\eta_a$  ranges from 0.75 to 0.85, and The mechanical efficiency  $\eta_m$  of the driver can range from 0.95 to 0.98. The overall efficiency,  $\eta_T$ , is defined as the product of the adiabatic efficiency,  $\eta_a$ , and the mechanical efficiency,  $\eta_m$ :

$$\eta_T = \eta_a \times \eta_m \quad (7)$$

We shall then proceed to compare the transportation capacity through the use of the cited equations between hydrogen and natural gas under the conditions shown in table 4 which in turn provide an example of calculation.

If we proceed to simplify the flow rate equations admitting that both gases operate under the same conditions we then realise that the ratio of flow capacity depends on three variables intrinsic to each gases – the gas compressibility factor  $Z$  the transmission factor  $F$  and the specific gravity  $G$ .

$$\nu = \frac{F_{hydrogen} \times \sqrt{\frac{G_{hydrogen} \cdot Z_{hydrogen}}{G_{gas} \cdot Z_{gas}}}}{F_{gas}} \quad (8)$$

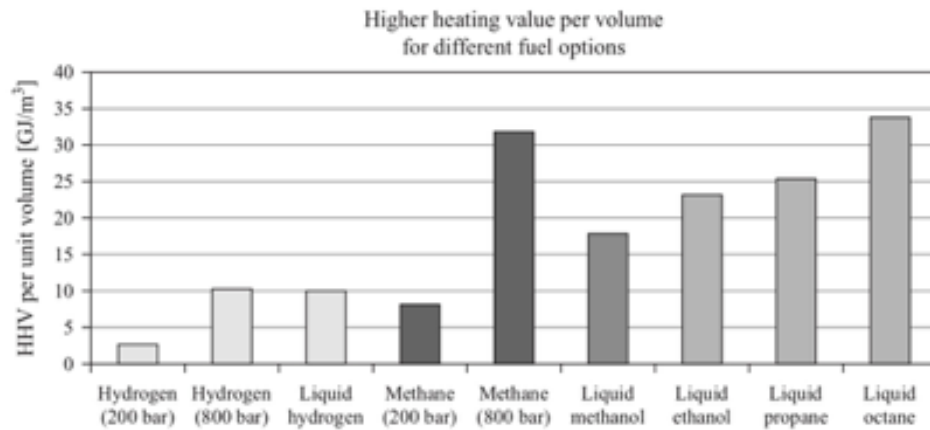


Fig.12 Volumetric HHV energy density of different fuels [14]

Table 5.2 Pipeline calculation (continuation)

Average pressure kPa	Compressibility factor at suction -	Compressibility factor at discharge -	Adiabatic efficiency -	Gas gravity -
7,2	1,2	1	0,8	0,07
6,6	1,2	1	0,8	0,07
5,9	1,2	1	0,8	0,07
5,3	1,2	1	0,8	0,07
4,3	1,2	1	0,8	0,07
3,7	1,2	1	0,8	0,07
7,2	0,90	0,95	0,8	0,6
6,6	0,90	0,95	0,8	0,6
5,9	0,90	0,95	0,8	0,6
5,3	0,90	0,95	0,8	0,6
4,3	0,90	0,95	0,8	0,6
3,7	0,90	0,95	0,8	0,6

Table 5.1 Pipeline calculation

Gas type	Pipeline Efficiency -	Specific Heat ratio -	Average gas temperature K	Inlet Temperature K	Discharge pressure MPa	Suction pressure MPa
Hydrogen	0,95	1,4	300	293	9	5
Hydrogen	0,95	1,4	300	293	8	5
Hydrogen	0,95	1,4	300	293	8	3
Hydrogen	0,92	1,4	300	293	7	3
Hydrogen	0,92	1,4	300	293	6	2
Hydrogen	0,92	1,4	300	293	5	2
Natural gas	0,95	1,27	300	293	9	5
Natural gas	0,95	1,27	300	293	8	5
Natural gas	0,95	1,27	300	293	8	3
Natural gas	0,92	1,27	300	293	7	3
Natural gas	0,92	1,27	300	293	6	2
Natural gas	0,92	1,27	300	293	5	2

**Table 5.3** Pipeline calculation (continuation)

Inne pipe Diameter	Pipe segment length	Compressor Power	Gas flow	Gas viscosity
mm	km	kW	m3/day	Poise
100	25	439,27	7,69E+05	9,00E-07
150	50	566,87	1,26E+06	9,00E-07
200	75	2655,26	2,63E+06	9,00E-07
250	100	2820,52	3,29E+06	9,00E-07
275	125	3821,86	3,32E+06	9,00E-07
300	150	2798,46	2,99E+06	9,00E-07
100	25	68,91	1,73E+05	1,14E-04
150	50	89,33	2,84E+05	1,14E-04
200	75	410,22	5,91E+05	1,14E-04
250	100	438,04	7,42E+05	1,14E-04
275	125	587,69	7,46E+05	1,14E-04
300	150	433,44	6,73E+05	1,14E-04

Knowing that hydrogen is characterised by a lower molecular weight and viscosity it is apparent that it flows 2 – 5 times faster than natural gas under the same conditions. Yet because of its lower heating value (HHV) the total energy carried is up to 40% lower than natural gas (**Figure 12**). Which in turn coincides with the finding of our simulation, which established a higher flow rate in every case coupled with a larger energy cost due to the demand of the compressor.

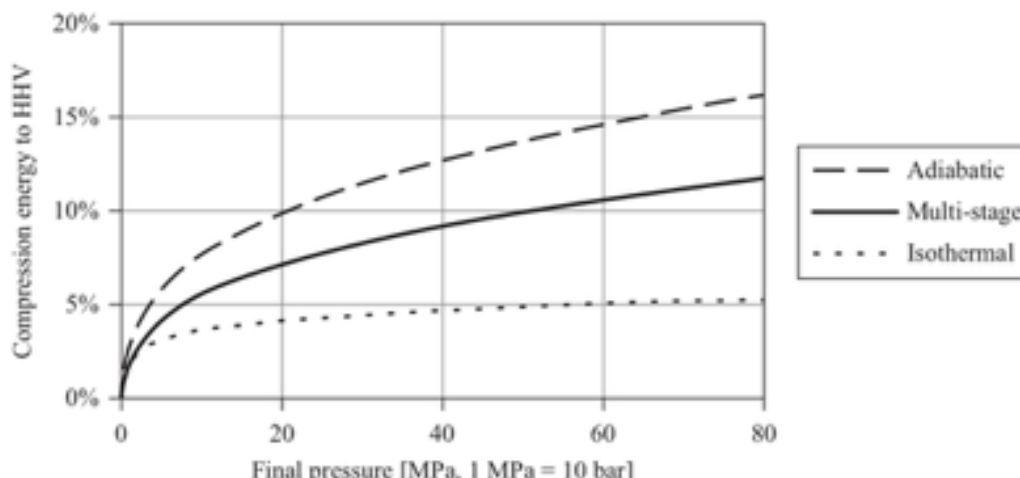


**Fig.13** Energy required for the compression of hydrogen compared to its higher heating values, HHV [14]

Alternatively those issues could be resolved through the use of part of the hydrogen to drive the compressor (as in the case of natural-gas pipelines), a change in the compression type; **Figure 13** shows that an isothermal compression is the least energy intensive process with the adiabatic compression consuming up to 10% of the higher heating values for our range of pressures, and a

raise in the driving pressures and pipe diameter.

Finally, hydrogen can affect the materials used for its transportation through the effects of hydrogen embrittlement and leakage due to corrosion and/or diffusion of the molecule.

The former effect is highly dependent on pressure, which if the pressure drop is neglected means that cracking due to hydrogen embrittlement must be driven by static stress. Nonetheless experience from the petroleum industry demonstrated that hydrogen assisted fatigue is also possible [15][16].

Since defects can induce to a higher concentration of stresses in pressurised materials, – defects caused by welds, corrosion, and third party damage –, the design of the structure should rely on fracture mechanics methods which impose severe mechanical conditions that can promote fracture phenomena that are not revealed by more conventional testing methods.

Knowing the local tensile stress normal to the crack line ( $\sigma_y$ ) we can relate it to the distance to the crack plane ahead of the crack tip ( $x$ ) and the stress intensity factor ( $K$ ):

$$\sigma_y = \frac{K}{\sqrt{2\pi x}} \quad (10)$$

That being said the stress intensity factor is proportional to the wall stress ( $\sigma_w$ ), ( $\beta$ ) a function of both defect and structure geometry, and ( $a$ ) the defect depth:

$$K = \beta \sigma_w \sqrt{\pi a} \quad (11)$$

Finally, the design parameter can be established through the stress intensity factor ( $K$ ) and the critical value of the stress intensity factor for propagation of the defect ( $K_c$ ) which depends on variables such as service environment:

$$K \geq K_c \Rightarrow \beta \sigma_w \sqrt{\pi a} \geq K_c \quad (12)$$

Defects can also extend by fatigue crack propagation:

$$\frac{da}{dN} = C \Delta K^n \quad (13)$$

The fatigue Crack Growth Rate ( $da/dN$ ) being the rate of cracking under specified loading conditions, ( $C$ ) and ( $n$ ) specific material and environment-dependent constants and ( $\Delta K$ ) the stress intensity factor range  $\Delta K = K_{max} - K_{min}$

Now that we defined the mathematical confines of fracture mechanics it is to be noted that this framework applies only when plastic deformation of the material is limited. – Considerable plastic deformation may add to the propagation of existing defect in which case the linear stress intensity factor ( $K$ ) may not apply accurately and elastic-plastic fracture mechanics methods should be considered.–

In the following we shall see the effect of gas pressure and impurities on the material as well as steel strength and composition.

As presented earlier higher pressures facilitate hydrogen embrittlement of steel, this can be explained by the increase of the quantity of hydrogen atoms dissolved in the steel as proved by the general form of Sievert's law:  $C = S\sqrt{f}$  showing that the concentration (C) is relative to the solubility (S), and the fugacity (f) both terms dependant on pressure and temperature.

To corroborate this explanation **Figure 14.1** to **14.2** show indeed a drop in the intensity factor (K) and an increase in the crack growth rate (da/dN) for higher gas pressure in especially low-alloy steel at pressures over 30MPa. Whereas, **Figure 14.3** indicates the persistence of the susceptibility to hydrogen embrittlement even at lower pressure, through the variation of the stress concentration factor.

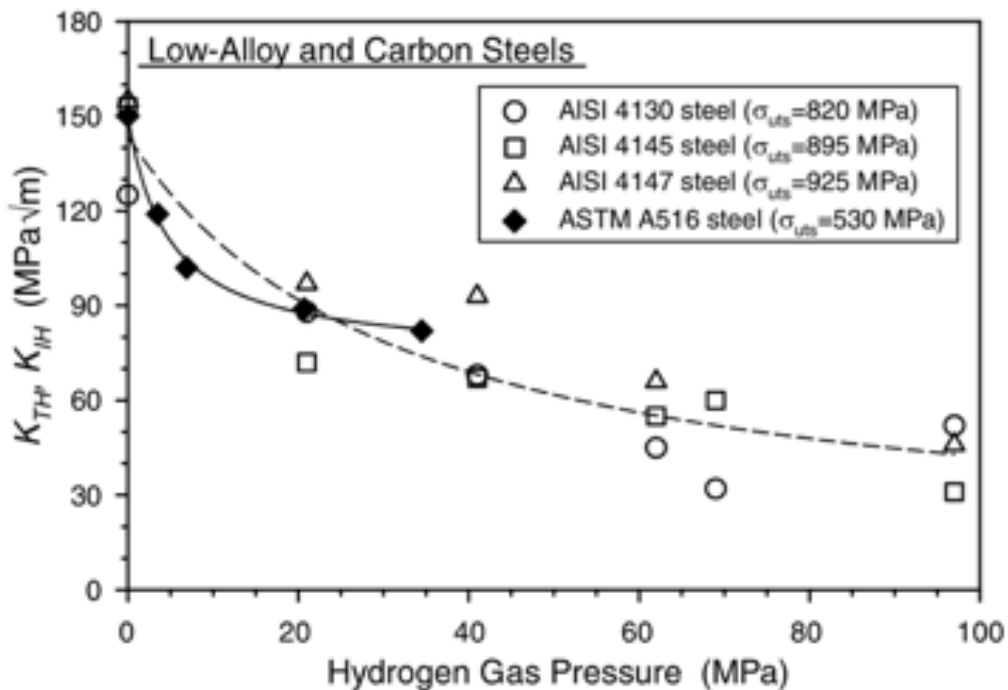
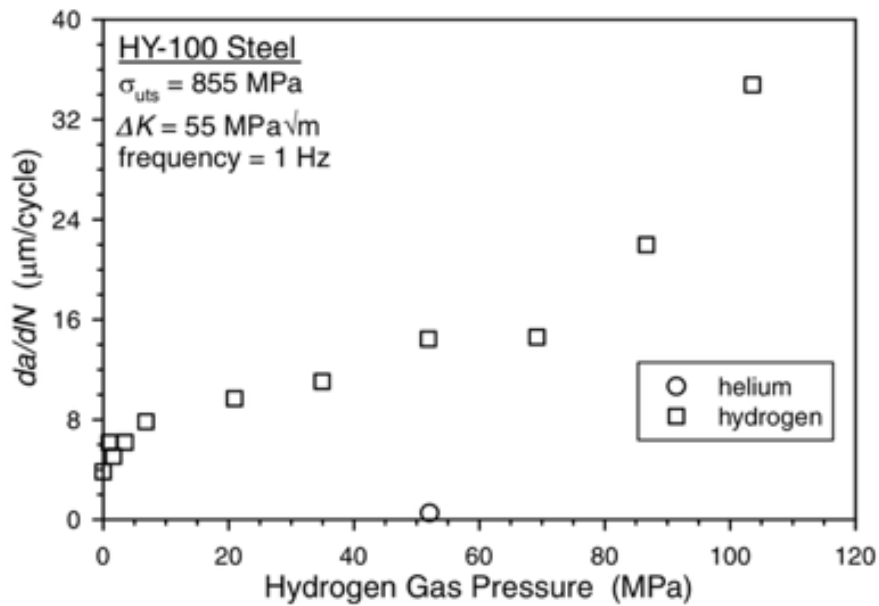
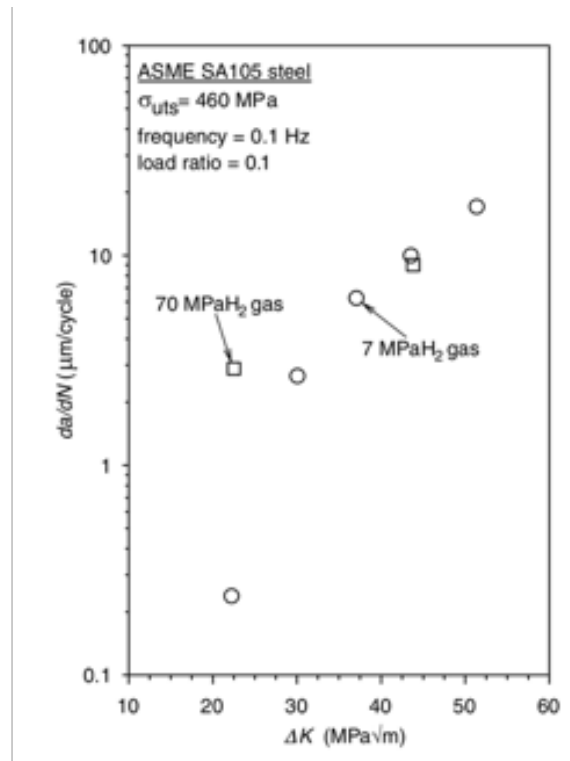


Fig.14.1 Effects of gas pressure on critical stress intensity factor [15]



**Fig. 14.2** Effect of hydrogen gas pressure on fatigue crack growth ( $da/dN$ ) at constant stress intensity factor range ( $\Delta K$ ) in a low-alloy steel [16]



**Fig. 14.3** Effect of hydrogen gas pressure on fatigue crack growth ( $da/dN$ ) at constant stress intensity factor range ( $\Delta K$ ) relationships for a carbon steel [17]



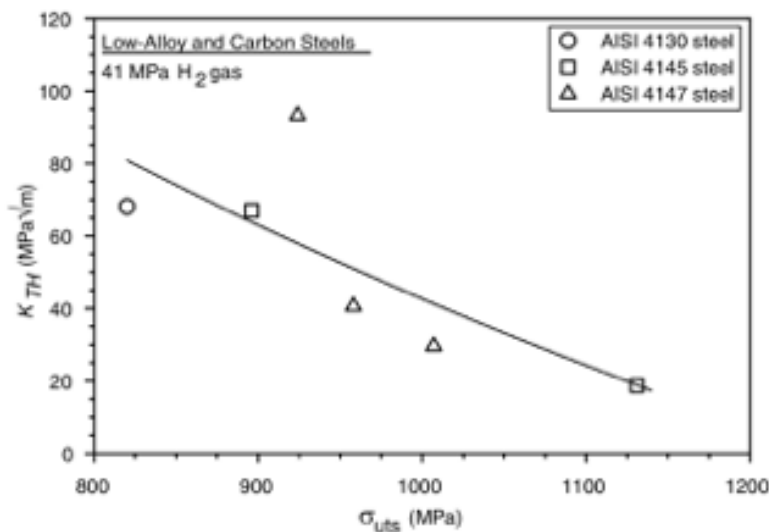


**Fig. 14.4** Effect of tensile strength on critical stress intensity factor for crack extension in hydrogen gas. Data are for low-alloy steel tested under static loading

**Figure 14.4** for instance demonstrate the impact of strength in the susceptibility to hydrogen embrittlement, as it compares various materials with different tensile strengths [18,19,20].

Similarly welding in carbon and low-alloy steels can cause undesirable changes in the microstructure of the material (e.g. creation of martensite) and create residual stress. Given that the effect of pressure affect welds in a similar fashion to that of the base metal, the strength and microstructure of welds then must be controlled to avoid hydrogen embrittlement.

Eventually a way to offset the sensitivity of the material to hydrogen embrittlement is through the control of material composition and impurities in the gas or via coatings/barriers thus preventing leakage:

To a degree the presence of low concentration of certain gases in the environment can alter the effect of hydrogen; though sulphur-bearing gases such as Hydrogen sulphide exacerbate the effect.

**Figure 15** shows the ratio of  $(da/dN)$  in hydrogen gas containing additives over  $(da/dN)$  in hydrogen gas only. It is therefore apparent that oxygen and carbon monoxide can mitigate the effects of hydrogen embrittlement, though it is to be noted that the mechanistic role of gas additives must be considered. As for example oxygen may impede the uptake of hydrogen in steel structure at first hand, but over a long period of the material can dissolve enough hydrogen to suffer embrittlement.



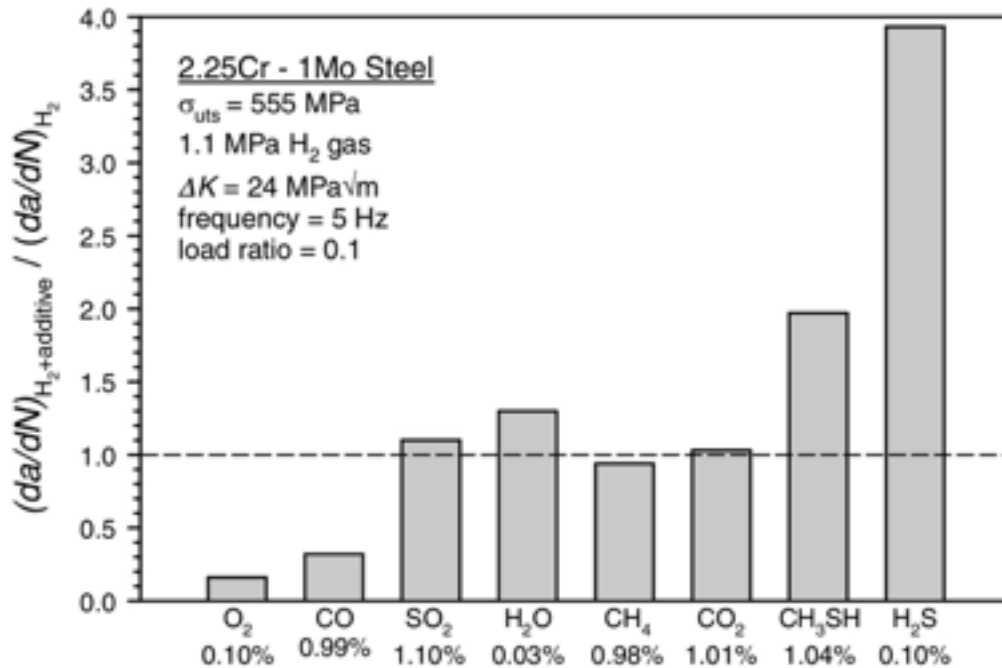


**Fig.15** Effect of gas additives on the fatigue crack growth rate ( $da/dN$ ) at constant stress intensity factor range ( $\Delta K$ ) for a low-alloy steel in hydrogen gas. [21]

Alternatively the concentration of common elements can be impactful as well. In **Figure.16** we observe the influence of the concentration of manganese, silicon, phosphorous, and sulphur in low-alloy steel revealing that an increase in the concentration of manganese and silicon are favourable to hydrogen embrittlement with sulphur and phosphorus having no effect.

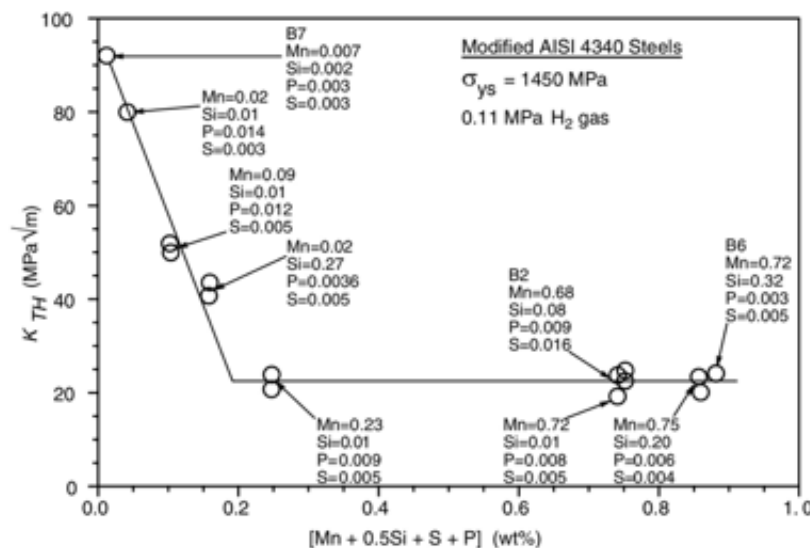


**Fig.16** Effects of steel composition on critical stress intensity factor for crack extension ( $K_{TH}$ ) in low-alloy steel. [23]

In addition while variation in concentration of sulphur and phosphorus had no effect on hydrogen embrittlement, the mere presence of the aforesaid elements is integral to the mechanism of such effect. Therefore a way to optimise against hydrogen embrittlement in low-alloy steels would be to minimise the bulk composition of the aforementioned elements thus diminishing the tendency for hydrogen-assisted fracture along the grain boundaries [22]. Unfortunately, carbon-steels do not exhibit fracture along the grain boundaries but rather cracks spread across the grains [23] ergo rendering impractical the lessening of elemental concentration.

Likewise, hydrogen barriers have been used to atone the effects of hydrogen corrosion (embrittlement) and deal with leakage, most of these are applied as external coatings; having low hydrogen solubility and slow hydrogen permeation, on metallic alloys by use of chemical or electrochemical processes.

**Table 6** Hydrogen permeability of various materials

Material	Permeability	Reference
Iron	$1.8 \times 10^{-10}$	[24]
Nickel	$1.2 \times 10^{-10}$	[24]
Ferritic steels	$3 \times 10^{-11}$	[24, 25]
Austenitic steels	$1.2 \times 10^{-11}$	[24]
Titanium carbide	$8 \times 10^{-15}$	[26, 27]
Tungsten	$4.3 \times 10^{-15}$	[24]
Aluminium oxide	$9 \times 10^{-17}$	[26, 27, 28]

## 5.2. Hydrogen storage

Several studies have been published on the storage of hydrogen by different techniques; these being:

- Compressed hydrogen gas
- Liquid hydrogen
- Solid storage of hydrogen

–More specifically, since the first two techniques can be applied by modifying hydrogen’s physical state in gaseous or liquid form, the third method can be divided into the following categories:

- Absorption in porous materials
- Absorbed on interstitial sites in a host metal
- Complex compounds

Of the various options, the two conventional and technically most advanced storage systems are based on the storage of pure hydrogen in pressurised or liquid form, which due to the purpose of our study in stationary systems are more relevant and thus will be focused on.

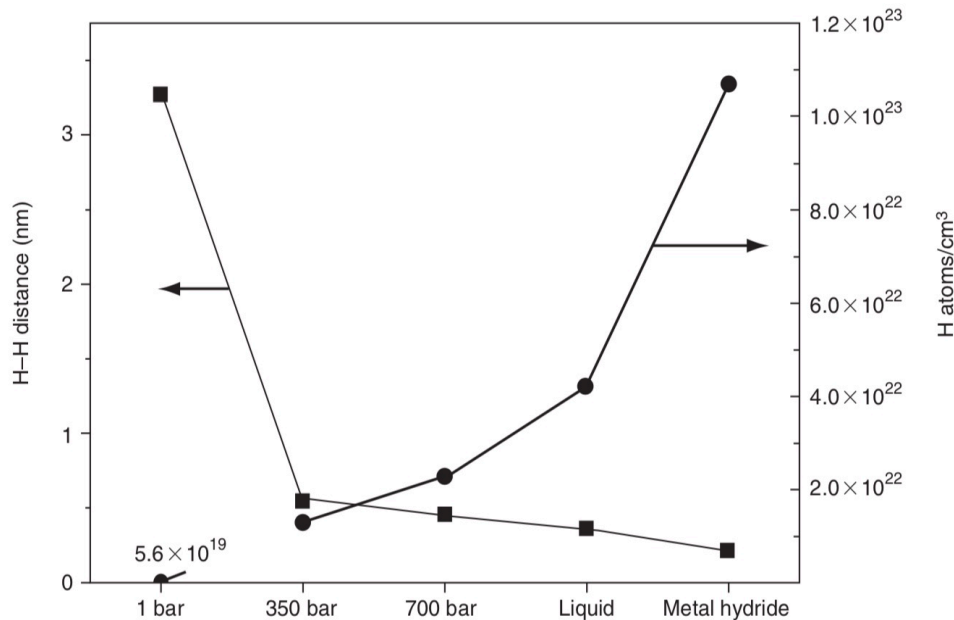


Fig. 17 Average hydrogen atom distance at various pressures [29]

As for the solid storage, this technology is more adequate in vehicles thus acting as a fuel cell capable of storing and releasing large amount of hydrogen under the right thermal conditions with the advantage of being lightweight and having a great hydrogen density.

The following sections shall outline some of the advantages, drawbacks and limitations of the various methods currently considered as storage options. As a fundamental comparison, **Figure 17** depicts the physical limits of different storage options as compressed gas, as a liquid, or chemically absorbed in a metal hydride, and **Figure 18** compares the volumetric and gravimetric density of some of the most common storage options, and clearly shows the theoretical potential of low volumetric densities for solid-state storage systems. However, there are further system requirements that need to be fulfilled.

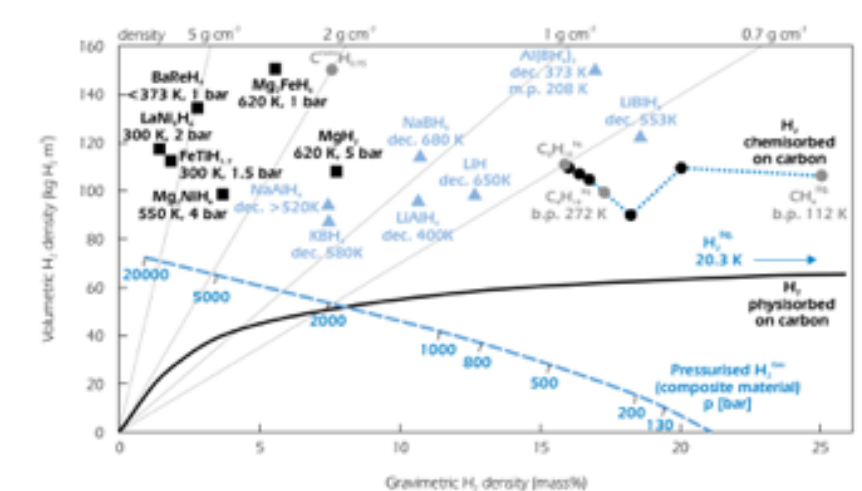
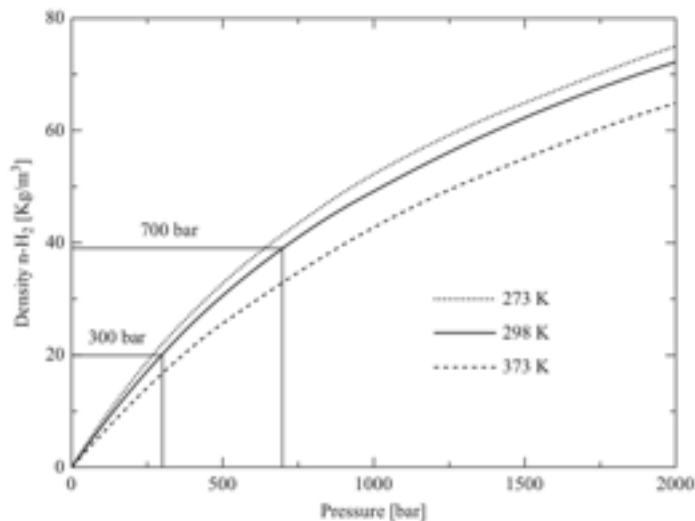


Fig. 18 Density for various H<sub>2</sub> storage systems, source Schlapbach and Züttel, Nature 2001

### 5.2.1. COMPRESSED HYDROGEN



**Fig. 19** Evolution of the volumetric density of normal H<sub>2</sub> as a function of pressure at three different temperatures [31]

For stationary applications as in our case, the volumetric storage density is the more important parameter, because weight does not necessarily play a role and does not reduce the overall efficiency of the stationary energy system.

**Figure 19** illustrates a plot of the volumetric density of normal hydrogen as a function of the pressure at three different temperatures. It can be easily observed that hydrogen density does not follow a linear function over the increase of pressure.

This said, we know that commonly high pressure gas steel cylinders, which are operated at a maximum pressure of about 200 bar are used as a base storage systems; these cylinders can employ different types of steel alloys depending on the tensile strength of the material, however the problem of diffusivity of hydrogen through steel is a major issue and therefore can limit the reliability of these systems.

Note as an example that austenitic steels have been employed for compressed natural gas storage applications, and given the proper permeation barrier can be adapted for a static hydrogen storage system.

Nonetheless lightweight composite tanks designed to endure higher pressures are also becoming more and more common. Cryogas, gaseous hydrogen cooled to near cryogenic temperatures, is another alternative that can be used to increase the volumetric energy density of gaseous hydrogen.

Composite tanks require no internal heat exchanger and may be usable for cryo-gas. Their main disadvantages are the large physical volume required, the fact that the ideal cylindrical shape makes it difficult to conform storage to available space, their high cost (500-600 USD/kg H<sub>2</sub>), and the energy penalties associated with compressing the gas to very high pressures. There are also

some safety issues that still have not been resolved, such as the problem of rapid loss of H<sub>2</sub> in an accident. The long-term effect of hydrogen on the materials under cyclic or cold conditions is also not fully understood. Hence, there is still need for more research and development, specifically in the following fields:

- Research on material embrittlement, using new ad hoc fracture mechanics techniques.
- Development of stronger and lower-cost construction materials, especially carbon fibres.
- Development of an efficient and clean (i.e. without oils) 1000-bar compressor.
- The consideration of hydride-type compressors utilising waste heat or solar energy.
- Development of techniques that recover the compression energy during vehicle operation.

Finally, a mechanical device that increases the pressure of the gas by reducing its volume achieves hydrogen compression. However, the low molar weight of hydrogen requires the use of a volumetric compressor rather than a centrifugal one in order to gain efficiency. Moreover, the energy used to compress gas does not only produce pressure differential, but also generates heat.

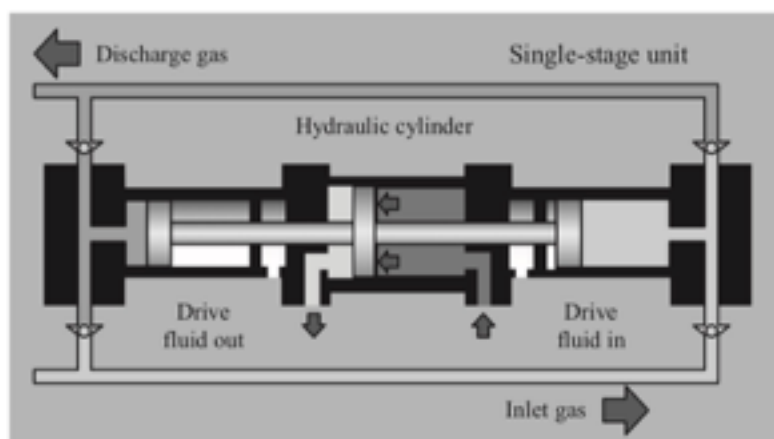


**Fig. 20.1** Schematic Diagram of a single-stage compression unit [32]

Furthermore, hydrogen compressors are categorised by mechanical and non-mechanical devices, with the mechanical one being a piston compressor in most cases; electro-hydraulically driven, As seen in **Figure 20.1**, representing a single-stage unit, the intensifier contains a hydraulic drive cylinder in the centre that is coupled by tie rods with two single-stage gas cylinders on each side. The fluid power drive provides the intensifier with high-pressure hydraulic oil. During operation, the gas fills the cylinder and then, the force of the hydraulic pressure acts on the hydraulic piston compressing the gas in the cylinder. Once compression is completed, the four-way valve redirects the hydraulic fluid, and the piston assembly moves in the opposite direction.

As it can be seen in **Figure 20.2**, In the case of a piston-metal diaphragm, the gas from the piston and related components is isolated by a set of metal diaphragms. The piston moves a column of hydraulic fluid, which in turn moves the diaphragm, set and displaces the gas to be compressed. As a consequence, the process is more isentropic than adiabatic, thus achieving a higher compression ratio.

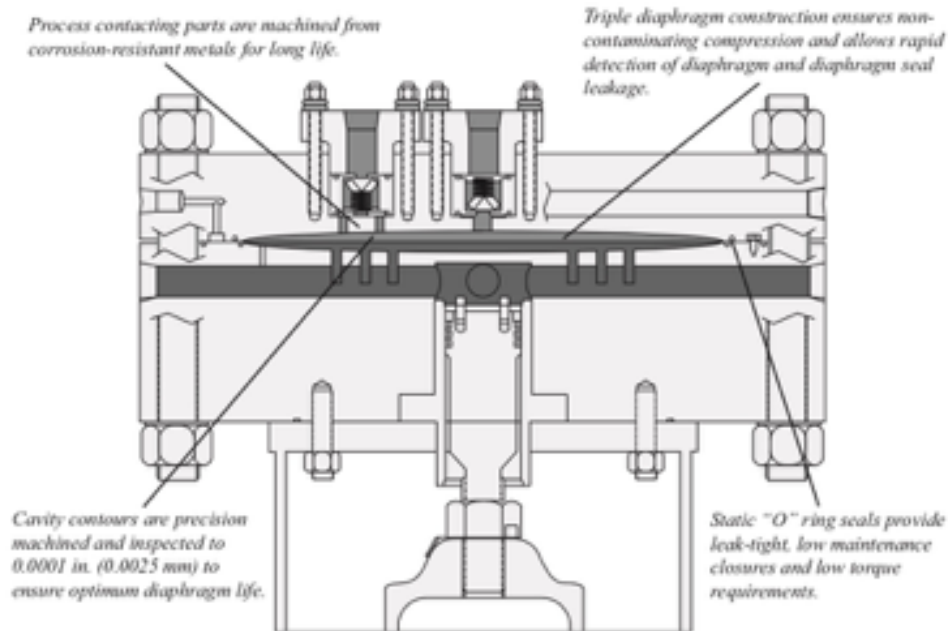


Fig. 20.2 Schematic Diagram of a metal diaphragm hydrogen compressor [32]

For both types of compression we find notable drawbacks, for instance in the case of single-stage compressors the containment of  $H_2$  becomes very difficult and requires specialised design adding to the risk of contamination from oils. As for the diaphragm compressor, its scale is relatively low therefore decreasing the possible output.

In addition to the mechanical compressors, we find in use non-mechanical devices, these types of compressors have several advantages, including lower capital, operating and maintenance costs and the absence of moving parts, which eliminates problems related to wear, noise and intensity of energy usage. Since hydrogen is completely separated from the hydraulic fluid, high purity hydrogen can be supplied.

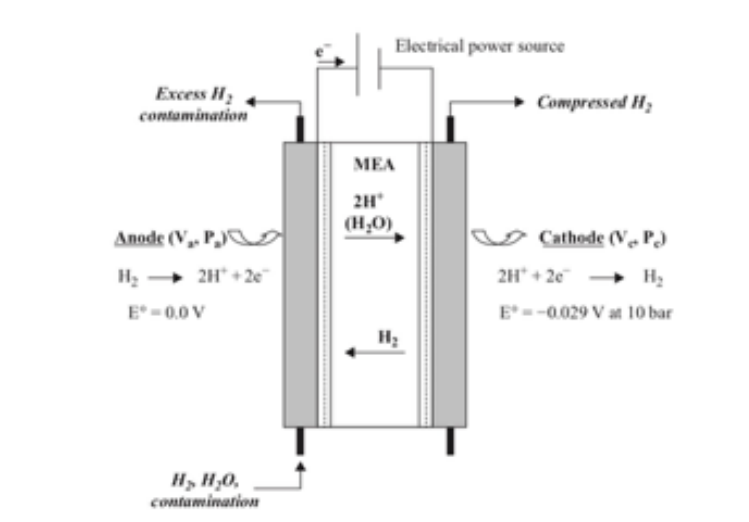


Fig. 21 Principle of the electrochemical hydrogen compressor [35]

In addition to the mechanical compressors, we find in use non-mechanical devices, these types of compressors have several advantages, including lower capital, operating and maintenance costs and the absence of moving parts, which eliminates problems related to wear, noise and intensity of energy usage. Since hydrogen is completely separated from the hydraulic fluid, high purity hydrogen can be supplied.

The electrochemical hydrogen compressor is used when small quantities of hydrogen have to be delivered in high pressure, because it is more efficient than the mechanical compressor in this regime [34]. The working principle is based on an electrochemical cell, composed of an anode, a membrane electrode assembly and a cathode, as it schematically represented in **Figure 21**.

When a potential difference is applied, the hydrogen at a pressure  $P_a$  is oxidised to  $H^+$  at the anode. These ions are transported through the membrane to the cathode, where they are reduced to hydrogen at a pressure  $P_c > P_a$ , if the cathode compartment is hermetically sealed. As long as hydrogen and power are supplied, this electrochemical reaction continues to compress hydrogen. A multi-stage electrochemical hydrogen compressor incorporates a series of membrane electrode assemblies. It should be noted that the process is selective for hydrogen, as the inert gas components cannot pass the membrane [33].

On the other hand, metal hydride hydrogen compressors are efficient and reliable thermally powered systems that use the properties of reversible metal hydride alloys to compress hydrogen without contamination. Either varying the type of the hydride or just modifying the formula of a reference alloy can obtain a wide range of different operation characteristics. The operating principle of the metal hydride hydrogen compressor is based on heat and mass transfer in the reaction bed during absorption and desorption process [33]. The advantages of metal hydride compression include simplicity in design and operation, absence of moving parts, compactness, safety and reliability, and on the most important, the possibility to consume waste industrial heat instead of electricity [34]. But more specifically, metal hydride compressors are simple and efficient pressure/temperature swing absorption-desorption systems. This allows not only controlling pressure by varying the temperature, but it also opens a new horizon for hydrogen separation and purification [34].

However, the drawbacks for these processes lie on their scalability notably for the metal hybrids, as they are a relatively new; we denote their first use in 1984.

### **5.2.2. LIQUID HYDROGEN**

The second method to store hydrogen is, to decrease its temperature at a constant pressure to obtain its liquid phase. Liquid hydrogen is stored in cryogenic tanks at around 20K at ambient pressure. The simplest hydrogen liquefaction cycle is the Linde cycle, based on the Joule-Thomson effect [36]. To minimise losses due to boiling this cycle gathers the surrounding air, which is dried and then liquefied by the energy released as the hydrogen increases in temperature. The cryogenically liquefied air at 82K flows through a water cooling jacket surrounding the inner tank and, thus, acts as a refrigerator causing a significant delay in the temperature increase of the hydrogen [37].

For the liquefaction of hydrogen, the isenthalpic process of pressure decrease (throttling) is used. A throttling process proceeds along a constant-enthalpy curve in the direction of decreasing pressure, which means that the process occurs from left to right on a T-s diagram (**Figure 22**).





If hydrogen is found in the region of liquid plus gas phase after the throttling (region of horizontal isobaric lines in the T–s diagram), part of it becomes liquid. The whole process is like this: hydrogen is first compressed and then cooled (under constant pressure) in a heat exchanger, before it passes through a throttle valve where it undergoes an isenthalpic Joule–Thomson expansion, producing some liquid. The cooled gas is then separated from the liquid and returned to the compressor to undergo the same process.

In other words, the pre-cooled gas is compressed at ambient pressure and then further cooled down in a heat exchanger. As part of the process, the hydrogen passes through ‘ortho–para’ conversion catalyst beds that convert most of the ‘ortho’ hydrogen into the ‘para’ form. These two types of hydrogen have different energy states. ‘Ortho’ hydrogen is less stable than ‘para’ at liquid hydrogen temperatures. It spontaneously changes to the ‘para’ form, releasing energy, which vaporises a portion of the liquid. By using a catalyst, such as platinum or hydrous ferric oxide, most of the hydrogen is converted into the more stable form during the liquefaction process.

In general the process consumes about 30% of the LHV of hydrogen [38] far off the theoretical 4MJ/kg predicted for the condensation of the gas at atmospheric pressure, this is due to the Carnot efficiency of the process being at around 7%. The overall efficiency is then further reduced by the so-called boil-off phenomenon. The stored cryogenic liquid starts to evaporate after a certain period of time, owing to unavoidable heat input into the storage vessel, leading to a loss of 2%–3% of evaporated hydrogen per day [39]. This cannot be prevented, even with a very effective vacuum insulation and heat-radiation shield in place. To prevent a high-pressure build-up, the overpressure must be released from the tank, via a catalytic converter.



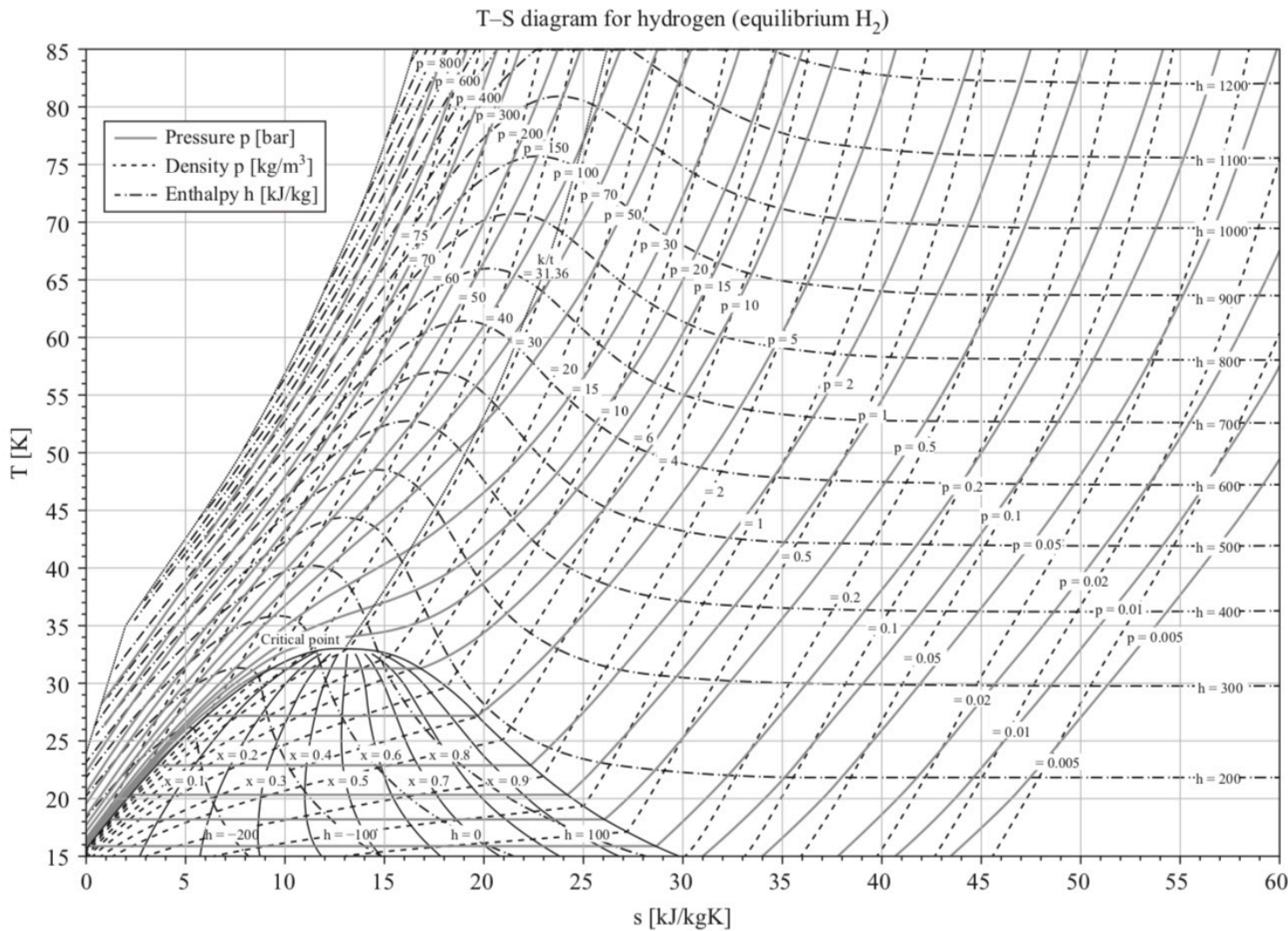


Fig. 22 T-s diagram for equilibrium hydrogen for temperatures from 15K to 85K [37]



### **5.2.3. CONCLUSION**

Compressed gas and liquid storage are the most commercially viable options today, but completely cost-effective storage systems have yet to be developed.

For instance, compressed hydrogen system's major disadvantage is that the already limited volumetric density does not increase proportionally with the operating pressure at high values. Furthermore, the fabrication costs of a 700 bar vessel are still too high, mostly because of the high costs of carbon fibres. A technological breakthrough is needed in this case.

For liquid hydrogen storage systems, the problems of cooling-down the so-called boil-off phenomenon have to be addressed. However, it is not possible to reduce the losses to zero and further insulation efforts or active cooling will increase the overall costs of the system.

As far as alternative storage systems are concerned, hybrid systems of a metal hydride and pressurised hydrogen seem to be most promising at the moment. It is a much safer option than the other methods, and systems of this kind can absorb or deliver large amounts of hydrogen even at temperatures below freezing point. However, the weight of such a system is still too high and has to be further reduced by using optimised storage materials.

Consequently this affects primarily the cost, in that any hydrogen solution will be more expensive than oil, owing to the inherent characteristics of hydrogen handling compared with liquid gasoline or diesel.

To conclude, the choice for the most economic option depends on transport volumes and transport distances. The most sound possibility could be to blend hydrogen with natural gas up to a certain extent and either separate the two at the delivery point, or use the mixture, e.g., in stationary combustion applications. To what extent this is feasible and reasonable (given that hydrogen is an expensive and valuable commodity), is still a matter of debate.

## 6. Current heat cycle

In the following section we shall discuss the different heat cycles developed for the adaptation of hydrogen combustion in gas turbines. Due to their complexity and that they only have been developed in the case of specific research, we shall keep a rather broad approach towards the description of the cycle, its components and its performance.

The most notable heat cycles, we have been able to identify are a variant of Brayton cycles, some use part of the hydrogen to cool down compressor stages in order to decrement the energy input needed, and optimise the pressure ratio.

Finally, the most prominent cycles we shall cite in this study are the Jericha cycle, the zero emission Graz cycle and the organic Rankine cycle.

### 6.1. Jericha cycle

Following their research on the Jericha cycle, (Sugista et. al, 1998) imply the importance of not using a conventional Brayton cycle, as not to generate tremendous amounts of NO<sub>x</sub>. Their paper [40] focuses on the comparison of a Rankine cycle and a top extracting cycle combined to a bottoming reheat cycle, which they describe as follows<sup>a</sup>.

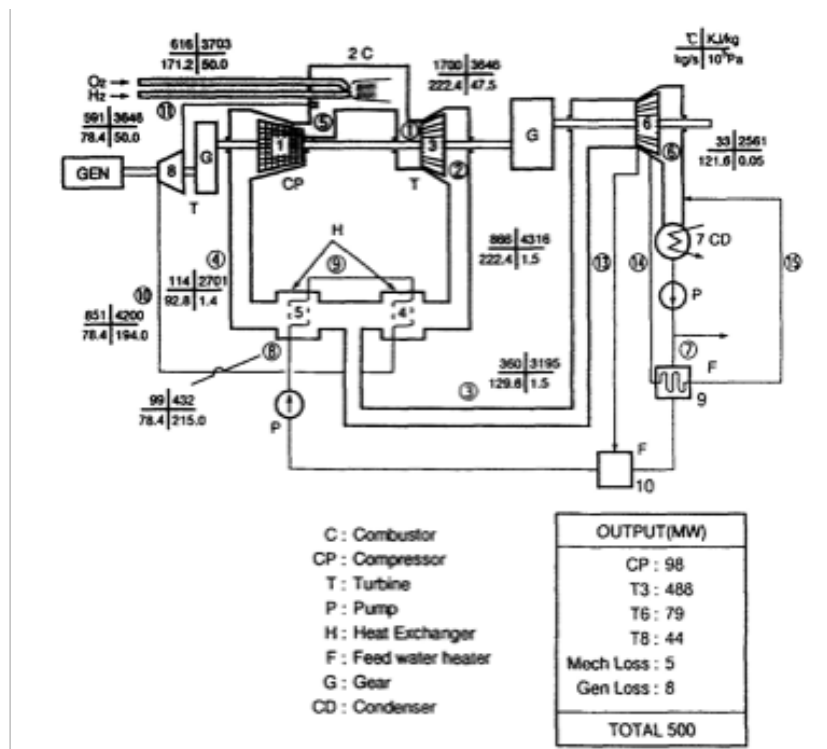


Fig. 23 Schematic of Jericha cycle [40]

<sup>a</sup> In order to keep this study concise we've only exposed the results of one of the cycles found in the paper

The topping cycle seen in **Figure 23** is a closed Brayton cycle containing a compressor (1), a turbine (3), heat exchanger (4,5) and combustor (2). Steam is extracted from between the heat exchanger and is expanded by the turbine and then pumped out. And the bottoming cycle is a closed reheat Rankine cycle formed by a heat exchanger (4,5,17), turbine (9,11,16), feed water heater (14,15) and a combustor (17).

After the steam is extracted between heat exchanger (4) and (5) it is expanded by turbine (6) and the hydrogen fuel and stoichiometric oxygen are combusted, the rest of the steam is pumped up, recuperated by heat exchanger (4) and (5), expanded by turbine (8) and mixed with the topping steam in the outlet of compressor (1).

In their research (Sugista et. al, 1998) operated under the assumptions of a constant 500MW total output, with maximum temperatures of 1973K and 1773K, topping pressure ratio of 35.7 and a 15% of bleed in order to cool the turbine.

Finally they accounted the following results for the cycle described above:

- A maximal thermal efficiency of 61.5% for a temperature of 1973K and 60.1% for 1773K
- Low maximum operating temperatures of the heat exchanger of 1139K
- And first stage turbine vane height of 77mm

In conclusion, their finding illustrates a thermal efficiency difference of 4.4% [40] between the combined cycle and the conventional Rankine cycle. Plus, the largest vane height of 77mm brings about an advantage in the manufacturing of complex cooling passages inside the vane, as well as the aerodynamic efficiency. They therefore conclude, that though these results are promising further research and iterations of the cycle are needed for a better-adapted cycle for hydrogen combustion.

## 6.2. Zero emission Graz-cycle

Our second researched cycle is the Zero emission Graz cycle, investigated by Wolfgang Sanz, Martin Braun, Herbert Jericha and Max F. Platzer in 2017 [41]. In their work the Graz Cycle, a zero-emission power plant based on the oxy–fuel technology, originally used with fossil fuel and pure oxygen combustion offering up to 65% of efficiency due to recompression of the working fluid, is adapted for hydrogen discharge.

Figure 24.1 and 24.2 illustrate respectively the temperature–entropy diagram of the cycle, and its flow scheme. This cycle basically consists of a high-temperature Brayton cycle and a low-temperature Rankine cycle, i.e. a combined cycle. The Brayton part consists of the combustion chamber (CC), the high-temperature turbine (HTT) and the compressors (C1/C2). The Rankine steam loop consists of the heat recovery steam generator (HRSG), high-pressure steam turbine (HPT), low-pressure steam turbine (LPT), condenser, condensate pump; deaerator<sup>a</sup> and finally the feed pump supplying high-pressure water to the HRSG.

---

<sup>a</sup> A device that is widely used for the removal of oxygen and other dissolved gases from the feed-water to steam-generating boilers.

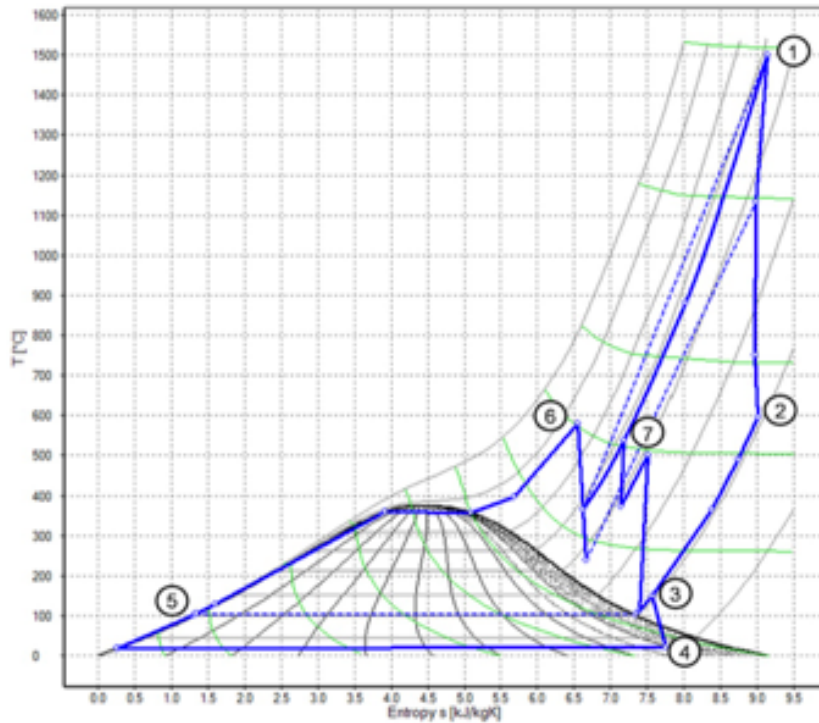


Fig. 24.1 Temperature–entropy diagram of the Graz cycle for Hydrogen/ oxygen combustion [41]

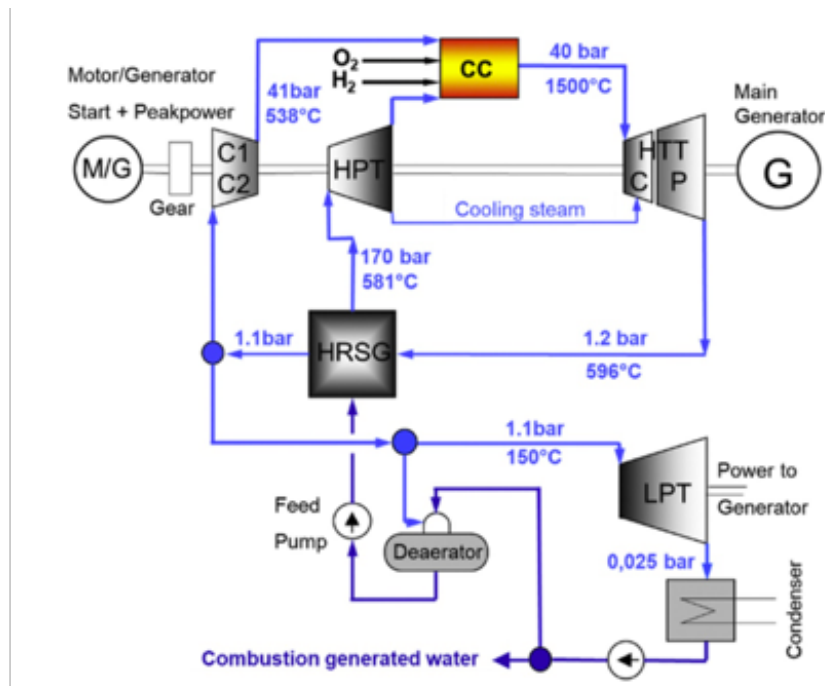


Fig. 24.2 Principle flow scheme of the Graz Cycle for hydrogen/oxygen combustion [41]





Herbet Jericha ET. Al [41] report the cycle as functioning in the following way: *“Pure hydrogen together with a stoichiometric mass flow of pure oxygen is fed to the combustion chamber, which is operated at a pressure of 40bar. The high purity can be obtained by producing hydrogen and oxygen with electrolyser supplied by electricity from renewable energy.*

*In order to obtain reasonable combustion temperatures steam stemming from the steam compressor as well as from the high pressure turbine are supplied to form the environment for the combustion process and to cool the burners and the liner. Previous experimentation has shown that an oxygen surplus of at least 3% is necessary for nearly complete fuel conversion. In this case a small amount of oxygen would accumulate in the cycle, which is extracted in the deaerator.*

*Steam leaves the combustion chamber at a mean temperature of 1773K (point 1 in the T-s diagram of **Figure 24.1**). The fluid is expanded to a pressure of 1.2 bar and 869K in the high temperature turbine (point 2). Cooling is performed with steam coming from the high-pressure turbine at 41.7 bar/ 637K for the high-pressure section and at 15 bar 513K for the low-pressure section. Cooling is assumed to an expansion temperature of 1023K, leading to a cooling mass flow of 21.8% of the HTT inlet mass flow.*

*After the HRSG (point 3) only 52% of the steam mass flow at 423K is further expanded in the LPT, a typical condensing turbine. For cooling water temperature of 283 K the LPT exit and thus condenser pressure is 0.025bar, which corresponds to a condenser temperature of 304.1K. The steam quality at the LPT exit is 89% (point 4).*

*After the condensate pump excess water stemming from the combustion process is separated, before the water is degassed in the deaerator (point 5). It is then further compressed in the feed pump and delivered to the HRSG. After preheating, evaporation and superheating steam of 170 bar and 854K is fed to the HPT (point 6). After the expansion it is used to cool the burners and the HTT stages as described above.*

*Nearly half of the cycle steam - the return flow after the HRSG - is compressed using the main cycle compressors C1 and C2 with intercooler and is fed to the combustion chamber with a temperature of 811K (point 7). Inter-cooling is performed to keep the compressor exit temperature at reasonable levels; its heat partially superheats the high-pressure steam.”*

Finally, the Graz Cycle in this work is based on the internal combustion of hydrogen with pure oxygen, so that a working fluid of nearly pure steam is obtained. The thermodynamic layout at the design point assumes state-of-the-art gas turbine technology with a peak cycle condition of 1773K and 40bar. At design point the net cycle efficiency is 68.5%, which is remarkably higher than the efficiency of modern power plants.

The high efficiency is obtained amongst others by the recompression of about half of the cycle fluid thus reducing the heat extraction out of the process. But this leads to a close interaction of the components so that the feasibility of part-load operation is studied.

These high efficiencies at part and full load make the Graz Cycle a promising candidate for the reconversion of hydrogen in a future energy system based on hydrogen as storage medium.

### 6.3. Regenerative reheat Brayton cycle

For the third cycle, we shall analyse the study made by (Y. S. H. Najjar et al 1990) [42], which compared a regenerative reheat Brayton cycle fuelled and cooled by hydrogen to that of a cooled by compressed air and fuelled by diesel.

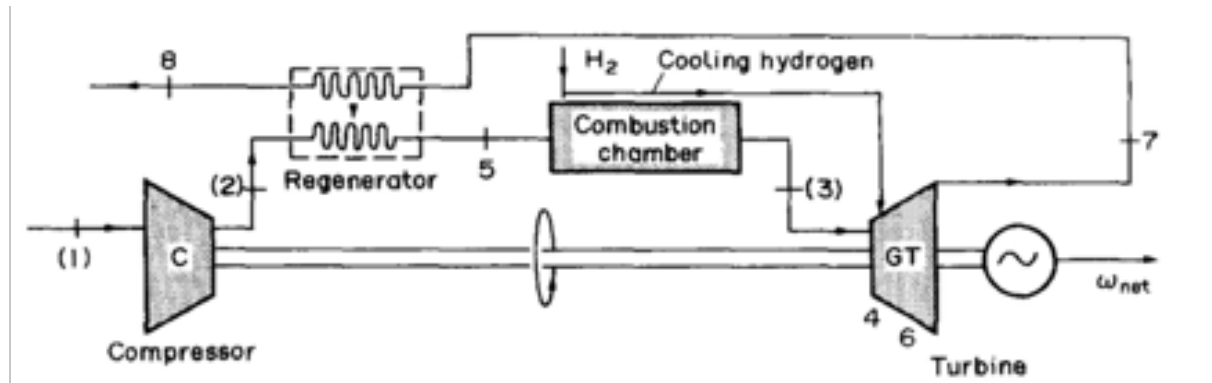


Fig. 25.1 Cycle configuration of a heat-exchange gas turbine engine using hydrogen as fuel and for cooling [42]

The layout of the configuration of the cycle according to **Figure 25.1** was that in the first stage air is drawn in through compressor (1) then directed to a heat exchanger (2) to undergo a first heating through exchange with exhaust gases (5) coming from Turbine (7), following previous step, the preheated compressed air and the hydrogen are discharged within the combustion chamber (3) with a little stream of hydrogen redirected for turbine fan cooling in the gas turbine (6) and then expanded for energy generation (4). Note that though it's not apparent in the diagram the expansion is in two phases given the regenerative aspect of the cycle.

According to Figure 24.2 the Brayton reheat cycle considered in this study is far from ideal, suffering inlet air pressures losses in the heat exchanger ( $\Delta P_{h_1}$ ) and the combustion chamber ( $\Delta P_{h_2}$ ), as well as exhaust gas pressure losses in the heat exchanger after expansion in turbine ( $\Delta P_{h_3}$ ). Moreover the authors of this study have taken into considerations the design point the following assumptions; a maximum combustion temperature of 1300K, a compression ratio of 7 and an effectiveness in the recuperator of 0.8.

Finally the results reported in the paper were positive, stating that improvement of performance is more remarkable when hydrogen fuel is used, with 50% improvement in power and 9% in efficiency. Moreover the excess hydrogen for turbine blade cooling seems to improve the performance in specific fuel consumption, power and overall thermal efficiency denoting lastly that the maximum combustion temperature had a superior relative effect to that of compression ratio.

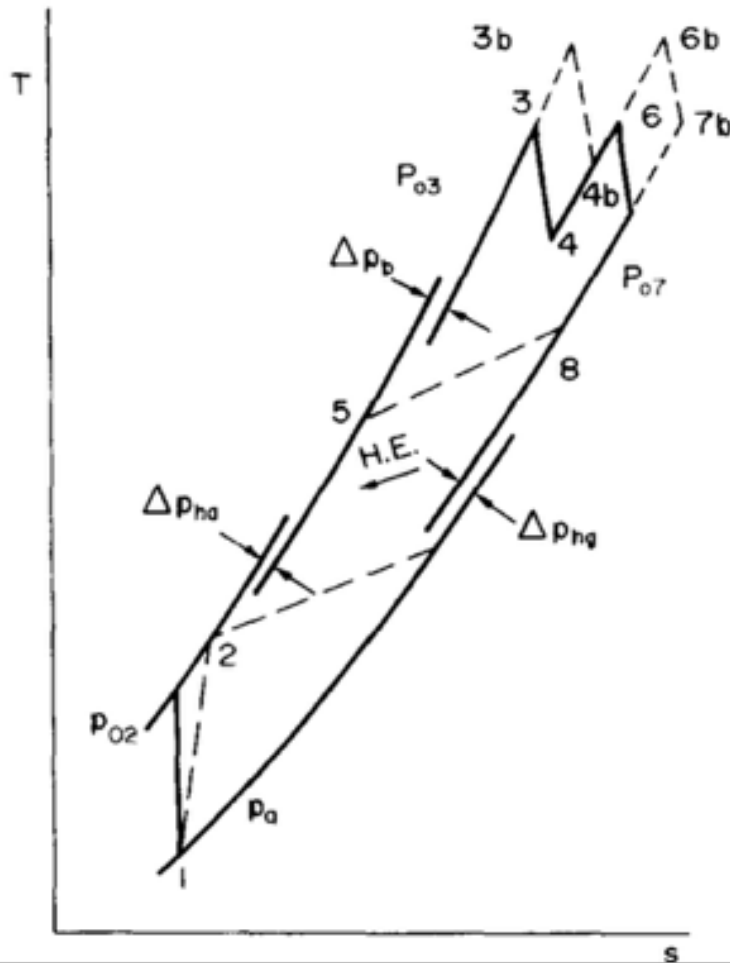


Fig. 25.2 T-S diagram of the cycle [42]

## 6.4. Conclusion

In conclusion as observed in all reported papers, we can recognise a clear advantage to the use of hydrogen in stationary gas turbines as opposed to conventional fuels. Likewise the coincidence of the reports cites a betterment of efficiency, though certain drawbacks can be alluded; High  $\text{NO}_x$  release and material deterioration, due to the high temperatures of combustion of hydrogen which implies the use of diluents like inert gases or exhaust gas recirculation [43], moreover we can conclude that further research is needed in the design of combustion and injection system for the adaptation of hydrogen as primary fuel, and that our preliminary review of the published papers is rather promising.



## 7. Thermodynamic analysis

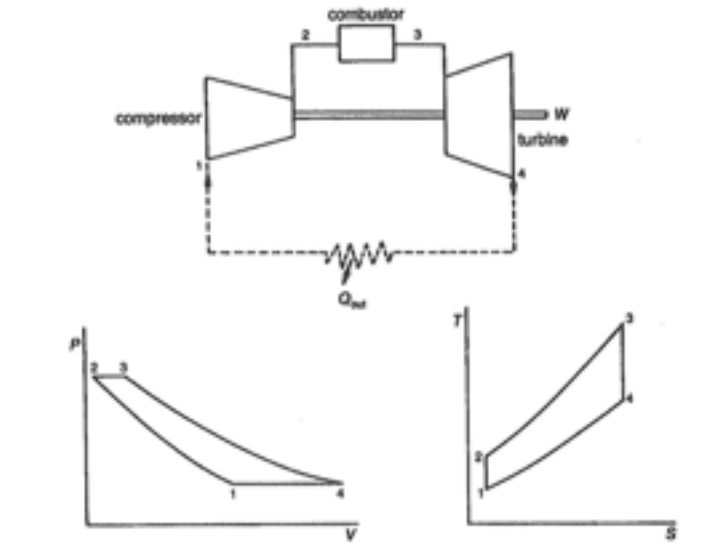


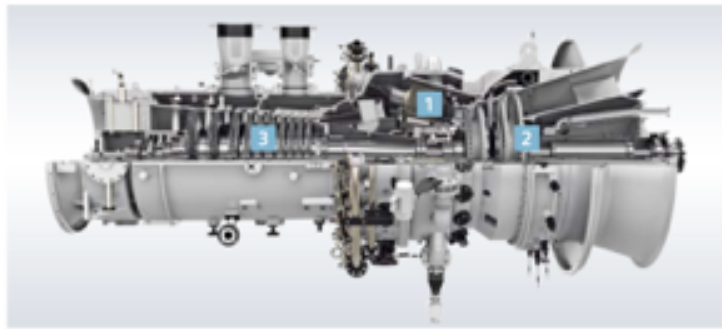
Fig. 26 The air-standard Brayton cycle

In this chapter we intent to retrieve some of the results presented prior, and analyse them more thoroughly through the configuration of a model.

The first part of this chapter is the mathematical discussion, where we lay out the primary bound conditions and assumptions of our model and present the mathematical formulas we used for the realisation of the thermodynamic analysis. Later on we will present all the results in relation to our model and discuss the implications that such results endue.

For this chapter we chose to base our study on the Siemens SGT-600 gas turbine illustrated in Figure 26, given its large use in the industry as well as its fuel flexibility (Natural gas and 20% – 90%  $H_2$ ). Table 6 shows the relevant characteristics of the turbo-machine [43–44].

Furthermore, we based our simulation on a simple Brayton cycle, which we consider quasi ideal deprived of reheat or regeneration (**Figure 26**) in order to simplify the calculations. Moreover, We've taken into account pressure losses occurring in the combustion chamber, without considering bleed for turbine blade cooling. Finally the initial condition for air intake were taken at atmospheric pressure, 300K of temperature and a 60% relative humidity; the introduction of wet air is important in order to lower the combustion temperatures and therefore the emissions of Nitric oxides.



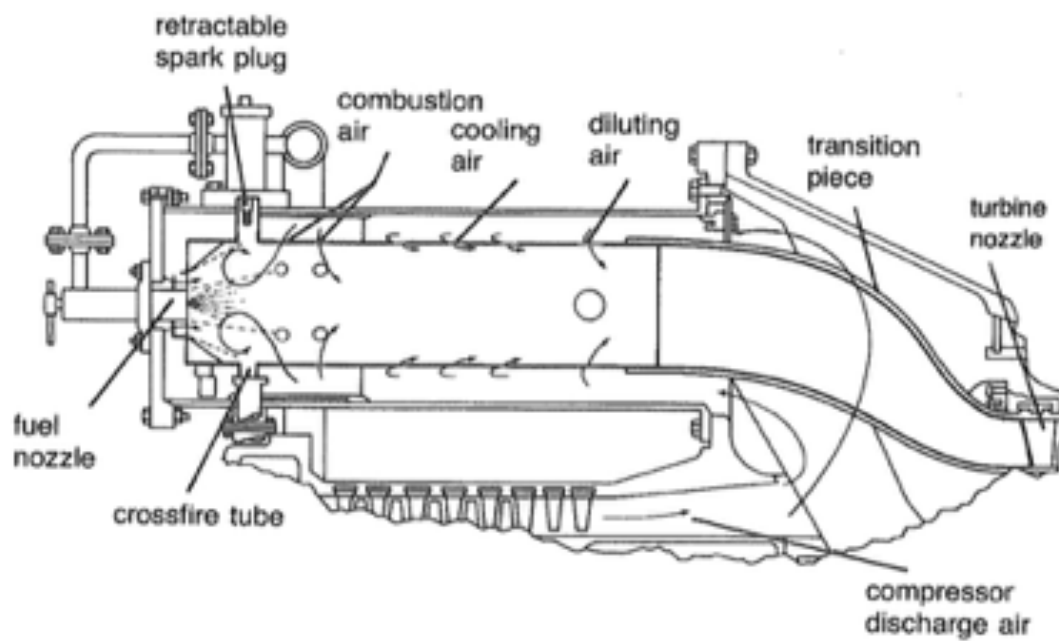
- 1 DLE combustion system**  
Well-proven and reliable dry low emissions (DLE) combustor with low emissions.
- 2 Power turbine**  
Two-stage uncooled free power turbine offers nominal shaft speed up to 7,700 rpm. For mechanical drive, it may operate at 50 to 105 percent of the nominal speed. The blades use interlocking shrouds for extra robustness.
- 3 Compressor**  
10-stage axial flow transonic compressor with three balancing planes accessible from the outside.

Fig. 27 Descriptive diagram of the SGT-600 gas turbine [43—44]

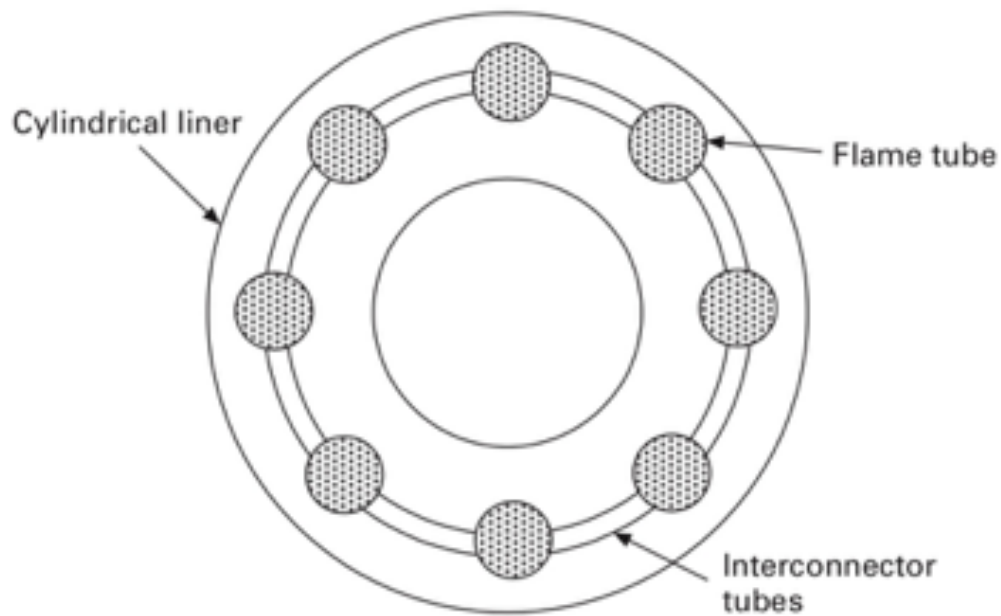
Table 7 Characteristics of the SGT-600 gas turbine [43—44]

Power generation	24,77 MW
Frequency	50/60Hz
Gas flow	80.4 Kg/s
Turbine Speed	7,700 rpm
Pressure Ratio	14:1
Injection pressure	24.5 bar
Compressor	10-Stage axial flow compressor
Combustion	DLE Burners in a Turbo-annular combustor

On the other hand **Table 7** provides us with the primary conditions of the selected gas turbine, describing gas intake flow of 80.4 kg/s, a pressure ratio of 14 and a pressure of injection of 24.5 bars. We've also chosen to ignore the pressure losses occurring in the diffuser for lack of knowledge of its geometry. Figure 28.1 explains the concept of a tubo-annular combustion where we can appreciate the trajectories of compressed intake air. The airflow enters a primary duct where it is directed towards the fuel nozzle to get a lean fuel/air mixture for a primary combustion. Part of the intake air is directed to a secondary combustion zone in order to cool the temperature and permeate the creation of nitric oxides and serve as cooling film for the combustion chamber casing. The advantage of a tubo-annular design is an even flame combustion due to the various nozzles surrounding the combustion duct (see **Figure 28.2**), this gives light to an even combustion flow hence allowing for an air/fuel requirement as low as 8—10% of the total needed (lean mixture) [45].

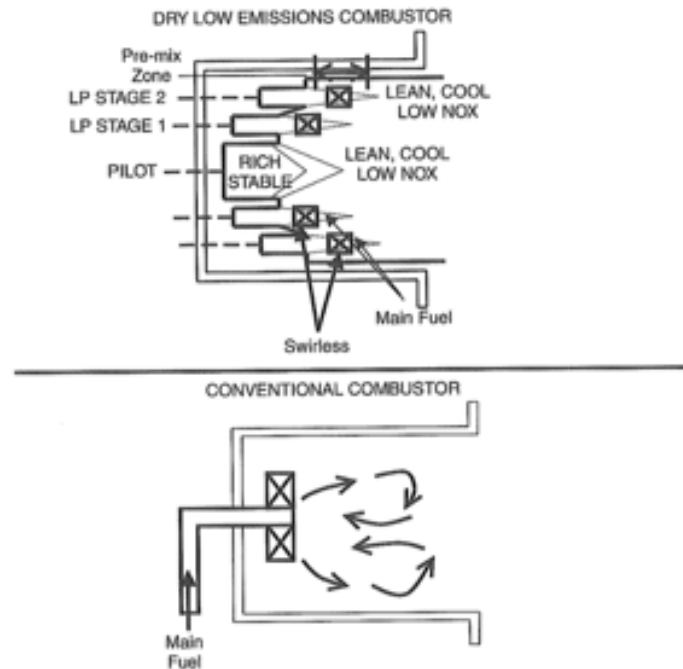


**Fig. 28.1** Tuboannular combustor for a heavy-duty gas turbine. (Courtesy of General Electric Company.) [45]

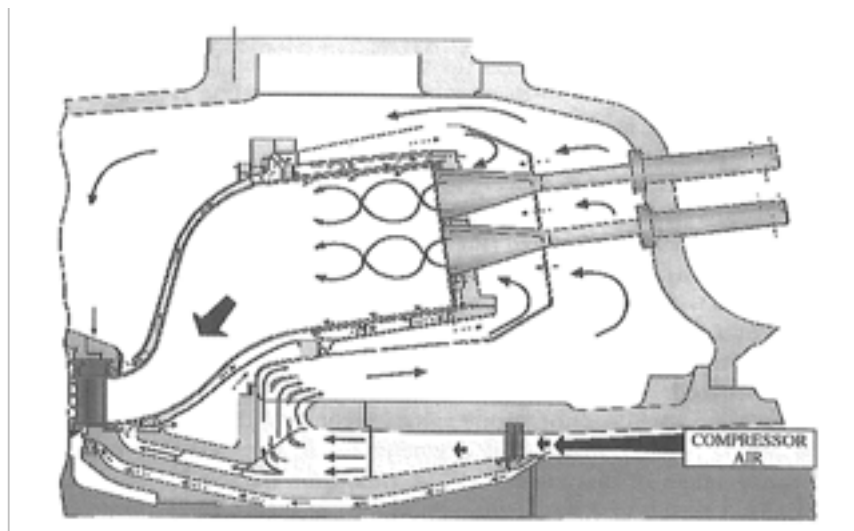


**Fig. 28.2** Cross-section of a tuboannular combustor

We also know that the combustion system operating in the turbine we've chosen, is a Dry low emission system, which takes the approach of burning about at least 75% of the gas at cool fuel lean condition to avoid any production of  $\text{NO}_x$ .



**Fig. 29.1** Schematic comparison of a typical DLE Combustor and a conventional combustor combustor [45]



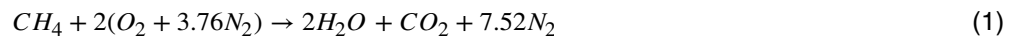
**Fig. 29.2** Schematics of a DLE Combustor (Courtesy of ALSTOM) [45]

Figure 29.1 and 29.2 illustrate the process of creation of swirls created by premixing up 60% of the fuel mass in the injector and re-infusing the rest of the gas in a secondary burn.

## 7.1. Mathematical model

### 7.1.1. ADIABATIC FLAME TEMPERATURE

Now that we know all the primary bound conditions for our model we will consider the ideal lean fuel/air reaction presented below, omitting all degradation reaction and energy equilibrium potential calculations due to the lack of resources and the complexities of the calculations that would ensue. Though it would be interesting to investigate the primary combustion properties for each fuel through an analysis of the free energy of Gibbs and thermochemical potential of each reaction we will just refer to those calculation as feasible through the Chemkin tool developed by NASA and mention some of that information later on in Appendix D.



Given the reaction process known and simplified the first step of our analysis is to investigate the adiabatic flame temperature for both fuel for the prior set condition and different fuel/air mixture. This in turn will allow us to estimate with a certain degree of confidence the maximum temperature reached within the primary zone of combustion.

The temperature rise depends on the amount of excess air used or the air-fuel ratio. The flame temperature has the highest value for using pure oxygen gas and it decreases by using air. So, the exact stoichiometric air is to be supplied for better result. With too large amount of excess air the flame temperature will be reduced. When the heat lose to the environment or diluted by the inert gases and there is an incomplete combustion. So, the temperature of the products will be less. The flame temperature is determined from the energy balance of the reaction at equilibrium. There are two type of adiabatic flame temperature: constant pressure adiabatic flame temperature and constant volume adiabatic flame temperature. In our case given that the acquisition of heat is isobaric we will consider the calculation of adiabatic flame temperature at constant pressure given by the following formulas:

We approximate the  $c_p$  of each of the gases using the curvefit coefficients encountered in appendix A:

$$\frac{c_p}{R} = a_1 + a_2T + a_3T^2 + a_4T^3 + a_5T^4 \quad (3)$$

And

$$\Sigma H_{products}(T_i, p) = \Sigma n_i(\Delta H_{fi}^0 + \bar{c}_p(T_f - T_{ref})) \quad (4)$$

From (1) and (2) we can derive the enthalpies of formation and reaction of the reactants and products, knowing that for gases like Hydrogen and Nitrogen the enthalpies of formation are null, and we solve for  $T_i(4)$  in an iterative form.

## 7.1.2. COMPRESSOR

Given that we idealised our Brayton cycle for our turbine, we can then assume an isentropic flow in the compressor, which therefore can be interpreted by the following:

The compressor discharge temperature can be calculated by:

$$T_2 = T_1 \left( \frac{P_2}{P_1} \right)^{\frac{\gamma-1}{\gamma}} \quad (1)$$

Furthermore we can estimate the adiabatic efficiency of the compressor through the following formula [42]:

$$\eta_{ad_c} = \frac{\left( \frac{P_2}{P_1} \right)^{\frac{\gamma-1}{\gamma}} - 1}{\frac{T_2}{T_1} - 1} \quad (2)$$

Equally for a better estimation, it would be advised to consider the dimensionless coefficient of specific speed and specific diameter characterising the compressor, and then directly attribute the values we need from the compressor map if available or provided by the manufacturer. In this section we shall provide in example.

We start by calculating the specific diameter and speed of the compressor through these formulas:

$$D_s = \frac{DH^{0.25}}{\sqrt{Q}} \quad (3)$$

$$N_s = \frac{N}{\sqrt{\gamma RT_1}} \quad (4)$$

$$Q_s = \frac{\dot{m}_{a1} \sqrt{\frac{RT_1}{\gamma}}}{P_1} \quad (5)$$

Here the values of N, Q and H represent the speed of the compressor shaft which in the case of a single shaft turbine is equal to the turbine speed, the volume rate or  $Q = \frac{\dot{m}_a}{\rho_a}$ , and finally the adiabatic head that can be calculated through the pressure rise and the change in density per stage.

**Figure 30.1** and **30.2** later shows us a typical compressor map, from which knowing the values of the specific speed and specific diameter one can extrapolate the compressor efficiency, which generally revolves around a normal value of 85%.

Finally we proceed to calculate the power absorbed by the compressor through the following formula:

$$W_c = \dot{m}_a \bar{c}_p (T_2 - T_1)$$

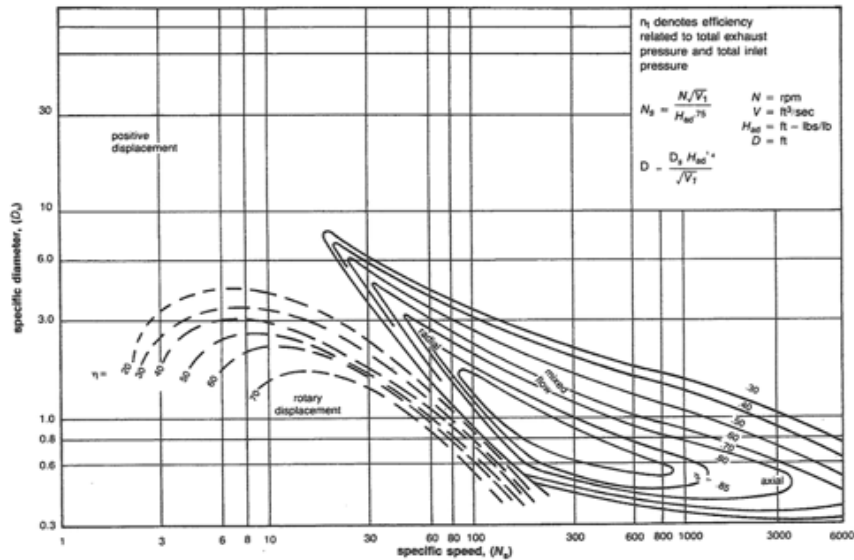


Fig. 30.1 Typical compressor map [45]

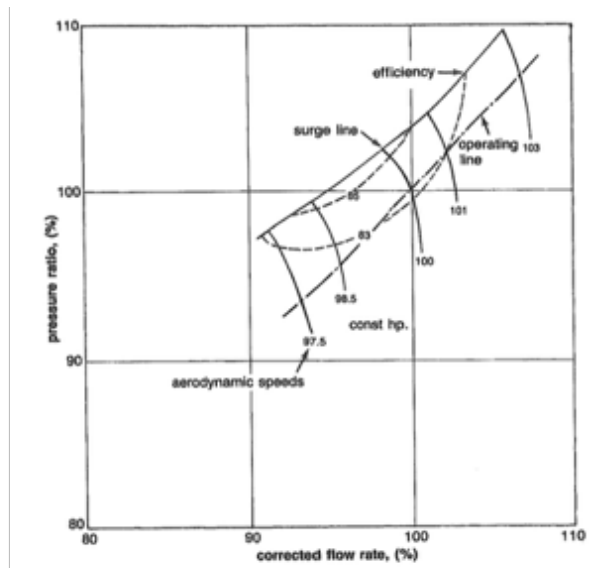


Fig. 30.2 Typical flow map for an axial flow compressor [45]

### 7.1.3. COMBUSTION CHAMBER

In the combustion chamber the overall pressure loss can be viewed as the sum of the frictional loss of pressure, loss of pressure due to the change of density endured by the gas through change of temperature and loss of pressure owed to the introduction of turbulences in the combustion flow. The current knowledge of friction in ordinary turbulent pipe flow at high Reynolds number suggest that the divergent of a non-dimensional expression of the dynamic head is relatively low across the range of Reynolds number under which combustion systems operate. This being said we could express the pressure los as a factor in the following formula:

$$PLF = K_1 + K_2 \left( \frac{T_3}{T_2} - 1 \right) \quad (1)$$

Where  $K_1$  and  $K_2$  are constants for a given combustor,  $T_3$  is the combustor exit temperature and  $T_3/T_2$  is the ratio of the stagnation temperature rise across the combustor.

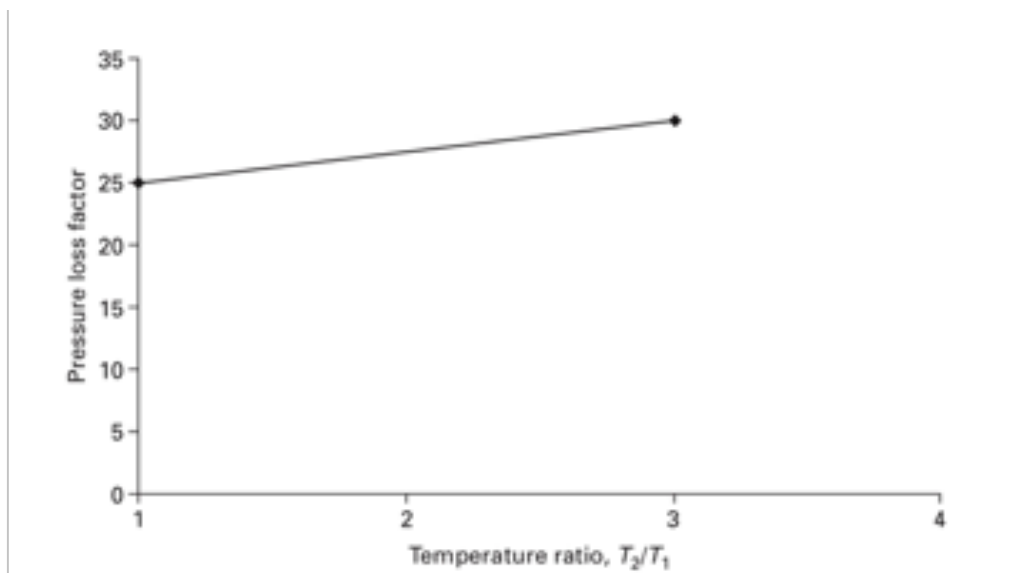


Fig. 31 Variation of the pressure loss factor with temperature ratio [46]

From **Figure 31** and the ratio of  $T_3/T_2$  we can get the pressure loss factor correspondent to our combustion chamber and extrapolator through the use of (2) in order to get the actual loss in pressure occurring in the combustion chamber.

$$\frac{\Delta P_{23}}{P_2} = PLF \left( \frac{\dot{m}_a \sqrt{\frac{RT_2}{\gamma}}}{P_2} \right)^2 \times \gamma \quad (2)$$



From (2) we can account for the inlet pressure of the turbine  $P_3$ , which allows us to estimate the average combustion temperature through compatibility of flow between the turbine and the compressor. Therefore through the equations of non-dimensional flow we can arrive to the expression (3) [47]:

$$\frac{\dot{m}_a \sqrt{T_3}}{P_3} = \frac{\dot{m}_a \sqrt{T_1}}{P_3} \cdot \sqrt{\frac{T_3}{T_1}} \quad (3)$$

Another estimate of the exit temperature of the combustion chamber, would be through the use of the adiabatic flame temperature and the consideration of the air/fuel ratios as seen in the beginning of this section that we've taken at a 8%—10%.

$$\phi = \frac{FAR}{FAR_s} = \frac{m}{m_s} \quad (4)$$

FAR corresponding to fuel air ratio and  $FAR_s$  corresponding to the stoichiometric fuel air ratio.

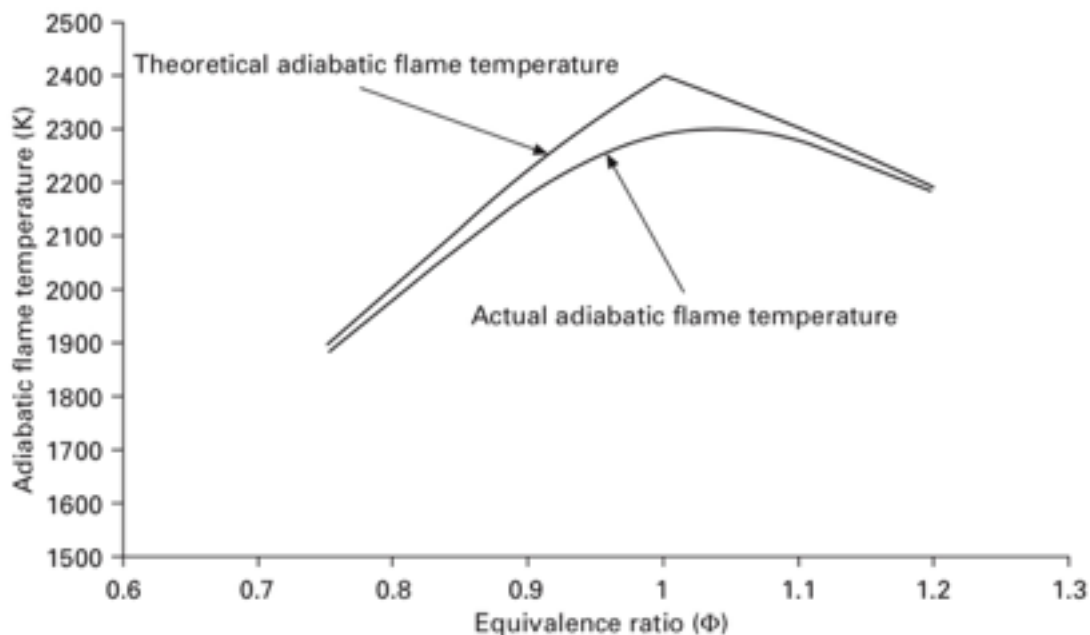


**Fig. 32** Effect of equivalence ratio on adiabatic flame temperature for  $CH_4$  [46]

In Figure 32 we appreciate the effects of the equivalence ratio on the adiabatic flame temperature, and we can observe as well how the actual adiabatic flame temperature approximates the theoretical one.

This being said we could assume with a fair degree of confidence, that the theoretical adiabatic flame temperature is the maximum temperature available in the combustion chamber. Using this assumption and the pattern factor formula for the dilution zone used to cool down the exhaust gases we arrive at (5):



$$PF = \frac{T_{max} - T_3}{T_3 - T_2} \quad (5)$$

Where PF is the pattern factor highlighting the overall temperature distribution,  $T_{max}$  is the maximum or peak temperature  $T_3$  is the average exit temperature, and  $T_2$  is the combustion inlet temperature and usually corresponds to the compressor discharge temperature. Admitting a satisfactory value for PF of 0.2 we can then estimate the average exit temperature.

Now that the value of  $T_3$  is estimated we can follow by estimating the heat input and the fuel flow needed to raise the temperature.

Since the work done in the combustion system is null the heat input is:

$$Q_{23} = c_p(T_3 - T_2) \quad (6)$$

Presumably the combustion efficiency is very high, ranging from 98.5% to 99.5%; the losses in efficiency can be accounted for through the apparition of carbon monoxides in the combustion.

For a given equivalence ratio and airflow rate, the fuel flow can be determined by:

$$\dot{m}_f = \phi \times \dot{m}_a \times FAR_s \quad (7)$$

Finally, the mass flow leaving the combustion chamber will be defined as:

$$\dot{m}_t = \dot{m}_f + \dot{m}_a \quad (8)$$

On a tangent, the other interesting consideration to make would be the estimation of the Nitric oxide, though the chemical reactions governing the formation of these pollutants are quite complex. Three predominant factors are; combustion temperature, pressure and humidity. There are other parameters that also affect the formation of these pollutants, such as fuel–air ratio, fuel and air mixing, combustor geometry and residence times. Various correlations have been proposed and validated and serve as a very useful means of predicting emissions from gas turbines.

On their paper Bakken and Skogly [48] proposed a correlation to predict  $NO_x$  for natural gas fired gas turbine that we can also assimilate for hydrogen discharge.

$$NO_x = 62P^{0.5}f^{1.4}e^{-\frac{635}{T_c}} \quad (9)$$

Where P is the combustion pressure in (Pa),  $T_c$  is the combustion temperature (K),  $f$  is the fuel–air ratio and  $NO_x$  is given in ppm at 15%  $O_2$  dry.

According to Bakken et. Al , the parameters should be corrected to standard condition (15°C and 1.013 Bar). This implies that  $NO_x$  is dependent on  $T_c / T_1$  and  $P / P_1$ , where  $T_1$  and  $P_1$  are the compressor inlet temperature and pressure respectively, rather than the combustion temperature,  $T_c$  and pressure, P.

### 7.1.4. TURBINE

First let us assume that our turbine works under normal operating speed range and that therefore its efficiency is  $\eta_t \approx 95\%$ , this is due to the fact that unlike the compressor, the turbine efficiency does not vary very much with pressure ratio and non-dimensional speed. Though, there is some decrease in the efficiency with pressure ratio at lower speeds but our prior assumption allows us to take the said value of efficiency to be true.

Moreover, we know that the exhaust pressure of our turbine  $P_4$  is atmospheric from our primary bound conditions. We can hence calculate the turbine exit temperature through (1) given that expansion work is taken as isentropic:

$$T_4 = T_3 \left( \frac{P_4}{P_3} \right)^{\frac{\gamma-1}{\gamma}} \quad (1)$$

Furthermore, we can effectively compute the work done by our turbine in (2)

$$W_t = \dot{m}_t \bar{c}_p (T_3 - T_4) \quad (2)$$

The net work done by the cycle (specific work) is the difference between the expansion and compression work:

$$W_{net} = \left( \bar{c}_p (T_3 - T_4) - \bar{c}_p (T_2 - T_1) \right) \cdot \dot{m}_t \quad (3)$$

And the cycle thermal efficiency is defined as the ratio of the net work done and the heat input. Hence the thermal efficiency is given by:

$$\eta_{th} = 1 - \frac{T_4 - T_1}{T_3 - T_2} \quad (4)$$

We can add on the adiabatic thermal efficiency as this equation for better view on the effect of the fuel:

$$\eta_{adt} = \frac{W_{net}}{\dot{m}_f LHV} \quad (5)$$

Finally, we can add in by calculating the specific fuel consumption through (6) :

$$SFC = \frac{3600}{\eta_{th} LHV} \quad (6)$$

Which is proportional to the lower heating value and the thermal efficiency calculated in (4).

## 7.2. Results and discussion

Table 8 is a list of the conditions we've taken into account for our calculations.

**Table 8** Primary conditions

Ambient Pressure (kPa)	100
Ambient temperature (K)	298
Inlet gas flow, $\dot{m}_a$ (kg/s)	80
Compressor output pressure, $P_2$ (kPa)	1400
Low heating value $H_2$ (MJ/kg)	119
Low heating value $CH_4$ (MJ/kg)	50
Stoichiometric fuel/air ratio $H_2$ , $f$	0.03
Stoichiometric fuel/air ratio $CH_4$ , $f$	0.06

In table 9 we will review the different results of adiabatic flame temperature for both gases.

**Table 9** Adiabatic flame temperatures

<i>Equivalence ratio, <math>\phi</math></i>	<i>Adiabatic flame temperature <math>H_2</math> (K)</i>	<i>Adiabatic flame temperature <math>CH_4</math> (K)</i>
0.30	1461.78	1332.60
0.35	1579.35	1436.78
0.40	1691.30	1537.28
0.45	1797.94	1634.28
0.50	1899.50	1727.96

As we can see, the adiabatic flame temperature for the conditions that we set – combustion chamber conditions of pressure = 1400kPa and temperature = 612 K shown in the next table – is about 10% higher for hydrogen discharge, this is primarily due to the difference in composition of combustion products of both gases as seen in eq (1) and (2) in paragraph A. One shall denote as

well that due to being a natural occurring element, hydrogen does not have a standard enthalpy of formation contrary to methane as it can be seen in appendix B through the JANAF tables. This means that the adiabatic flame temperature in the case of hydrogen solely depends on the difference between the standard enthalpy of formation of water and the enthalpies of reaction.

**Table 10** Results for full 100% load

Parameters	Results for H <sub>2</sub>	Results for CH <sub>4</sub>
Equivalence ratio ( $\phi$ )	0,30	0,40
P <sub>2</sub> (kPa)	1.400,00	1.400,00
P <sub>3</sub> (kPa)	1.399,36	1.399,36
P <sub>4</sub> (kPa)	100,00	100,00
T <sub>2</sub> (K)	612,15	612,15
T <sub>3</sub> (K)	1.418,50	1.383,09
T <sub>4</sub> (K)	733,23	715,10
W <sub>c</sub> (kJ/kg)	283,42	283,42
W <sub>t</sub> (kJ/kg)	786,69	766,85
W <sub>net</sub> (MW)	24,94	24,41
$\dot{m}_f$ (kg/s)	0,82	1,86
$\dot{m}_t$ (kg/s)	80,82	81,86
$\eta_{turbine}$	0,95	0,95
$\eta_{compressor}$	0,87	0,87
$\eta_{burner}$	1,00	1,00
$\eta_{th}$	0,45	0,44
$\eta_g$	0,37	0,36
SFC (kg/kW)	0,06	0,15
NO <sub>x</sub> (ppm)	68,62	214,53

**Table 10** compares the values we would expect from hydrogen and natural gas discharge; note that the thermal efficiencies are rather high given the idealised cycle we are using. This could lead us to errors in calculation, but given the comparative nature of this study, errors in values can be discarded through normalisation. Additionally if we compare the values found in **Table 10** to what the manufacturer expects from the turbine as seen in **Figure 33** we see a 10% of error between values of exhaust temperature and heat rate; within margin of acceptable error.

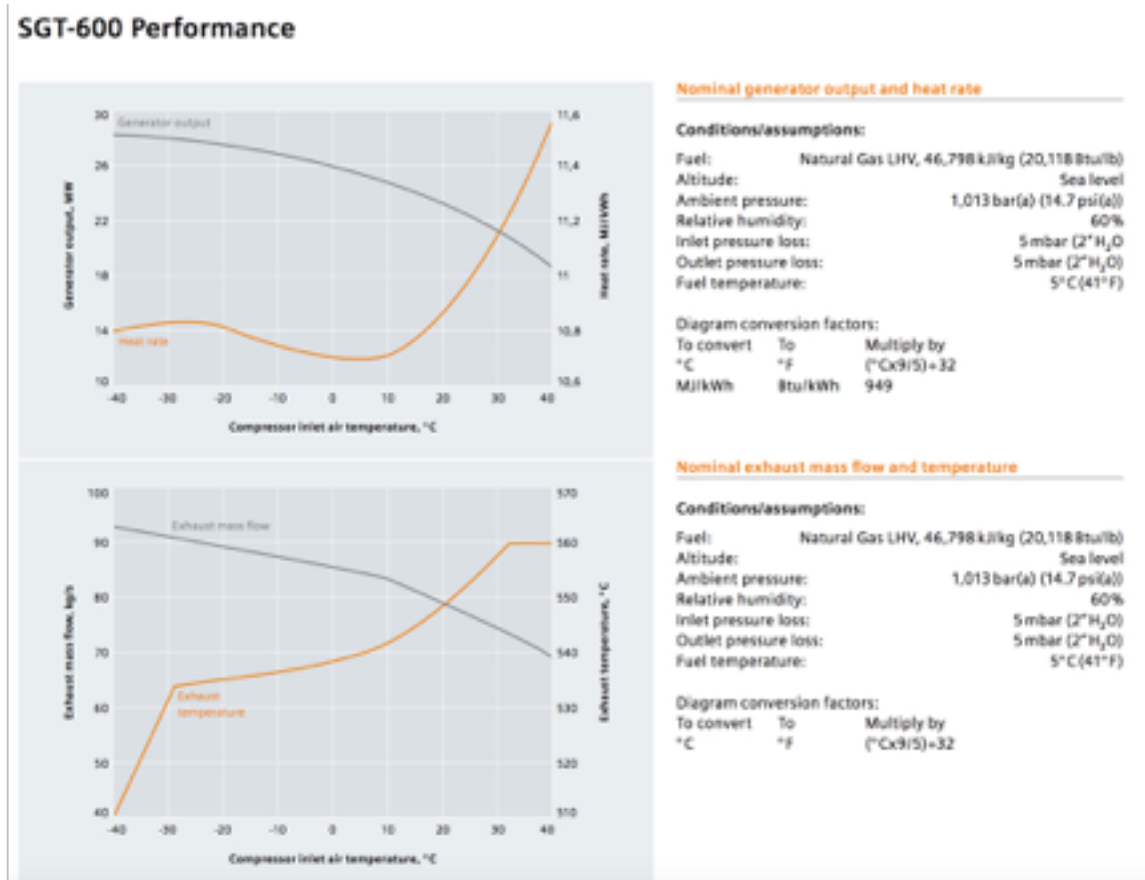


**Fig. 33** Performance of the SGT—600, courtesy of Siemens GmbH

Subsequently, as we can observe that differences in the equivalence ratio may produce effects on the net work output of the turbine, we plot the ratio of the output as function of  $\phi$  and we find out as it is apparent in **Figure 34**, that the behaviour of the ratio is roughly parabolic, meaning that it peaks in the region of  $\phi = 0.35$  and 24% raise in net work done by the turbine. This consequently means that for a certain load the fuel consumption for hydrogen will be much lower as expressed by the differences in SFC between both fuels, yet as we approximate to the stoichiometric region the differences in work output tend to equalise as increments in temperature are ever so infinitesimal getting to a certain range.

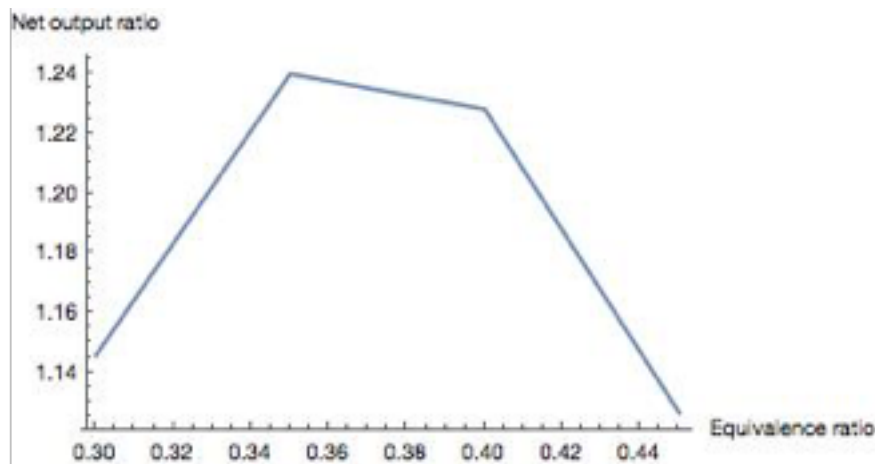


**Fig. 34** Comparison of net outputs

For the pollutants, we denote a reduction in the emissions of nitric oxides as well as the absence of carbon oxides due to the nature of the fuel. The explanation for the reduction of emissions of nitric oxides is explained by the fact that the estimation we've used for this calculation relies on the fuel/air ratio as a principal parameter. Hence knowing that hydrogen needs very little oxygen for combustion we understand the given trend though the flame temperature affects very little the emissions. In reality the emissions we've found should be much lower because of the type of burner that is used in the turbine but the formula doesn't really adjust for flame recirculation and swirls.

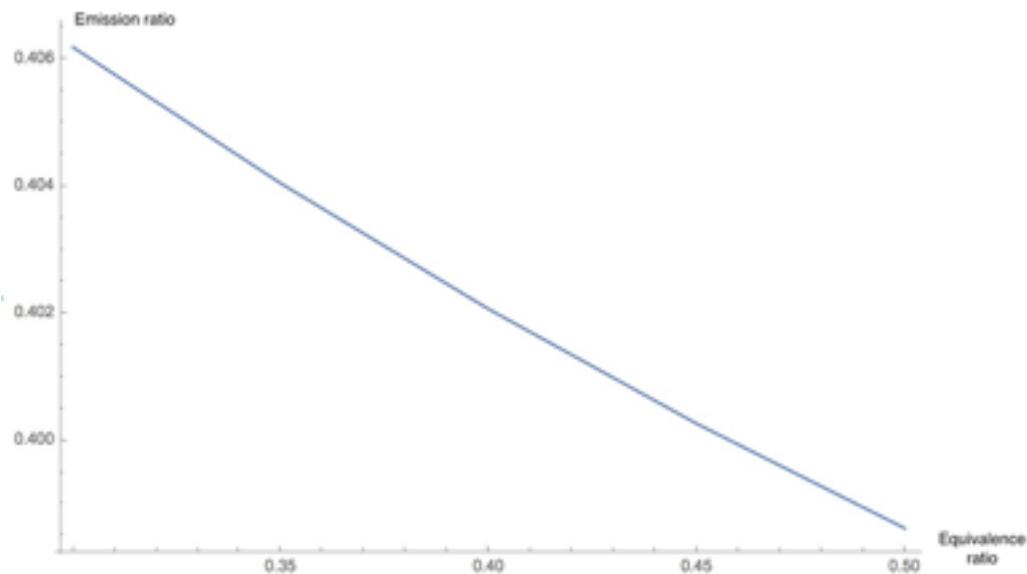


**Fig. 35** Comparison of NO<sub>x</sub> emissions

On the other hand, we do not see any major improvements in the thermal efficiency as we ignore



major losses in temperature and pressure through idealisation of the cycle. The fact being that through a simple Brayton cycle it is not possible to appreciate the real advantages of hydrogen as a fuel. For instance as observed in Chapter 7 paragraph C the use of hydrogen as coolant allows for up to an 8% increment in the thermal efficiency. As well as the high flame speed of the fuel permits for a compact design of the turbine and ease in the manufacturing of parts.

In conclusion, we can see from our basic model some of the apparent improvements that such fuel can allow without any real modification to the cycle. If reheat and regeneration with a combined cycle consume such fuel, it is theorised that gross efficiencies of up to 68% could follow [49].





## 8. Hydrogen safety, standard and regulation

### 8.1. Standards and regulation

In this chapter we will go through the established standards regulating the production, transport and use of hydrogen.

Given that hydrogen is largely in use throughout the industry, be it in food, petroleum or electronic endeavours we can find an extensive set of codes and standards regulating its entire usage. As the use of hydrogen as an energy carrier for consumer markets is expected to grow, the development and promulgation of codes and standards for this use are essential to establish a market environment receptive to commercial hydrogen products and systems, and therefore there's a dire need to expand on the existing norms established by the different bodies of regulation.

Moreover hydrogen standards are typically written under a consensus process by technical committees, for example in the United States, organisations such as the American Society of Mechanical Engineers (ASME) set standards for pressure vessels, pipelines, and piping; the Compressed Gas Association (CGA) for pressure vessel operation and maintenance; and the Underwriters Laboratories (UL) for product certification. Whereas in Europe, the European committee of standardisation, sets regulatory rules in agreement with the International Organisation for Standardisation (ISO), which get applied and reassessed by local governments, as in the case of Spain with the UNE norms from the AENOR.

Furthermore, the route of a complete standardisation of hydrogen as an energy carrier comes through the compliance of requirement of quality of the product, safety and recommendations which lay ground to norms of use and testing of the product. Certain of these norms, given the similarity of the use to natural gas take inspiration in the directive for transportation and handling of said energy carrier and therefore an analogy can be seen with the DIR. 2003/55 and ISO 9001 for quality assessment, DIR. 2006/42, 97/23/EC, 1999/92, 94/9 for storage and processing facilities, though the transportation be it by pipeline is assessed at a national level.

Nonetheless, as mentioned earlier hydrogen specific standards are existing and in use and can be found in:

- ISO/TC 197: in the field of systems and devices for the production, storage, transport, measurement and use of hydrogen.
- ISO 22734-2:2011: applicable to hydrogen generators and its safety and performance requirements.
- ISO DIS 15399: applicable to gaseous hydrogen cylinders and tubes for stationary storage.
- ISO/TR 15916:2015: guidelines for the use of hydrogen in its gaseous and liquid forms as well as its storage in either of these or other forms (hydrides).

For our case, we will also cite the existing regulatory normative in Spain:

- UNE-ISO/TR 15916 IN: basic considerations for the safety of hydrogen systems. (ISO/TR 15916:2004).
- UNE-ISO 14687: (ISO 14687:1999 + ISO 14687:1999/Cor. 1:2001), hydrogen fuel. Product specification.
- UNE-ISO 16110-1: safety in hydrogen generators using fuel processing technologies.
- UNE-ISO 22734-1: hydrogen generators using water electrolysis process.

It is to be taken under consideration that the listed norms do not provided the full extent of the existent regulations, both nationally or internationally but just provide the key standards we have taken into account for the specifics of our study.

On the other hand, confidence in hydrogen to become a safe “public fuel” in the EU depends on the following points [50]:

- Existing set of EU-wide regulations and technical standards relevant for hydrogen applications to be implemented on national level for practical use.
- Commitment and participation of authorities, R&D institutions and commercial companies in the development and implementation of technical solutions, regulations and standards related to hydrogen safety.
- Global collaboration in the development of internationally harmonised rules, which is specifically important for global vehicle and fuel markets.
- Validation of safe applications, codes and standards in demonstration projects.
- Continuous and systematic governmental and industrial funding for competence building.
- Measures to improve level of expertise in authorities and organisations assisting in approval processes.
- Communication between industries working on standards, which ensure safe products.

## **8.2. Hydrogen safety**

First we will provide a brief history of the history of incidences involving hydrogen, and the gravity of those accidents through Table.11 [51].

In actuality the list isn't complete, and the databases should be extensively updated. Yet, these characteristic examples shows the liability of hydrogen to major chemical accidents, though posing a considerable risk not only for onsite, but also for offsite damage as well.

**Table. 11** Summary of accidents related to hydrogen

Year	Date	Location	Origin of Accident	Death	Injury	Evacuated
2001	05.01	Oklahoma (trailer), OK, USA	Fire	1	1	15
2001	04.18	Labadie, MO, USA	Fire	NA	NA	NA
2000	09.14	Pardies	Fire and explosion	NA	NA	NA
2000	09.03	Gonfreville-Lorcher	Explosion	—	12	—
1999	05.07	Panipat, India	Fire	5	—	—
1999	04.08	Hillsborough, USA	Fire and explosion	3	50	38
1998	09.15	Torch, Canada	Fire	NA	NA	NA
1998	06.08	Auzouer, Touraine	Explosion and fire	—	1	200
1998	04.25	France	Fire	NA	NA	NA
1996	NA	United States	Explosion and fire of a transmission pipe	—	—	—
1994	NA	Japan	Fire in a desulfurization unit	—	2	—
1993	NA	Russia	Cloud explosion	—	4	—
1992	04.22	Jarrie	Fire	1	2	—
1992	01.18	Pennsylvania, USA	Fire	1	3	—
1992	NA	Japan	Explosion and fire in a refinery hydrogenation unit	9	8	—
1992	01.16	Sodegaura, Japan	Explosion	10	7	—
1992	01.08	Wilmington, USA	Leakage	—	16	—
1992	NA	Hong Kong	Hydrogen explosion in a power plant	2	19	—
1992	NA	U.S. nuclear power plant	Fire and explosion	NA	NA	NA
1991	06.09	Pardies	Fire	NA	NA	NA
1991	02.14	Daesan, Korea	Explosion	—	2	—
1991	10.-	Hamau-Frankfurt, Germany	Explosion	NA	NA	NA
1990	07.25	Birmingham, UK	Fire and gas cloud	—	>60	70,050
1990	04.29	Ottmarsheim	Fire	NA	NA	NA
1989	NA	United States	Pipeline failure and jet fire	7	8	—
1989	10.23	Pasadena, Houston, TX, USA	Explosion	22	100	NA
1988	06.15	Genoa, Italy	Explosion	3	2	15,000
1986	01.28	Challenger, USA	Explosion	7	—	—
1984	05.25	Tempelhof-feld, Germany	Explosion	NA	NA	NA
1984	10.13	Waziers, France	Fire	NA	NA	NA
1980	NA	EU chemical industries	Fire and explosion	NA	NA	NA
1978	06.12	United States	Fire	—	9	—
1975	NA	Ilford, Esses	Explosion	1	—	—
1937	05.06	Hindenburg, Lakehurst, NJ, USA	Fire	36	NA	NA

Furthermore, we can recognise part of the cause related to these incidents as issues linked to mechanical or material failure due to the effects of hydrogen embrittlement, over-pressurisation, boiling liquid expanding vapour explosion (BLEVE), and human error.

In the following section we will discuss the safety guidelines required through the standards we considered earlier.

Following UNE-ISO/TR 15916 IN, and according to what is presented in Table.10 the primary concern around the use of hydrogen is the risk of combustion, which is largely dependant on the

physical state of hydrogen.

Moreover the document assesses the non toxicity of hydrogen, though in confined spaces the risk of asphyxia is existent through the displacement of oxygen, additionally it is also noted that burning hazards can occur through hydrogen manipulation. Such liabilities are present by direct or close exposure to hot gases produced by the combustion, and UV light originating from the flame, in addition to the high risk of frostbite emanating from the handling of cold hydrogen gas and or liquid hydrogen.

Finally the paper advises for the following precautions and guideline in order to handle properly and avoid any risk linked to the manipulation of hydrogen:

### **8.2.1. General consideration and risk control**

An important principle for the safe use of hydrogen is to look for designs and operations that minimise the severity of the consequences of a potential mishap. This can be done in several ways, such as the following:

- The amount of hydrogen that is stored and that is involved in an operation should be minimised.
- Hydrogen should be isolated from oxidants, hazardous materials, and dangerous equipment.
- People and facilities should be separated from the potential effects of fire, explosion, or detonation caused by the failure of the hydraulic equipment or storage systems.
- Hydrogen systems should be elevated or vented above other installations.
- The accumulation of hydrogen/oxidant mixtures in confined spaces should be prevented.
- Personnel exposure should be minimised, and the use of personal protective equipment, alarms and warning devices (including fire and smoke detectors), and the control area around the hydrogen system should be insured.
- Good maintenance should be practiced, such as keeping access routes and evacuation clear and keeping hydrogen systems free of dirt and debris.
- Safe operating requirements should be met, such as working in pairs when operating in hazardous situations.



## **8.2.2. Design risks**

### ✓ **Material selection**

For the material selection the standard prescribes the following considerations:

- Compatibility with hydrogen (considering aspects such as hydrogen embrittlement, hydrogen attack, porosity, permeability, and diffusion).
- Compatibility with contiguous materials (combining properties under changes in temperature and pressure, for example, and the effect of such changes in the shape and dimensions of the materials).
- Compatibility with the conditions of use (effects of temperature and pressure, for example, on ductility, and expansion / contraction, property changes associated with changes in operating conditions).
- Compatibility with the surrounding environment or exposure (for example, a corrosive environment or high temperature due to a hydrogen fire or fire of nearby materials).
- Toxicity (the use of a material that is in some toxic mode, for example during manufacture, should be considered only when absolutely necessary).
- Failure mode (for example, fast break due to slow tactile separation).
- Ability to manufacture in the desired form (for example, machining, welding, and bending).
- Price.
- Availability.

Even though a given material may be susceptible to hydrogen embrittlement, the material can still be used in hydrogen service. For example, bottles of compressed gas that have been used successfully for many years for the storage and transport of compressed hydrogen gas are commonly made of 4130X alloy steel.

### ✓ **Storage unit considerations:**

The following guidelines apply to both gaseous hydrogen systems and liquid hydrogen systems unless only one of them is specified. The storage containers for hydrogen should be:

- Designed, manufactured and tested at an appropriate pressure defined in standards and regulations applicable to the pressure vessel.
- Built with appropriate materials.
- Insulated with the appropriate thermal insulation (especially containers that store LH<sub>2</sub>).

- Equipped with a discharge valve, as close to the container as possible.
- Equipped with a pressure control system (especially containers that store liquid hydrogen).
- Equipped with an approved venting system.
- Equipped with pressure relief devices to prevent overpressure.
- Located according to the requirements included in standards where distance is related to the amount of hydrogen.
- Provided with the appropriate label.

Liquid hydrogen tanks that are emptied and brought to environmental conditions should be checked regularly due to the accumulation of impurities such as oxygen and nitrogen. This can be done as part of a regular maintenance. The accumulation of oxygen in the stored hydrogen should not exceed 2% by volume when the mixture is allowed to warm to a gaseous state in confinement.

### ✓ **Hydrogen transmission lines:**

Pipes must be designed, manufactured and tested in accordance with standards of recognised prestige, using suitable materials with appropriate flexibility (such as expansion joints, hooks, and offsets). The lines must be located according to recognised standards far from power lines and buried pipes should be avoided whenever possible, in the contrary case, the effects of galvanic corrosion, the difficulty in performing a visual inspection of the integrity of the line, and the possibility of a leak that can be directed to a non-hazardous location should be considered.

Galvanic corrosion may occur, particularly when the humidity is present in dissimilar metals, and should be fitted in the pipes. The most corrosive material will be the most attacked and should be used as a female part.

Adequate supports, guides and anchors must be used, with the help of adequate pressure relief devices and insulation. The content and direction of the flow must be labelled.

Strong welding is preferable for pipe assemblies; however, flanged splices, threads, plugs, or sliding or compression fittings may be used depending on the operating conditions. Joint sealants and threads are suitable for the service of gaseous hydrogen. Some of these types of joints, joints, and sealants are not suitable for use at low temperatures. The bayonet assembly is commonly used for connections in liquid hydrogen tubing where connection and disconnection are frequent (for example, in load lines). If this is not possible, hydrogen detectors or fire detectors should control the regions around the junctions. The joints between soft welding (low melting point) should not be used in the hydrogen service.

Finally, non-metallic lines can work properly for short-term use if adequate ventilation and hydrogen detectors are provided.

### **8.2.3. Elimination of ignition source**

#### **✓ *Prevention of oxidant mixtures:***

The prevention of the formation of unwanted mixtures of hydrogen/oxidant is a key factor to prevent fire, deflagration or detonation. This is done by keeping the hydrogen/oxidant mixture separated. Some of the techniques that can be used to achieve this goal are:

- **Purging:** A system should be purged with an inert gas to remove air before introducing hydrogen into the system, and the system should be purged of hydrogen before being opened to air.
- **Leak-free system:** A system containing hydrogen should be subjected to a leak test and not leak before admitting hydrogen. Periodic leakage tests should be performed and if a leak is found it should be repaired.
- **Elimination:** The venting of hydrogen should be carried out in the open air by means of venting systems duly located and designed.
- **Ventilation:** A closed space, such as a room or a building, in which the hydrogen could accumulate should have adequate ventilation to prevent the formation of a combustible mixture.
- **Positive pressure maintenance:** Hydrogen systems, especially liquid hydrogen systems, should be kept at positive pressure to prevent air from entering the system from the outside.
- **Periodic heating of liquid hydrogen systems:** The liquid storage containers should be heated sufficiently from time to time so that impurities such as air can be vaporised and purged from the system.
- **Filters:** A filter can be used in a liquid hydrogen system to capture impurities that might include solid air. Such filters should be periodically isolated, heated, and purged to eliminate any impurities.

#### **✓ *Elimination of ignition sources:***

Installations using hydrogen should be protected from lightning by lightning rods, aerial cable, and ground rods suitably connected. Lightning strikes may cause inducing sparks; therefore, all equipment in a building should be bonded and grounded to prevent sparks. Static electricity may be generated in moving machinery belts or in flowing fluids containing solid or liquid particles. The measures taken to limit electrostatic charge generation and accumulation include bonding and grounding of all metal parts within a system, use of conductive machinery belts, personnel clothes made of antistatic fibres, and conductive and non-sparking floors. Sparks may also be generated by other mechanisms such as friction and impact. Even spark-proof tools can cause ignitions because the energy required for ignition of flammable hydrogen–air mixtures are extremely small.

For mechanical sources, one must avoid friction, mechanical fracture or mechanical vibration that may heat the gas to its auto-ignition temperature.



Finally, The following phenomena are considered as potential thermal sources of ignition:

- Open flames and/or hot surfaces (for example, welding and smoking cigarettes by staff).
- Leaks (for example, combustion engines and exhaust manifolds).
- Explosive charges (for example, charges used in construction, in fireworks, or in pyrotechnic devices).
- Catalysts and reactive chemical materials. High temperatures can result from the interaction of hydrogen with catalysts or with other chemical reactants. Some applications that use these materials include recombined hydrogen emitted by lead-acid batteries to produce water and hydrogen detection instruments.
- Resonance ignition from repeated shock waves that can occur in a system in which fluids move.
- Heating caused by high-speed jets, as could occur with an exhaust manifold.
- Shock waves and/or fragments, as could happen with the rupture of a tank or container.

✓ ***Elimination of detonation sources:***

The potential for deflagration and detonation should be valued in the designs of hydrogen facilities and operations. Strategies to minimise the potential for flame acceleration or detonation include:

- Bypass of confinement where flammable hydrogen mixtures may be formed.
- Use of flame suppressors, small holes, or channels to prevent deflagration and detonation in the system.
- Use of diluents and water spray systems to retard the acceleration of the flame.

If the potential for deflagration and detonation cannot be eliminated, then this possibility should be taken into account in the design and operation of the hydrogen system. This includes designs with sufficient strength to withstand high pressures or remote operations to protect facilities and personnel.

#### **8.2.4. Detection consideration**

The final consideration requested by the norm is the adoption of the adequate detection system, such that the level of concentration the alarm would be able to detect would be 1% of hydrogen per volume in the air, which is equivalent to 25% of the lower limit of flammability. This level should provide the time necessary to respond appropriately, with actions such as stopping the system, evacuating personnel, or other measures when necessary.



In parallel the proper fire detection system has to be in place with the capacity of detecting false positive and high sensibility for hydrogen flames.

## 9. Economical analysis

In this chapter we will try to analyse the effect of adopting hydrogen as a fuel on the price of the kW supplied by a gas turbine.

For this section we had to take into account a lot of assumptions and previsions set by several articles [52]. Beforehand, it is primordial to choose the economically advantageous production method for hydrogen, and subsequently select the adequate transportation method. From there we can estimate the selling price range of hydrogen and elaborate according to chapter 8 paragraph C the final cost of the supplied kWh.

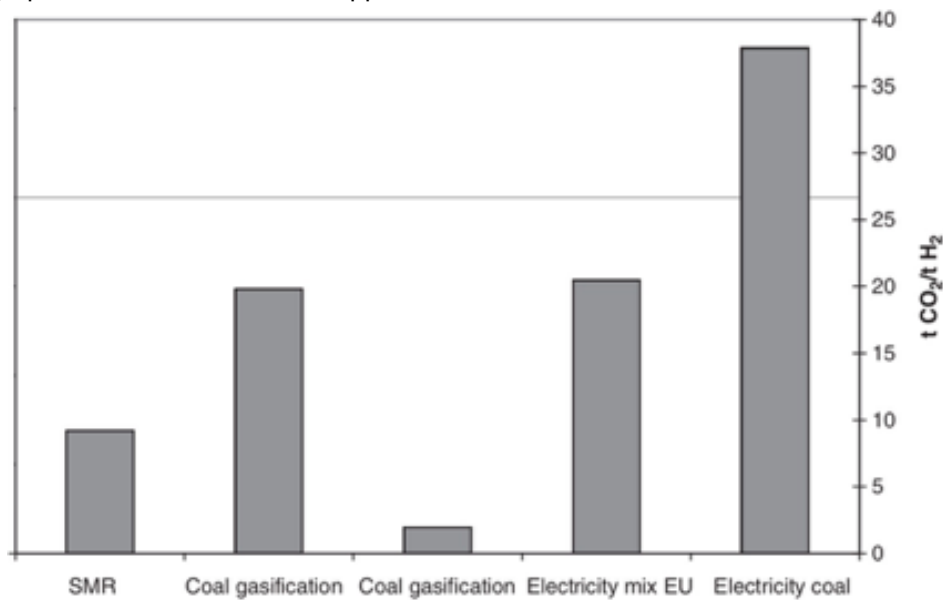


Fig. 36 CO<sub>2</sub> emission from H<sub>2</sub> production. [53]

In chapter 5 we've displayed some methods of hydrogen production though some of the most widespread in the industry were not mentioned (steam reforming from ethanol and biogas) given their similarities with other processes and their heavy carbon footprint as seen in **Figure 36** showing the specific CO<sub>2</sub> emissions for various hydrogen production technologies. With the exception of electrolysis from EU grid-mix electricity, the highest CO<sub>2</sub> emissions are incurred for hydrogen from coal.

In chapter 5 we've displayed some methods of hydrogen production though some of the most widespread in the industry were not mentioned (steam reforming from ethanol and biogas) given their similarities with other processes and their heavy carbon footprint as seen in **Figure 36** showing the specific CO<sub>2</sub> emissions for various hydrogen production technologies. With the exception of electrolysis from EU grid-mix electricity, the highest CO<sub>2</sub> emissions are incurred for hydrogen from coal.

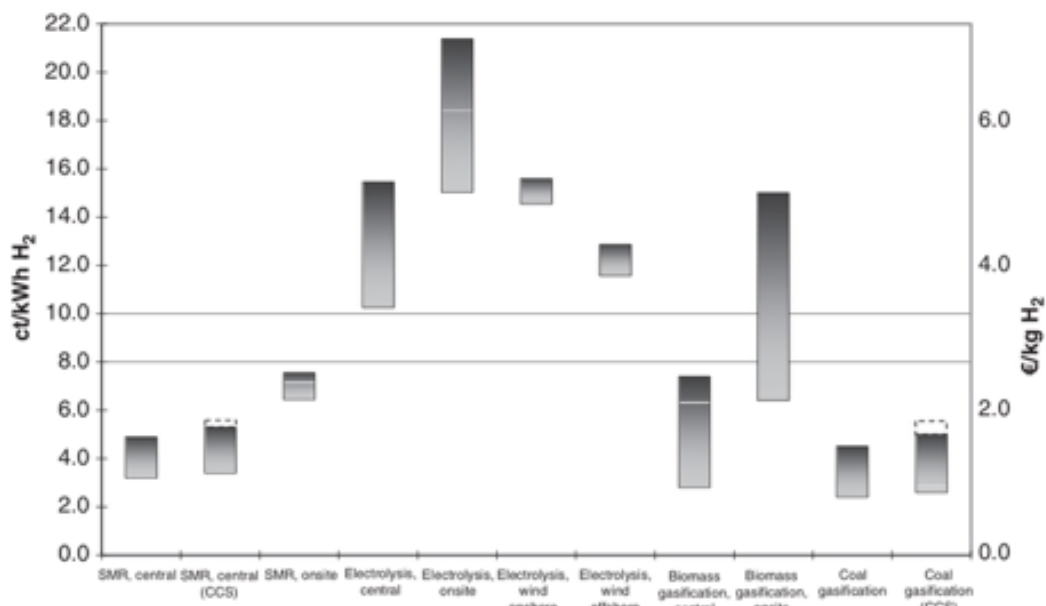


Fig. 37 Hydrogen production costs. [53]

Furthermore comparing the costs of production of hydrogen as seen in **Figure 37** we find out that the most attractive price for hydrogen production, taking into consideration carbon emissions is through Steam methane reforming (SMR) with a price range of [3–5] ct€/kWh H<sub>2</sub>.

In the other hand, the estimation of the cost of transportation would be through the comparison of the diverse methods we've presented earlier. Though it is observe that the price of transportation and distribution can be directly correlated to distance, flux and mass flow.

In our case; the study of hydrogen as an energy source, we are interested in a constant flux of hydrogen, that depending on the amount of energy generated we necessitate up to ( $\Gamma = SFC \times W_{net}$ ) 2.5t/day. The other variables to take into account are the distribution and transportation distance from production sites; for our case (the Spanish peninsula) and from **Figure 11.1** in chapter 6 we note that the major concentration of production hubs are in north-western Europe, though we can denote some major hubs revolving around the Catalan region. If we extrapolate involving certain data found for the natural gas distribution [54–61] we find that the average transportation distance revolves around 300km and the average distribution is of 50km.

Hence, for a short distance and relatively large quantities, pipelines distribution and transport can be favoured, as the capital costs depend largely on the operating distances when the operating costs can stay constant, the opposite of which is true in other method of distribution.

In the other hand, as reported in hart et. Al (1997) [62] losses due to evaporation, heating and leakage are relatively low in pipelines, as we can observe in **Figure 38** representing the relation between transportation distance and the energy cost as a fraction of LHV of hydrogen [63], which make the choice of opting for pipeline transmission in our case more attractive.

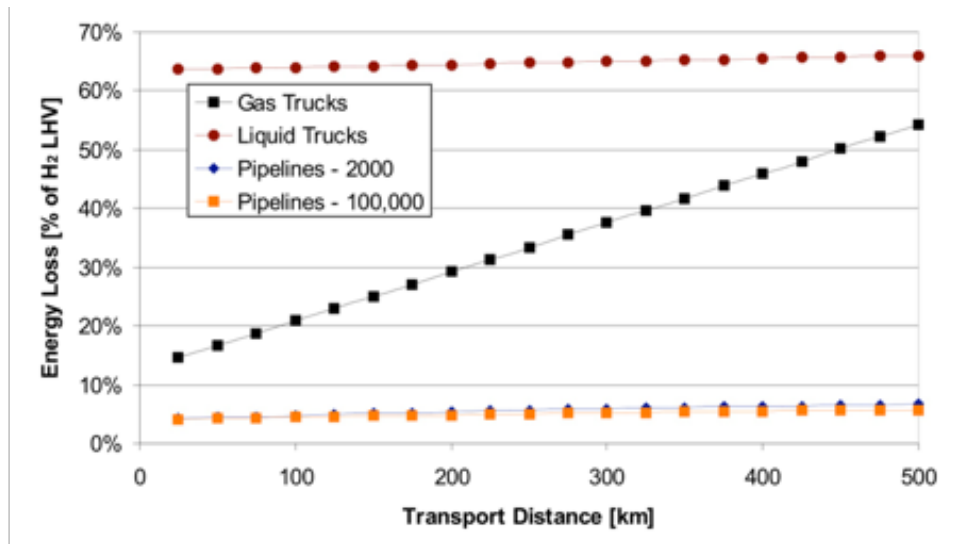


Fig. 38 Transportation energy loss. [63]

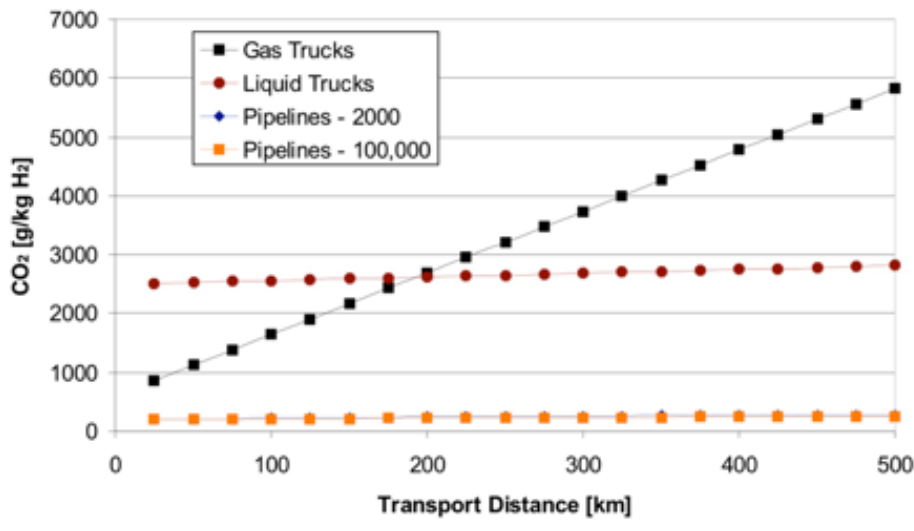


Fig. 39 CO<sub>2</sub> emissions due to different modes of transportation . [63]

In addition, we can also observe difference in carbon emissions between the different modes of transportation. **Figure 39** [63] illustrates the CO<sub>2</sub> emissions associated with the different transport modes and shows a very similar trend to that shown in **Figure 38**. The difference between these two graphs has to do with the relative amount of CO<sub>2</sub> emissions associated with electricity production (assuming a particular grid mix) and diesel fuel usage, the differences in energy densities between compressed and liquid hydrogen do account for the characteristic changes in carbon emissions, as gas trucks need to transport more compressed hydrogen in order to attain a similar energy concentration.

Finally, according to the MOREhys model (Model for Optimisation of Regional Hydrogen Supply) developed as a novel tool to assess the introduction of hydrogen as a fuel by means of an energy-system analysis<sup>a</sup> we can derivate the following tables (Table 12.1 – Table 12.3) of the projection of cost estimates.

**Table 12.1** Estimated costs of hydrogen transportation and distribution through pipeline [53—61]

		Transport		Distribution	
<b>Technical data</b>					
Diameter	m	0.25	0.25	0.25	0.10
Capacity	MWh <sub>H<sub>2</sub></sub>	100	600	1500	2.4
Inlet pressure	bar	30	30	30	30
Outlet pressure	bar	30	30	30	30
Lifetime	years	30	30	30	30
<b>Economic data</b>					
Specific investment pipeline: min.	k€/km	500	500	500	180
Specific investment pipeline: Reference	k€/km	560	560	560	250
Specific investment pipeline: max.	k€/km	620	620	620	350
Specific investment compressor	k€/km	10	60	140	0
Fixed costs <sup>a</sup>	% Investment/year	1	1	1	1
Variable costs, compressor <sup>b</sup>	ct/MWh <sub>H<sub>2</sub></sub> /km	0.093	0.42	0.64	0.0001
Average distance	km	300	300	300	50
<b>Total costs</b>	<b>ct/kWh<sub>H<sub>2</sub></sub></b>	<b>2.51</b>	<b>0.57</b>	<b>0.40</b>	<b>9.30</b>
Share annualised investment	%	90	71	47	91
Share fixed costs	%	9	7	4	9
Share variable costs	%	1	22	49	0

Notes:

<sup>a</sup> Maintenance, etc.

<sup>b</sup> Electricity price: 4.4 ct/kWh.

\*Note that the conversion from kWh H<sub>2</sub> to kg H<sub>2</sub> is of 33.3kWh/kg taken from the energy density of hydrogen [64].

<sup>a</sup> The MOREHyS model has been applied as a supporting tool for the hydrogen infrastructure analysis within the integrated EU project Hyways to develop the European Hydrogen Energy Roadmap (see [www.hyways.de](http://www.hyways.de)).

**Table 12.2** Techno-economic data of hydrogen liquefaction [53–61]

<b>Technical data</b>					
Capacity	MW <sub>H<sub>2</sub></sub>	10	50	100	300
Capacity	t LH <sub>2</sub> /day	7	36	72	216
Annual full load, hours	h/yr	8000	8000	8000	8000
Inlet pressure	bar	30	30	30	80
Specific electricity demand	kWh <sub>el</sub> /kWh <sub>H<sub>2</sub></sub>	0.40	0.33	0.31	0.22
Electrical nominal power	MW <sub>el</sub>	3.9	16.7	31.2	66.6
Theoretical demand of work	kWh/kWh <sub>H<sub>2</sub></sub>	0.084	0.084	0.084	0.073
Carnot efficiency	%	21	25	27	33
Lifetime	years	30	30	30	30
<b>Economic data</b>					
Specific investment	€/kW <sub>H<sub>2</sub></sub>	2800	1500	1000	733
Fixed costs <sup>a</sup>	% Invest/year	2.5	2.5	2.5	2.5
Variable costs <sup>b</sup>	ct/kWh <sub>H<sub>2</sub></sub>	1.76	1.45	1.36	0.97
Year of availability		Today	Today	Today	2020
<b>Total costs</b>	<b>ct/kWh<sub>H<sub>2</sub></sub></b>	<b>6.35</b>	<b>3.91</b>	<b>3.00</b>	<b>2.17</b>
Share annualised investment	%	58	51	45	45
Share fixed costs	%	14	12	10	10
Share variable costs	%	28	37	45	45

Notes:

<sup>a</sup>Maintenance, labour etc.

<sup>b</sup>Electricity price: 4.4 ct/kWh.

**Table 12.3** Estimated costs of hydrogen transportation and distribution through trucks [53—61]

		300 km (one way)	50 km (one way)
<b>Technical data</b>			
Gross weight truck (including H <sub>2</sub> load)	t	40	40
Transport capacity	t	3.5	3.5
Max. energy delivered per trip	MWh	117	117
Average driving speed	km/h	50	50
Time for loading and unloading	h	1.5	1.5
Number of trips per day		1	4
Capacity	MWh <sub>H<sub>2</sub></sub>	8.6	33.3
Annual full load hours	h/year	3240	3360
Fuel consumption (diesel) <sup>a</sup>	l/100 km	35	35
Lifetime	years	10	10
<b>Economic data</b>			
Investment	k€	500	500
Number of drivers		1	1
Wage	€/h	50	50
Working days per year		240	240
Fixed costs <sup>a</sup>	% Investment/a	2	2
Variable costs <sup>b</sup>	ct/(MWh <sub>H<sub>2</sub></sub> km)	0.24	0.24
<b>Total costs</b>	<b>ct/kWh<sub>H<sub>2</sub></sub></b>	<b>1.05</b>	<b>0.26</b>
Share annualised investment	%	28	29
Share fixed costs	%	59	62
Share variable costs	%	13	9

Notes:

<sup>a</sup>Maintenance, etc.

<sup>b</sup>Diesel price: 0.8 €/l.

As we can see, from all the data we've presented the most appealing mode of transportation of distribution would be through pipeline, setting therefore the final price of hydrogen to the plant at a range of [3.97— 16.81] ct€/kWh H<sub>2</sub>.

In contrast, according to the European office [65] of statistics the price of natural gas to the non-household consumer has been averaging the 3 ct€/kWh NG with an expected value attaining the 2.49 ct€/kWh NG later this. This shows a clear discrepancy between both products of a maximum of 675%. This in turn shows the heavy economical toll that an early adaptation to hydrogen as fuel source could bring to the energy industry.

Yet according to “Prospects for Hydrogen and Fuel Cells (IEA, Dec. 2005)” and “Energy Technology Perspectives (IEA, June 2006)” hydrogen could likely gain a significant market share in the coming decades thus benefiting from the economy of scale and therefore rendering its price

more palatable for the industry, in addition advances in technologies such as metal hybrids and betterment in the efficiencies of compression and liquefaction would decrease the overall transportation prices. Finally the introduction of a carbon tax by the European Union, could incentivise further development of an emerging hydrogen economy; as the adoption of these taxes would suppose an additional cost of up to 35€/t CO<sub>2</sub>.

Finally let us analyse the effect such price difference would assume on the final end consumer. Note that the end consumer gets as of today (2018) in Spain a base price according to the European office of statistics [65] of 22.96 ct€/kWh.

Now we will calculate the supposed price of the kWh in a best-case scenario with a hydrogen fuel cost to the plant of 3.97 ct€/kWh H<sub>2</sub> which translates into a final cost of 1.32201€/kg H<sub>2</sub>.

We know as a courtesy of Siemens GmbH that the capital cost C<sub>0</sub> of one of their SGT-600 gas turbine is of 5,000,000.00€. On the other hand we've calculated that the daily need of carburant to fuel our turbine is of 2.5t/day hence the annual fuel cost for the plant would be evaluated as:

$$M = 2500 \times 1.32201 \times 333.33$$

Assuming that our turbine works for 8000 hours a year. Therefore, we find that: M = 1,101,663.98€ per annum. Finally we need to estimate the annual cost of operation and maintenance. According to the IEA and the U.S. DoE the estimated O&M cost for a CCGT plant in Spain is averaged at a 36.67\$/MWh [73] for a 7% discount rate given relative risk for heavy weight industry. This translates into a final O&M price of:

$$OM = 36.67 \times 0.86 \times 24.94 \times 8000 \Rightarrow OM = 6,292,102.62€$$

Finally, we need to assess the charge factor ( $\beta$ ) that is given through the equation (1) knowing that our turbine has service cycle of about 17 years according to the manufacturer.

$$\beta = \left[ \frac{i(i+1)^N}{(1+i)^N - 1} \right] \quad (1)$$

With N being the service cycle in years and,  $i$  the discount rate. This yields a value for the charge factor of  $\beta = 0.102$ . Therefore the current cost of production will equate:

$$PE = \beta C_0 + M + (OM) \quad (2)$$

From (2) we find that the cost of production is equal to  $PE = 7,905,892.57€$

Subsequently the unitised cost of production will then depend on the overall efficiency of the plant and the hour of operation.

$$YE = \frac{PE}{\eta_g H} \quad (3)$$

Which in turn yields a final value of  $YE \approx 2,000€/kW$ , it is to be noted that our turbine though for energy generation is not meant to generate energy for the particular but rather as solution industrial solution to provide energy for the main plant and therefore for a bigger turbine this price might scale down.



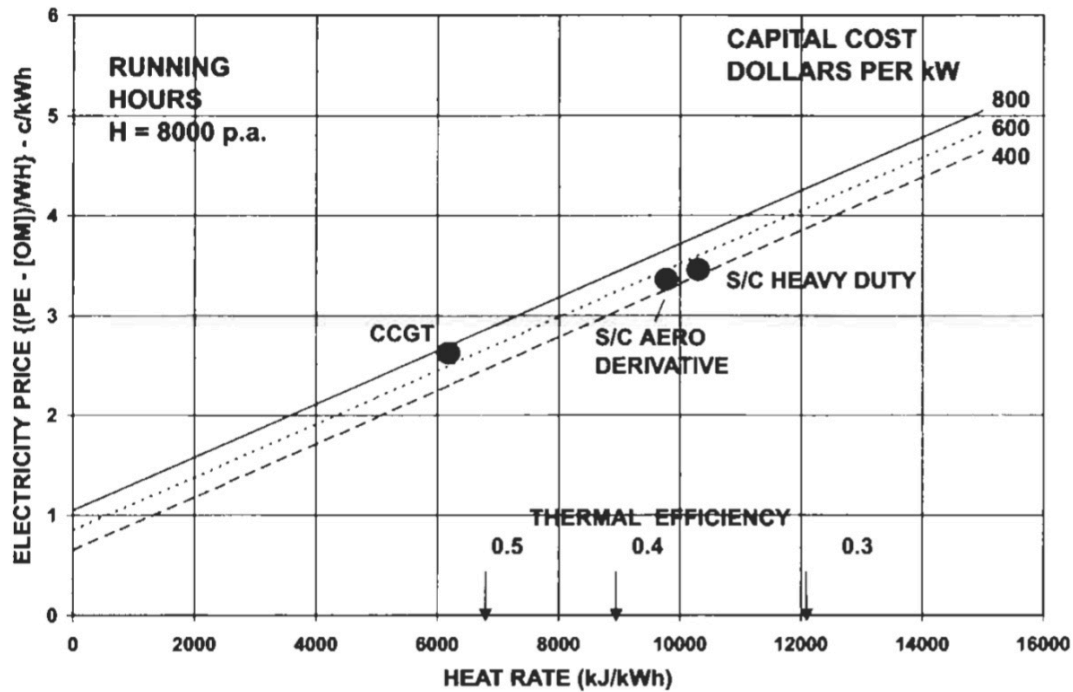


Fig. 40 Electricity price for typical gas turbine plants – running hours 8000 [76]

Ultimately if we take a look at **Figure 40** we see that for a typical CCGT plant the highest capital cost per kW is of 1088€ adjusted for inflation. This can relate to at least the double of electricity price for the end consumer, which in the case of the Spanish household translates into paying 46ct€/kWh instead of 22.96ct€/kWh.





## 10. Conclusion

In conclusion, as we've seen hydrogen is an attractive energy carrier, from its properties and as we've explored in the thermodynamic analysis an adapted working cycle for hydrogen discharge could further improve on efficiencies, work output and fuel consumption. We refer especially to the case of the zero emission Graz cycle that was reported to attain efficiencies as high as 68%.

Nonetheless from our own analysis we've noted that hydrogen does in fact impact the net output given the high temperature of its flame. A better exploitation of this effect would be through the development of better materials for the turbine, capable of withstanding higher temperatures, as the temperature limit for most design is at around 1800K. Another solution is the use of better cooling associated with the employment of ceramics and shielding surfaces to protect from high temperatures.

Nevertheless, the advantages of employing hydrogen as a fuel are clearly apparent and beneficial – from performance to pollutants diminution.

However, we've seen that serious drawbacks were causing notable issues. First the financial aspect; being rather costly to produce and to transport, this impedes the total adoption of the Hydrogen as an energy source.

The high cost of production could be avoided by adoption of the economy of scale, where by popularization of the fuel, the capital cost of inversion could though remaining the same can be evenly more distributed on the production capacity being scaled up.

The other drawback being in the transport and distribution, as we've seen the total adoption of existing natural gas pipeline infrastructure is not feasible due to hydrogen embrittlement, which only permits for a partial refurbishment of such infrastructure. As for the transport through pressurised vessels, the low density of hydrogen renders the logistics of such transportation and distribution, be it by rail or on board vehicle, a complicated and costly task:

- $LH_2$  → boil-off, leakage through permeation and energy consumption for cooling
- $CGH_2$  → leakage through permeation, pressurisation, high cost of materials

Hence the only viable solution so far for a large-scale consumption of hydrogen would be through the initial investment on an adapted hydrogen infrastructure estimated to be at circa 1.2 trillion \$ U.S according to the IAE, and the development of new way to store hydrogen.

Lastly, as we have seen through this paper hydrogen adoption for energy production is feasible and appealing from a technical standpoint. Yet we will have to wait for a betterment of current technology and a large initial investment from several governments in order to see a shift in energy carriers.



## 11. References

- [1] K. K. Kuo. Principles of Combustion. John Wiley, New York, 1986.
- [2] T. Poinso and D. Veynante. Theoretical and numerical combustion. R.T. Edwards, 2nd edition, 2005.
- [3] McCarty, R. D., Hord, J. and Roder, H.M., Selected properties of hydrogen (engineering design data), U.S. Department of Commerce, National Bureau of Standards, Washington, DC, NBS Monograph 168, February 1981.
- [4] Benz, F.J. Bishop, C.V. and Pedley, M. D., Ignition and Thermal Hazards of Selected Aerospace Fluids: Overview, Data, and Procedures. RD-WSTF-0001, NASA White Sands Test Facility, Las Cruces, NM, USA, October 1988.
- [6] Alternative fuels data center, Properties of fuel, DOE report, August 2005
- [7] Hydrogen fuel cell engines, and related technologies, Colleges of the desert, Palm desert, CA, 2001
- [8] Cleveland CJ, Chronologies, top ten lists, and world clouds. Handbook of Energy 2014;2:309–322.
- [9] Dunn S, History of hydrogen. Encyclopaedia of Energy 2004;3:241–252.
- [10] Hirscher M (ed.). Handbook of hydrogen storage: new materials for future energy storage. Weinheim: Wiley-VCH Verlag GmbH & Co. KGaA; 2010.
- [11] Frost W., Aspliden C., Characteristics of the wind, Fundamental Concepts of Wind Turbine Engineering, D.A. Spera, Ed., ASME Press, New York, 1994, Chapter 8.
- [12] Bechrakis D.A., McKeogh E.J., Gallagher P.D., Simulation and operational assessment for a small autonomous wind-hydrogen energy system, Energ. Convers. Manag., 47, 46–59, 2006.
- [13] Gibson TL, Kelly NA (2008) Optimization of solar powered hydrogen production using photo- voltaic electrolysis devices. Int J Hydrogen Energy 33:5931–5940
- [14] Scholz, W., Processes for industrial production of hydrogen and associated environmental effect, Gas Sep. Purif., 7, 131, 1993.
- [15] Li Kaiwen, Yu Bin & Zhang Tao (2017): Economic analysis of hydrogen production from steam reforming process
- [16] Nagata, S. et al., Fabrication of high temperature solid electrolyte fuel cell and power generation test (in Japanese), J. High Temp. Soc., 7, 217, 1981.
- [17] Bossel U, Eliasson B, Energy and the hydrogen economy, US DOE, EERE, [http://www.afdc.energy.gov/pdfs/hyd\\_economy\\_bossel\\_eliasson.pdf](http://www.afdc.energy.gov/pdfs/hyd_economy_bossel_eliasson.pdf).
- [18] Hydrogen Transportation Pipelines, IGC.121/04/E, European Industrial Gases Association, Brussels, 2004.



- [19] Hydrogen Pipeline Working Group Workshop, U.S. Department of Energy, Augusta, GA, 2005. ([www.eere.energy.gov/hydrogenandfuelcells/wkshp\\_hydro\\_pipe.html](http://www.eere.energy.gov/hydrogenandfuelcells/wkshp_hydro_pipe.html)).
- [20] Robinson, S.L. and Stoltz, R.E., Toughness losses and fracture behavior of low strength carbon-manganese steels in hydrogen, in *Hydrogen Effects in Metals*, Bernstein, I.M. and Thompson, A.W., Eds., American Institute of Mining, Metallurgical, and Petroleum Engineers, New York, 1981, pp. 987–995.
- [21] Walter, R.J. and Chandler, W.T., *Influence of Gaseous Hydrogen on Metals Final Report*, NASA-CR-124410, NASA, Marshall Space Flight Center, AL, 1973.
- [22] Walter, R.J. and Chandler, W.T., Cyclic-load crack growth in ASME SA-105 grade II steel in high-pressure hydrogen at ambient temperature, in *Effect of Hydrogen on Behavior of Materials*, Thompson, A.W. and Bernstein, I.M., Eds., The Metallurgical Society of AIME, Warrendale, PA, 1976, pp. 273–286.
- [23] Sandoz, G., A unified theory for some effects of hydrogen source, alloying elements, and potential on crack growth in martensitic AISI 4340 steel, *Metallurgical Transactions*, 3, 1169–1176, 1972.
- [24] Nelson, H.G. and Williams, D.P., Quantitative observations of hydrogen-induced, slow crack growth in a low alloy steel, in *Stress Corrosion Cracking and Hydrogen Embrittlement of Iron Base Alloys*, Staehle, R.W., Hochmann, J., McCright, R.D., and Slater, J.E., Eds., NACE, Houston, TX, 1977, pp. 390–404.
- [25] Hinotani, S., Terasaki, F., and Takahashi, K., Hydrogen embrittlement of high strength steels in high pressure hydrogen gas at ambient temperature, *Tetsu-To-Hagane*, 64, 899–905, 1978.
- [26] Fukuyama, S. and Yokogawa, K., Prevention of hydrogen environmental assisted crack growth of 2.25Cr-1Mo steel by gaseous inhibitors, in *Pressure Vessel Technology*, Vol. 2, Verband der Technischen Überwachungs-Vereine, Essen, Germany, 1992, pp. 914–923.
- [27] Bandyopadhyay, N., Kameda, J., and McMahon, C.J., Hydrogen-induced cracking in 4340-type steel: effects of composition, yield strength, and H<sub>2</sub> pressure, *Metallurgical Transactions*, 14A, 881–888, 1983.
- [28] Robinson, S.L. and Stoltz, R.E., Toughness losses and fracture behavior of low strength carbon-manganese steels in hydrogen, in *Hydrogen Effects in Metals*, Bernstein, I.M. and Thompson, A.W., Eds., American Institute of Mining, Metallurgical, and Petroleum Engineers, New York, 1981, pp. 987–995.
- [29] Brimhall, J.L., E.P. Simonen, and R.H. Jones, Data Base on Permeation, Diffusion, and Concentration of Hydrogen Isotopes in Fusion Reactor Materials, Fusion Reactor Materials Semiannual Progress Report, DOE/ER-0313/16, 1994.
- [30] Forcey, K.S. et al, Hydrogen transport and solubility in 316L and 14914 steels for fusion reactor applications, *Journal of Nuclear Materials*, 160, 117 (1988).



- [31] Hollenberg, G.W. et al., Tritium/hydrogen barrier development, *Fusion Engineering and Design*, 28, 190. (1995).
- [32] Perujo, A. and K.S. Forcey, Tritium permeation barriers for fusion technology, *Fusion Engineering and Design*, 28, 252. (1995).
- [33] Serra, E. et al., Hydrogen permeation measurements on alumina, *Journal of the American Ceramic Society*, 88, 15. (2005).
- [34] The Hydrogen economy, opportunities and challenges edited by Michael Ball and Martin Wietschel, p. 311. Cambridge
- [35] A. Niedzwiecki (Quantum Technologies): “Storage”, Proc. Hydrogen Vision Meeting, US DOE, Washington, 15-16 Nov. 2001 ([http://www.eere.energy.gov/hydrogenandfuelcells/pdfs/hv\\_report\\_12-17.pdf](http://www.eere.energy.gov/hydrogenandfuelcells/pdfs/hv_report_12-17.pdf)).
- [36] Encyclopédie des gaz, Air Liquide, Division scientifique. Amsterdam: Elsevier; 1976.
- [37] Léon A (ed.). Hydrogen technology. Berlin Heidelberg: Springer-Verlag; 2008.
- [38] Weast RC, Astle MJ, Beyer WH, CRC handbook of chemistry and physics. Boca Raton, FL: CRC Press; 1983.
- [39] Berry RL, Raynor GV, The crystal chemistry of the Laves Phases. *Acta Crystallographica* 1953;6:178–186.
- [40] Lototsky MV, Yartys VA, Pollet BG, Bowman Jr. RC, Metal hydride hydrogen compressors: a review. *International Journal of Hydrogen Energy* 2014;11:5818–5851.
- [41] Züttel A, Materials for hydrogen storage, *Materials Today*; 2003.
- [42] Bossel, U., Eliasson, B. and Taylor, G. (2005). The Future of the Hydrogen Economy: Bright or Bleak? Report E08, 26 February 2005, European Fuel Cell Forum, [www.efcf.com/reports](http://www.efcf.com/reports).
- [43] Gstrein G, Klell M, Properties of hydrogen. Institute for Internal Combustion Engines and Thermodynamics, Graz University of Technology; 2004.
- [44] Hydrogen Transmission in Pipelines and Storage in Pressurised and Cryogenic Tanks Ming Gao and Ravi Krishnamurthy – Hydrogen fuel production and storage edited by B. Gupta, CRC Press, Taylor & Francis Group.
- [45] Eberle, U., Arnold, G. and von Helmholt, R. (2006). Hydrogen storage in metal–hydrogen systems and their derivatives. *Journal of Power Sources*, 154 (2)
- [46] A study of thermodynamic cycle and system configurations of hydrogen combustion turbines, H. SUGISITA Takasago R & D Center, Mitsubishi Heavy Industries Ltd., H. MORI and K. UEMATSU Takasago Machinery Works Mitsubishi Heavy Industries Ltd.
- [47] Adapting the zero-emission Graz Cycle for hydrogen combustion and investigation of its part load behaviour, Wolfgang Sanz, Martin Braun, Herbert Jericha, Max F. Platzer, Institute for Thermal Turbomachinery and Machine Dynamics, Graz University of Technology, Graz, Austria, AeroHydro Research & Technology Associates, Pebble



Beach, CA, USA, 15 February 2018

- [48] Hydrogen fuelled and cooled gas turbine, Y. S. H. Najjar, Mechanical Engineering Department, Thermal King Abdulaziz University, P.O. Box 9027, Jeddah, Saudi Arabia, 9 May 1990
- [49] Concept of hydrogen fired gas turbine cycle with exhaust gas recirculation: Assessment of combustion and emissions performance, Mario Ditarantoa, Hailong Lib, Terese Løvåsc, SINTEF Energy Research, Trondheim, Norway, Mälardalen University, Västerås, Sweden, Norwegian University of Science and Technology, Trondheim, Norway, 3 April 2015
- [50] [https://www.energy.siemens.com/co/pool/hq/power-generation/gas-turbines/SGT-600/downloads/SGT-600\\_GT\\_PowerGen\\_EN.pdf](https://www.energy.siemens.com/co/pool/hq/power-generation/gas-turbines/SGT-600/downloads/SGT-600_GT_PowerGen_EN.pdf)
- [51] SGT–600 fact sheet courtesy of Siemens GMBH
- [52] Gas Turbine Engineering Handbook, Second edition, Meherwan P. Boyce, Gulf Professional Publishing
- [53] R. J. Kee, F. M. Rupley, J. A. Miller, M. E. Coltrin, J. F. Grcar, E. Meeks, H. K. Moffat, A. E. Lutz, G. Dixon- Lewis, M. D. Smooke, J. Warnatz, G. H. Evans, R. S. Larson, R. E. Mitchell, L. R. Petzold, W. C. Reynolds, M. Caracotsios, W. E. Stewart, P. Glarborg, C. Wang, and O. Adigun, Chemkin Collection, Release 3.6, Reaction Design, Inc., San Diego, CA (2000).
- [54] Stull, D. R., Prophet, H., & United States. (1971). JANAF thermochemical tables. Washington, D.C: U.S. Dept. of Commerce, National Bureau of Standards.
- [55] Applied combustion, Second edition, L.L. Faulkner, Colombus division, Battelle Memorial Institute and department of Mechanical engineering, The Ohio State University, Columbus, Ohio
- [56] A. M. Y. Razak, Industrial gas turbines, performances and operability, Woodhead Publishing limited, Cambridge England
- [57] H. Cohen, G. F. C. Rogers, H. I. H. Saravanamutto, Gas turbine Theory, 4<sup>th</sup> edition, Longman group limited, ISBN: 0-582-23632-0
- [58] Bakkan, L.E. and Skogly, L., ASME Paper 95-GT-399, 1995.
- [59] Advanced gas turbine cycles, J.H. Horlock F.R. Eng., F.R.S., Whittle laboratory, Cambridge, U.K. 2003 ISBN 0-08-044273-0
- [60] Fliess B, Gonzales F, Kim J, Schonfeld R. The use of international standards in technical regulation, OECD Trade Policy. Working Papers, No. 102. Paris: OECD Publishing; 2010. pp. 1e150.
- [62] Renewable hydrogen energy regulations, codes and standards: Challenges faced by an EU candidate country, Sudi Apaka, Erhan Atayb, Güngör Tuncerc, Beykent University, Faculty of Economics and Administrative Sciences, Sisli-Ayazaga Kampüsü, 34396,



Istanbul, Türkiye, Trakya University, Faculty of Economics and Administrative Sciences, Istanbul, Turkey, Beykent University, Department of Industrial Engineering, Istanbul, Turkey

- [63] After Rigas, F. and Sklavounos, S., *Int. J. Hydrogen Energ.*, 30, 1501, 2005; Rosyid, O.A., *System-Analytic Safety Evaluation of the Hydrogen Cycle for Energetic Utilization*, Dissertation, Otto-von-Guericke University, Magdeburg, Germany, 2006.
- [64] Bossel, U., Eliasson, B. and Taylor, G. (2005). *The future of the hydrogen economy: bright or bleak?* European Fuel Cell Forum, February 2005. [www.efcf.com/reports](http://www.efcf.com/reports).
- [65] *The Hydrogen economy, opportunities and challenges* edited by Michael Ball and Martin Wietschel, p 305. Cambridge
- [66] Amos, W. (1998). *Costs of Storing and Transporting Hydrogen*. Report NREL/TP- 570-25106. National Renewable Energy Laboratory Colorado/US Department of Energy.
- [67] Castello, P., Tzimas, E., Moretto, P. and Peteves, S. D. (2005). *Techno-Economic Assessment of Hydrogen Transmission & Distribution Systems in Europe in the Medium and Long Term*. Joint Research Centre (JRC), Report EUR 21586 EN. Petten, The Netherlands: The Institute for Energy.
- [68] Bossel, U. and Eliasson, B. (2003). *Energy and the hydrogen economy*. European Fuel Cell News, January 2003. [www.efcf.com/reports](http://www.efcf.com/reports).
- [69] Bossel, U., Eliasson, B. and Taylor, G. (2005). *The future of the hydrogen economy: bright or bleak?* European Fuel Cell Forum, February 2005. [www.efcf.com/reports](http://www.efcf.com/reports).
- [70] Castello, P., Tzimas, E., Moretto, P. and Peteves, S. D. (2005). *Techno-Economic Assessment of Hydrogen Transmission & Distribution Systems in Europe in the Medium and Long Term*. Joint Research Centre (JRC), Report EUR 21586 EN. Petten, The Netherlands: The Institute for Energy.
- [71] Syed, M. T., Sherif, S. A., Veziroglu, T. N. and Sheffield, J. W. (1998). *An economic analysis of three hydrogen liquefaction systems*. *International Journal of Hydrogen Energy*, 23 (7), 565-576.
- [72] Valentin, B. (2001). *Wirtschaftlichkeitsbetrachtung einer Wasserstoffinfrastruktur für Kraftfahrzeuge*. Diploma thesis. Munster, Germany: University of Applied Sciences Munster and Linde Gas AG.
- [73] <http://www.europarl.europa.eu/document/activities/cont/201106/20110628ATT22856/20110628ATT22856EN.pdf>
- [74] Hart, D. (1997). *Hydrogen Power: The Commercial Future of the Ultimate Fuel*, London, UK Financial Times Energy Publishing.
- [75] DETERMINING THE LOWEST-COST HYDROGEN DELIVERY MODE, Christopher Yang, and Joan Ogden, Institute of Transportation Studies, Department of Environmental Science and Policy University of California, Davis, CA 95616 USA



- [76] Zittel, Werner & Wurster, Reinhold & Bolkow, Ludwig. Advantages and Disadvantages of Hydrogen. Hydrogen in the Energy Sector. Systemtechnik Gmbitt. 1996.







## Appendixes

### Appendix A: Curvefit coefficient for thermodynamic properties

#### A.1– Curvefit coefficient for fuels specific heat and enthalpy for reference state of zero enthalpy of the elements

See reference [58] in order to find the source.

$$c_p \text{ (kJ/kmol-K)} = 4.184(a_1 + a_2\theta + a_3\theta^2 + a_4\theta^3 + a_5\theta^{-2}),$$

$$\hat{h}^\circ \text{ (kJ/kmol)} = 4184(a_1\theta + a_2\theta^2/2 + a_3\theta^3/3 + a_4\theta^4/4 - a_5\theta^{-1} + a_6),$$

where  $\theta = T \text{ (K)}/1000$

Formula	Fuel	MW	a <sub>1</sub>	a <sub>2</sub>	a <sub>3</sub>	a <sub>4</sub>	a <sub>5</sub>	a <sub>6</sub>
CH <sub>4</sub>	Methane	16.043	-0.29149	26.327	-10.610	1.5656	0.16573	-18.331
C <sub>3</sub> H <sub>8</sub>	Propane	44.096	-1.4867	74.339	-39.065	8.0543	0.01219	-27.313
C <sub>6</sub> H <sub>14</sub>	Hexane	86.177	-20.777	210.48	-164.125	52.832	0.56635	-39.836
C <sub>8</sub> H <sub>18</sub>	Isooctane	114.230	-0.55313	181.62	-97.787	20.402	-0.03095	-60.751
CH <sub>3</sub> OH	Methanol	32.040	-2.7059	44.168	-27.501	7.2193	0.20299	-48.288
C <sub>2</sub> H <sub>5</sub> OH	Ethanol	46.07	6.990	39.741	-11.926	0	0	-60.214
C <sub>8.26</sub> H <sub>13.5</sub>	Gasoline	114.8	-24.078	256.63	-201.68	64.750	0.5808	-27.562
C <sub>7.76</sub> H <sub>13.1</sub>		106.4	-22.501	227.99	-177.26	56.048	0.4845	-17.578
C <sub>10.3</sub> H <sub>18.7</sub>	Diesel	148.6	-9.1063	246.97	-143.74	32.329	0.0518	-50.128

## A.2– Curvefit coefficient for thermodynamic properties of (C–H–O–N) systems

See reference [57] to find source

$$c_p/R_u = a_1 + a_2 T + a_3 T^2 + a_4 T^3 + a_5 T^4$$

$$h^o/R_u T = a_1 + \frac{a_2}{2} T + \frac{a_3}{3} T^2 + \frac{a_4}{4} T^3 + \frac{a_5}{5} T^4 + \frac{a_6}{T}$$

$$s^o/R_u = a_1 \ln T + a_2 T + \frac{a_3}{2} T^2 + \frac{a_4}{3} T^3 + \frac{a_5}{4} T^4 + a_7$$

Species	T(K)	a <sub>1</sub>	a <sub>2</sub>	a <sub>3</sub>	a <sub>4</sub>	a <sub>5</sub>	a <sub>6</sub>	a <sub>7</sub>
CO	1,000–5,000	0.03025078E+02	0.14426885E-02	-0.05630827E-05	0.00183813E-09	-0.06910951E-13	-0.14268350E+05	0.06108217E+02
	300–1,000	0.03262431E+02	0.15119498E-02	-0.03881755E-04	0.05581944E-07	-0.02474951E-10	-0.14310339E+05	0.04848997E+02
CO <sub>2</sub>	1,000–5,000	0.04453623E+02	0.03380148E-01	-0.12784105E-05	0.02393996E-08	-0.16690333E-13	-0.04896696E+06	-0.09553959E+01
	300–1,000	0.02275724E+02	0.09922072E-01	-0.10409113E-04	0.06066686E-07	-0.02117280E-10	-0.04833731E+06	0.03188488E+02
H <sub>2</sub>	1,000–5,000	0.02991423E+02	0.07000644E-02	-0.05633828E-06	-0.09231579E-10	0.15827519E-14	-0.08350340E+04	-0.13551101E+01
	300–1,000	0.03298324E+02	0.08249443E-02	-0.0843015E-05	-0.09475434E-09	0.04134872E-13	-0.10235209E+04	-0.03294094E+02
H	1,000–5,000	0.02900000E+02	0.00000000E+00	0.00000000E+00	0.00000000E+00	0.00000000E+00	0.02547162E+06	-0.0460176E+01
	300–1,000	0.02900000E+02	0.00000000E+00	0.00000000E+00	0.00000000E+00	0.00000000E+00	0.02547162E+06	-0.0460176E+01
OH	1,000–5,000	0.02882730E+02	0.10139743E-02	-0.02276877E-05	0.02174683E-09	-0.05126305E-14	0.03886888E+05	0.0598712E+02
	300–1,000	0.03637266E+02	0.01850938E-02	-0.16761646E-05	0.02387202E-07	-0.08435442E-11	0.03606781E+05	0.13588605E+01
H <sub>2</sub> O	1,000–5,000	0.02872185E+02	0.03056293E-01	-0.06730260E-05	0.12009964E-09	-0.06391638E-13	-0.02989921E+06	0.06862817E+02
	300–1,000	0.0386842E+02	0.03474982E-01	-0.06354696E-04	0.06964581E-07	-0.02566588E-10	-0.03020011E+06	0.02980232E+02
N <sub>2</sub>	1,000–5,000	0.02926640E+02	0.14879768E-02	-0.05684760E-05	0.10097038E-09	-0.06733351E-13	-0.09227977E+04	0.05980528E+02
	300–1,000	0.03298677E+02	0.14082464E-02	-0.07963272E-04	0.05641515E-07	-0.02444854E-10	-0.10208999E+04	0.05950372E+02
N	1,000–5,000	0.02480268E+02	0.10661458E-03	-0.07465337E-06	0.01879652E-09	-0.10239839E-14	0.05611004E+06	0.0448758E+02
	300–1,000	0.02503071E+02	-0.02180018E-03	0.05420529E-06	-0.05647560E-09	0.02099904E-12	0.05609990E+06	0.04167566E+02
NO	1,000–5,000	0.03245435E+02	0.12691383E-02	-0.05015890E-05	0.09169283E-09	-0.06275419E-13	0.09900840E+05	0.06417293E+02
	300–1,000	0.03376541E+02	0.12530634E-02	-0.03302750E-04	0.05217810E-07	-0.02446262E-10	0.09917961E+05	0.05829390E+02
NO <sub>2</sub>	1,000–5,000	0.04482899E+02	0.02462429E-01	-0.10422585E-05	0.01976902E-08	-0.13917168E-13	0.02261292E+05	0.09883985E+01
	300–1,000	0.02670600E+02	0.07838500E-01	-0.08863864E-04	0.06161714E-07	-0.02320150E-10	0.029962901E+05	0.11612071E+02



## Appendix B: Thermodynamic properties

### B.1– Methane (CH<sub>4</sub>)

Methane (CH <sub>4</sub> )		March 31, 1961				
MW = 16.043						
$\bar{h}_f^0 = -17.895$ kcal/gmole						
$T$		$\bar{C}_p^0$	$\bar{h}(T) - \bar{h}(T_0)$	$\bar{s}^0(T)$	$\Delta G^0(T)$	$\log K_p$
0	0	0.000	-2.396	0.000	-15.991	infinite
100	180	7.949	-1.601	35.706	-15.400	33.656
200	360	8.001	-0.805	41.222	-13.909	15.198
298	536	8.518	0.000	44.490	-12.145	8.902
300	540	8.535	0.016	44.543	-12.110	8.822
400	720	9.680	0.923	47.144	-10.066	5.500
500	900	11.076	1.960	49.453	-7.845	3.429
600	1,080	12.483	3.138	51.597	-5.493	2.001
700	1,260	13.813	4.454	53.622	-3.046	0.951
800	1,440	15.041	5.897	55.548	-0.533	0.146
900	1,620	16.157	7.458	57.385	2.029	-0.493
1,000	1,800	17.160	9.125	59.141	4.625	-1.011
1,100	1,980	18.052	10.887	60.819	7.247	-1.440
1,200	2,160	18.842	12.732	62.424	9.887	-1.801
1,300	2,340	19.538	14.652	63.960	12.535	-2.107
1,400	2,520	20.150	16.637	65.431	15.195	-2.372
1,500	2,700	20.688	18.679	66.840	17.859	-2.602
1,600	2,880	21.161	20.772	68.191	20.520	-2.803
1,700	3,060	21.579	22.910	69.486	23.189	-2.981
1,800	3,240	21.947	25.086	70.730	25.854	-3.139
1,900	3,420	22.273	27.298	71.926	28.522	-3.281
2,000	3,600	22.562	29.540	73.076	31.187	-3.408
2,100	3,780	22.820	31.809	74.183	33.851	-3.523
2,200	3,960	23.050	34.103	75.250	36.511	-3.627
2,300	4,140	23.256	36.418	76.279	39.173	-3.722
2,400	4,320	23.441	38.753	77.273	41.833	-3.809
2,500	4,500	23.608	41.106	78.233	44.483	-3.889
2,600	4,680	23.758	43.474	79.162	47.141	-3.962
2,700	4,860	23.894	45.857	80.062	49.791	-4.030
2,800	5,040	24.018	48.253	80.933	52.440	-4.093
2,900	5,220	24.131	50.660	81.778	55.093	-4.152

K	°R	$\frac{\text{cal}}{\text{gmole} \cdot \text{K}}$	$\frac{\text{kcal}}{\text{gmole}}$	$\frac{\text{cal}}{\text{gmole} \cdot \text{K}}$	$\frac{\text{kcal}}{\text{gmole}}$	—
---	----	--	------------------------------------	--	------------------------------------	---

Note that the tables have been adapted from the Chemkin [53] and JANAF [54] databases.  
1 cal/gmole K = 4.1842 kJ/kgmol K



Methane (CH<sub>4</sub>)

MW = 16.043

$\bar{h}_f^0 = -17.895$  kcal/gmole

$T$		$\bar{C}_p^0$	$\bar{h}(T) - \bar{h}(T_0)$	$\bar{s}^0(T)$	$\Delta G^0(T)$	$\log K_p$
3,000	5,400	24.233	53.079	82.597	57.736	-4.206
3,100	5,580	24.327	55.507	83.394	60.381	-4.257
3,200	5,760	24.413	57.944	84.167	63.026	-4.304
3,300	5,940	24.493	60.389	84.920	65.669	-4.349
3,400	6,120	24.565	62.842	85.652	68.309	-4.391
3,500	6,300	24.633	65.302	86.365	70.951	-4.430
3,600	6,480	24.695	67.768	87.060	73.589	-4.467
3,700	6,660	24.752	70.241	87.737	76.231	-4.503
3,800	6,840	24.806	72.719	88.398	78.872	-4.536
3,900	7,020	24.855	75.202	89.043	81.511	-4.568
4,000	7,200	24.901	77.690	89.673	84.150	-4.598
4,100	7,380	24.944	80.162	90.288	86.785	-4.626
4,200	7,560	24.984	82.678	90.890	89.429	-4.653
4,300	7,740	25.022	85.179	91.478	92.063	-4.679
4,400	7,920	25.057	87.683	92.054	94.700	-4.704
4,500	8,100	25.090	90.190	92.617	97.335	-4.727
4,600	8,280	25.121	92.701	93.169	99.983	-4.750
4,700	8,460	25.150	95.214	93.710	102.625	-4.772
4,800	8,640	25.177	97.730	94.240	105.268	-4.793
4,900	8,820	25.203	100.249	94.759	107.912	-4.813
5,000	9,000	25.227	102.771	95.268	110.552	-4.832
5,100	9,180	25.250	105.295	95.768	113.198	-4.851
5,200	9,360	25.272	107.821	96.259	115.844	-4.869
5,300	9,540	25.292	110.349	96.740	118.501	-4.886
5,400	9,720	25.311	112.879	97.213	121.145	-4.903
5,500	9,900	25.330	115.411	97.678	123.799	-4.919
5,600	10,080	25.347	117.945	98.134	126.449	-4.935
5,700	10,260	25.364	120.481	98.583	129.106	-4.950
5,800	10,440	25.379	123.018	99.024	131.762	-4.965
5,900	10,620	25.394	125.557	99.458	134.428	-4.979
6,000	10,800	25.409	128.097	99.885	137.081	-4.993

K	°R	$\frac{\text{cal}}{\text{gmole} \cdot \text{K}}$	$\frac{\text{kcal}}{\text{gmole}}$	$\frac{\text{cal}}{\text{gmole} \cdot \text{K}}$	$\frac{\text{kcal}}{\text{gmole}}$	—
---	----	--	------------------------------------	--	------------------------------------	---

Note that the tables have been adapted from the Chemkin [53] and JANAF [54] databases.  
1 cal/gmole K = 4.1842 kJ/kgmol K



## B.2– Carbon monoxide (CO)

Carbon Monoxide (CO)

September 30, 1965

$MW = 28.01055$

$\bar{h}_f^0 = -26.417$  kcal/gmole

$T$		$\bar{C}_p^0$	$\bar{h}(T) - \bar{h}(T_0)$	$\bar{s}^0(T)$	$\Delta G^0(T)$	$\log K_p$
0	0	0.000	-2.072	0.000	-27.200	infinite
100	180	6.956	-1.379	39.613	-28.741	62.809
200	360	6.957	-0.683	44.435	-30.718	33.566
298	536	6.965	0.000	47.214	-32.783	24.029
300	540	6.965	0.013	47.257	-32.823	23.910
400	720	7.013	0.711	49.265	-34.975	19.109
500	900	7.121	1.417	50.841	-37.144	16.235
600	1,080	7.276	2.137	52.152	-39.311	14.318
700	1,260	7.450	2.873	53.287	-41.468	12.946
800	1,440	7.624	3.627	54.293	-43.612	11.914
900	1,620	7.786	4.397	55.200	-45.744	11.108
1,000	1,800	7.931	5.183	56.028	-47.859	10.459
1,100	1,980	8.057	5.983	56.790	-49.962	9.926
1,200	2,160	8.168	6.794	57.496	-52.049	9.479
1,300	2,340	8.263	7.616	58.154	-54.126	9.099
1,400	2,520	8.346	8.446	58.769	-56.189	8.771
1,500	2,700	8.417	9.285	59.348	-58.241	8.485
1,600	2,880	8.480	10.130	59.893	-60.284	8.234
1,700	3,060	8.535	10.980	60.409	-62.315	8.011
1,800	3,240	8.583	11.836	60.898	-64.337	7.811
1,900	3,420	8.626	12.697	61.363	-66.349	7.631
2,000	3,600	8.664	13.561	61.807	-68.353	7.469
2,100	3,780	8.698	14.430	62.230	-70.346	7.321
2,200	3,960	8.728	15.301	62.635	-72.335	7.185
2,300	4,140	8.756	16.175	63.024	-74.311	7.061
2,400	4,320	8.781	17.052	63.397	-76.282	6.946
2,500	4,500	8.804	17.931	63.756	-78.247	6.840
2,600	4,680	8.825	18.813	64.102	-80.202	6.741
2,700	4,860	8.844	19.696	64.435	-82.153	6.649
2,800	5,040	8.863	20.582	64.757	-84.093	6.563
2,900	5,220	8.879	21.469	65.069	-86.028	6.483

K	°R	$\frac{\text{cal}}{\text{gmole} \cdot \text{K}}$	$\frac{\text{kcal}}{\text{gmole}}$	$\frac{\text{cal}}{\text{gmole} \cdot \text{K}}$	$\frac{\text{kcal}}{\text{gmole}}$	—
---	----	--	------------------------------------	--	------------------------------------	---

Note that the tables have been adapted from the Chemkin [53] and JANAF [54] databases.  
1 cal/gmole K = 4.1842 kJ/kgmol K





Carbon Monoxide (CO)

$MW = 28.01055$

$\bar{h}_f^0 = -26.417 \text{ kcal/gmole}$

$T$		$\bar{C}_p^0$	$\bar{h}(T) - \bar{h}(T_0)$	$\bar{s}^0(T)$	$\Delta G^0(T)$	$\log K_p$
3,000	5,400	8.895	22.357	65.370	-87.957	6.407
3,100	5,580	8.910	23.248	65.662	-89.878	6.336
3,200	5,760	8.924	24.139	65.945	-91.795	6.269
3,300	5,940	8.937	25.032	66.220	-93.707	6.206
3,400	6,120	8.949	25.927	66.487	-95.609	6.145
3,500	6,300	8.961	26.822	66.746	-97.509	6.088
3,600	6,480	8.973	27.719	66.999	-99.400	6.034
3,700	6,660	8.984	28.617	67.245	-101.286	5.982
3,800	6,840	8.994	29.516	67.485	-103.164	5.933
3,900	7,020	9.004	30.416	67.718	-105.039	5.886
4,000	7,200	9.014	31.316	67.946	-106.908	5.841
4,100	7,380	9.024	32.218	68.169	-108.774	5.798
4,200	7,560	9.033	33.121	68.387	-110.630	5.756
4,300	7,740	9.042	34.025	68.599	-112.483	5.717
4,400	7,920	9.051	34.930	68.807	-114.333	5.679
4,500	8,100	9.059	35.835	69.011	-116.177	5.642
4,600	8,280	9.068	36.741	69.210	-118.012	5.607
4,700	8,460	9.076	37.649	69.405	-119.845	5.573
4,800	8,640	9.084	38.557	69.596	-121.672	5.540
4,900	8,820	9.092	39.465	69.784	-123.497	5.508
5,000	9,000	9.100	40.375	69.967	-125.315	5.477
5,100	9,180	9.107	41.285	70.148	-127.132	5.448
5,200	9,360	9.115	42.196	70.325	-128.941	5.419
5,300	9,540	9.123	43.108	70.498	-130.741	5.391
5,400	9,720	9.130	44.021	70.669	-132.542	5.364
5,500	9,900	9.138	44.934	70.836	-134.336	5.338
5,600	10,080	9.145	45.849	71.001	-136.129	5.312
5,700	10,260	9.153	46.763	71.163	-137.919	5.288
5,800	10,440	9.160	47.679	71.322	-139.698	5.264
5,900	10,620	9.167	48.595	71.479	-141.473	5.240
6,000	10,800	9.175	49.513	71.633	-143.249	5.218

K	°R	$\frac{\text{cal}}{\text{gmole} \cdot \text{K}}$	$\frac{\text{kcal}}{\text{gmole}}$	$\frac{\text{cal}}{\text{gmole} \cdot \text{K}}$	$\frac{\text{kcal}}{\text{gmole}}$	—
---	----	--	------------------------------------	--	------------------------------------	---

Note that the tables have been adapted from the Chemkin [53] and JANAF [54] databases.  
1 cal/gmole K = 4.1842 kJ/kgmol K



### B.3– Carbon dioxide (CO<sub>2</sub>)

Carbon Dioxide (CO<sub>2</sub>)

September 30, 1965

$MW = 44.00995$

$\bar{h}_f^0 = -94.054$  kcal/gmole

$T$		$\bar{c}_p^0$	$\bar{h}(T) - \bar{h}(T_0)$	$\bar{s}^0(T)$	$\Delta G^0(T)$	$\log K_p$
0	0	0.000	-2.238	0.000	-93.965	infinite
100	180	6.981	-1.543	42.758	-94.100	205.645
200	360	7.734	-0.816	47.769	-94.191	102.922
298	536	8.874	0.000	51.072	-94.265	69.095
300	540	8.896	0.016	51.127	-94.267	68.670
400	720	9.877	0.958	53.830	-94.335	51.540
500	900	10.666	1.987	56.122	-94.399	41.260
600	1,080	11.310	3.087	58.126	-94.458	34.405
700	1,260	11.846	4.245	59.910	-94.510	29.506
800	1,440	12.293	5.453	61.522	-94.556	25.830
900	1,620	12.667	6.702	62.992	-94.596	22.970
1,000	1,800	12.980	7.984	64.344	-94.628	20.680
1,100	1,980	13.243	9.296	65.594	-94.658	18.806
1,200	2,160	13.466	10.632	66.756	-94.681	17.243
1,300	2,340	13.656	11.988	67.841	-94.701	15.920
1,400	2,520	13.815	13.362	68.859	-94.716	14.785
1,500	2,700	13.953	14.750	69.817	-94.728	13.801
1,600	2,880	14.074	16.152	70.722	-94.739	12.940
1,700	3,060	14.177	17.565	71.578	-94.746	12.180
1,800	3,240	14.269	18.987	72.391	-94.750	11.504
1,900	3,420	14.352	20.418	73.165	-94.751	10.898
2,000	3,600	14.424	21.857	73.903	-94.752	10.353
2,100	3,780	14.489	23.303	74.608	-94.746	9.860
2,200	3,960	14.547	24.755	75.284	-94.744	9.411
2,300	4,140	14.600	26.212	75.931	-94.735	9.001
2,400	4,320	14.648	27.674	76.554	-94.724	8.625
2,500	4,500	14.692	29.141	77.153	-94.714	8.280
2,600	4,680	14.734	30.613	77.730	-94.698	7.960
2,700	4,860	14.771	32.088	78.286	-94.683	7.664
2,800	5,040	14.807	33.567	78.824	-94.662	7.388
2,900	5,220	14.841	35.049	79.344	-94.639	7.132

K	°R	$\frac{\text{cal}}{\text{gmole} \cdot \text{K}}$	$\frac{\text{kcal}}{\text{gmole}}$	$\frac{\text{cal}}{\text{gmole} \cdot \text{K}}$	$\frac{\text{kcal}}{\text{gmole}}$	—
---	----	--	------------------------------------	--	------------------------------------	---

Note that the tables have been adapted from the Chemkin [53] and JANAF [54] databases.  
1 cal/gmole K = 4.1842 kJ/kgmol K





Carbon Dioxide (CO<sub>2</sub>)

$MW = 44.00995$

$\bar{h}_f^0 = -94.054$  kcal/gmole

$T$		$\bar{C}_p^0$	$\bar{h}(T) - \bar{h}(T_0)$	$\bar{s}^0(T)$	$\Delta G^0(T)$	$\log K_p$
3,000	5,400	14.873	36.535	79.848	-94.615	6.892
3,100	5,580	14.902	38.024	80.336	-94.587	6.668
3,200	5,760	14.930	39.515	80.810	-94.560	6.458
3,300	5,940	14.956	41.010	81.270	-94.531	6.260
3,400	6,120	14.982	42.507	81.717	-94.495	6.074
3,500	6,300	15.006	44.006	82.151	-94.462	5.898
3,600	6,480	15.030	45.508	82.574	-94.421	5.732
3,700	6,660	15.053	47.012	82.986	-94.379	5.574
3,800	6,840	15.075	48.518	83.388	-94.331	5.425
3,900	7,020	15.097	50.027	83.780	-94.286	5.283
4,000	7,200	15.119	51.538	84.162	-94.237	5.149
4,100	7,380	15.139	53.051	84.536	-94.186	5.020
4,200	7,560	15.159	54.566	84.901	-94.130	4.898
4,300	7,740	15.179	56.082	85.258	-94.072	4.781
4,400	7,920	15.197	57.601	85.607	-94.015	4.670
4,500	8,100	15.216	59.122	85.949	-93.954	4.563
4,600	8,280	15.234	60.644	86.284	-93.885	4.460
4,700	8,460	15.254	62.169	86.611	-93.818	4.362
4,800	8,640	15.272	63.695	86.933	-93.746	4.268
4,900	8,820	15.290	65.223	87.248	-93.678	4.178
5,000	9,000	15.306	66.753	87.557	-93.603	4.091
5,100	9,180	15.327	68.285	87.860	-93.528	4.008
5,200	9,360	15.349	69.819	88.158	-93.450	3.927
5,300	9,540	15.371	71.355	88.451	-93.361	3.850
5,400	9,720	15.393	72.893	88.738	-93.280	3.775
5,500	9,900	15.415	74.433	89.021	-93.190	3.703
5,600	10,080	15.437	75.976	89.299	-93.104	3.633
5,700	10,260	15.459	77.521	89.572	-93.017	3.566
5,800	10,440	15.481	79.068	89.841	-92.918	3.501
5,900	10,620	15.503	80.617	90.106	-92.820	3.438
6,000	10,800	15.525	82.168	90.367	-92.724	3.377

K	°R	$\frac{\text{cal}}{\text{gmole} \cdot \text{K}}$	$\frac{\text{kcal}}{\text{gmole}}$	$\frac{\text{cal}}{\text{gmole} \cdot \text{K}}$	$\frac{\text{kcal}}{\text{gmole}}$	—
---	----	--	------------------------------------	--	------------------------------------	---

Note that the tables have been adapted from the Chemkin [53] and JANAF [54] databases.  
1 cal/gmole K = 4.1842 kJ/kgmol K



## B.4- Hydrogen (H<sub>2</sub>)

Hydrogen (H <sub>2</sub> )		March 31, 1961				
MW = 2.016						
$\bar{h}_f^0 = 0.000$ kcal/gmole						
$T$		$\bar{C}_p^0$	$\bar{h}(T) - \bar{h}(T_0)$	$\bar{s}^0(T)$	$\Delta G^0(T)$	$\log K_p$
0	0	0.000	-2.024	0.000	0.000	0.000
100	180	5.393	-1.265	24.387	0.000	0.000
200	360	6.518	-0.662	28.520	0.000	0.000
298	536	6.892	0.000	31.208	0.000	0.000
300	540	6.894	0.013	31.251	0.000	0.000
400	720	6.975	0.707	33.247	0.000	0.000
500	900	6.993	1.406	34.806	0.000	0.000
600	1,080	7.009	2.106	36.082	0.000	0.000
700	1,260	7.036	2.808	37.165	0.000	0.000
800	1,440	7.087	3.514	38.107	0.000	0.000
900	1,620	7.148	4.226	38.946	0.000	0.000
1,000	1,800	7.219	4.944	39.702	0.000	0.000
1,100	1,980	7.300	5.670	40.394	0.000	0.000
1,200	2,160	7.390	6.404	41.033	0.000	0.000
1,300	2,340	7.490	7.148	41.628	0.000	0.000
1,400	2,520	7.600	7.902	42.187	0.000	0.000
1,500	2,700	7.720	8.668	42.716	0.000	0.000
1,600	2,880	7.823	9.446	43.217	0.000	0.000
1,700	3,060	7.921	10.233	43.695	0.000	0.000
1,800	3,240	8.016	11.030	44.150	0.000	0.000
1,900	3,420	8.108	11.836	44.586	0.000	0.000
2,000	3,600	8.195	12.651	45.004	0.000	0.000
2,100	3,780	8.279	13.475	45.406	0.000	0.000
2,200	3,960	8.358	14.307	45.793	0.000	0.000
2,300	4,140	8.434	15.146	46.166	0.000	0.000
2,400	4,320	8.506	15.993	46.527	0.000	0.000
2,500	4,500	8.575	16.848	46.875	0.000	0.000
2,600	4,680	8.639	17.708	47.213	0.000	0.000
2,700	4,860	8.700	18.575	47.540	0.000	0.000
2,800	5,040	8.757	19.448	47.857	0.000	0.000
2,900	5,220	8.810	20.326	48.166	0.000	0.000

K	°R	$\frac{\text{cal}}{\text{gmole} \cdot \text{K}}$	$\frac{\text{kcal}}{\text{gmole}}$	$\frac{\text{cal}}{\text{gmole} \cdot \text{K}}$	$\frac{\text{kcal}}{\text{gmole}}$	—
---	----	--	------------------------------------	--	------------------------------------	---

Note that the tables have been adapted from the Chemkin [53] and JANAF [54] databases.  
1 cal/gmole K = 4.1842 kJ/kgmol K



Hydrogen (H<sub>2</sub>)

$MW = 2.016$

$\bar{h}_f^0 = 0.000$  kcal/gmole

$T$		$\bar{c}_p^0$	$\bar{h}(T) - \bar{h}(T_0)$	$\bar{s}^0(T)$	$\Delta G^0(T)$	$\log K_p$
3,000	5,400	8.859	21.210	48.465	0.000	0.000
3,100	5,580	8.911	22.098	48.756	0.000	0.000
3,200	5,760	8.962	22.992	49.040	0.000	0.000
3,300	5,940	9.012	23.891	49.317	0.000	0.000
3,400	6,120	9.061	24.794	49.586	0.000	0.000
3,500	6,300	9.110	25.703	49.850	0.000	0.000
3,600	6,480	9.158	26.616	50.107	0.000	0.000
3,700	6,660	9.205	27.535	50.359	0.000	0.000
3,800	6,840	9.252	28.457	50.605	0.000	0.000
3,900	7,020	9.297	29.385	50.846	0.000	0.000
4,000	7,200	9.342	30.317	51.082	0.000	0.000
4,100	7,380	9.386	31.253	51.313	0.000	0.000
4,200	7,560	9.429	32.194	51.640	0.000	0.000
4,300	7,740	9.472	33.139	51.762	0.000	0.000
4,400	7,920	9.514	34.088	51.980	0.000	0.000
4,500	8,100	9.555	35.042	52.194	0.000	0.000
4,600	8,280	9.595	35.999	52.405	0.000	0.000
4,700	8,460	9.634	36.961	52.612	0.000	0.000
4,800	8,640	9.673	37.926	52.815	0.000	0.000
4,900	8,820	9.711	38.895	53.015	0.000	0.000
5,000	9,000	9.748	39.868	53.211	0.000	0.000
5,100	9,180	9.785	40.845	53.405	0.000	0.000
5,200	9,360	9.822	41.825	53.595	0.000	0.000
5,300	9,540	9.859	42.809	53.783	0.000	0.000
5,400	9,720	9.895	43.797	53.967	0.000	0.000
5,500	9,900	9.930	44.788	54.149	0.000	0.000
5,600	10,080	9.965	45.783	54.328	0.000	0.000
5,700	10,260	10.000	46.781	54.505	0.000	0.000
5,800	10,440	10.034	47.783	54.679	0.000	0.000
5,900	10,620	10.067	48.788	54.851	0.000	0.000
6,000	10,800	10.100	49.796	55.020	0.000	0.000

K	°R	$\frac{\text{cal}}{\text{gmole} \cdot \text{K}}$	$\frac{\text{kcal}}{\text{gmole}}$	$\frac{\text{cal}}{\text{gmole} \cdot \text{K}}$	$\frac{\text{kcal}}{\text{gmole}}$	—
---	----	--	------------------------------------	--	------------------------------------	---

Note that the tables have been adapted from the Chemkin [53] and JANAF [54] databases.  
1 cal/gmole K = 4.1842 kJ/kgmol K



## B.5– Water vapour (H<sub>2</sub>O)

Water Vapor (H<sub>2</sub>O)

March 31, 1961

MW = 18.016

$\bar{h}_f^0 = -57.798$  kcal/gmole

$T$	$\bar{C}_p^0$	$\bar{h}(T) - \bar{h}(T_0)$	$\bar{s}^0(T)$	$\Delta G^0(T)$	$\log K_p$	
0	0	0.000	-2.367	0.000	-57.103	infinite
100	180	7.961	-1.581	36.396	-56.557	123.600
200	360	7.969	-0.784	41.916	-55.635	60.792
298	536	8.025	0.000	45.106	-54.636	40.048
300	540	8.027	0.015	45.155	-54.617	39.786
400	720	8.186	0.825	47.484	-53.519	29.240
500	900	8.415	1.654	49.334	-52.361	22.886
600	1,080	8.676	2.509	50.891	-51.156	18.633
700	1,260	8.954	3.390	52.249	-49.915	15.583
800	1,440	9.246	4.300	53.464	-48.646	13.289
900	1,620	9.547	5.240	54.570	-47.352	11.498
1,000	1,800	9.851	6.209	55.592	-46.040	10.062
1,100	1,980	10.152	7.210	56.545	-44.712	8.883
1,200	2,160	10.444	8.240	57.441	-43.371	7.899
1,300	2,340	10.723	9.298	58.288	-42.022	7.064
1,400	2,520	10.987	10.384	59.092	-40.663	6.347
1,500	2,700	11.233	11.495	59.859	-39.297	5.725
1,600	2,880	11.462	12.630	60.591	-37.927	5.180
1,700	3,060	11.674	13.787	61.293	-36.549	4.699
1,800	3,240	11.869	14.964	61.965	-35.170	4.270
1,900	3,420	12.048	16.160	62.612	-33.786	3.886
2,000	3,600	12.214	17.373	63.234	-32.401	3.540
2,100	3,780	12.366	18.602	63.834	-31.012	3.227
2,200	3,960	12.505	19.846	64.412	-29.621	2.942
2,300	4,140	12.634	21.103	64.971	-28.229	2.682
2,400	4,320	12.753	22.372	65.511	-26.832	2.443
2,500	4,500	12.863	23.653	66.034	-25.439	2.224
2,600	4,680	12.965	24.945	66.541	-24.040	2.021
2,700	4,860	13.059	26.246	67.032	-22.641	1.833
2,800	5,040	13.146	27.556	67.508	-21.242	1.658
2,900	5,220	13.228	28.875	67.971	-19.838	1.495

K	°R	$\frac{\text{cal}}{\text{gmole} \cdot \text{K}}$	$\frac{\text{kcal}}{\text{gmole}}$	$\frac{\text{cal}}{\text{gmole} \cdot \text{K}}$	$\frac{\text{kcal}}{\text{gmole}}$	—
---	----	--	------------------------------------	--	------------------------------------	---

Note that the tables have been adapted from the Chemkin [53] and JANAF [54] databases.  
1 cal/gmole K = 4.1842 kJ/kgmol K



Water Vapor (H<sub>2</sub>O)

$MW = 18.016$

$\bar{h}_f^0 = -57.798 \text{ kcal/gmole}$

$T$		$\bar{c}_p^0$	$\bar{h}(T) - \bar{h}(T_0)$	$\bar{s}^0(T)$	$\Delta G^0(T)$	$\log K_p$
3,000	5,400	13.304	30.201	68.421	-18.438	1.343
3,100	5,580	13.374	31.535	68.858	-17.034	1.201
3,200	5,760	13.441	32.876	69.284	-15.630	1.067
3,300	5,940	13.503	34.223	69.698	-14.223	0.942
3,400	6,120	13.562	35.577	70.102	-12.818	0.824
3,500	6,300	13.617	36.936	70.496	-11.409	0.712
3,600	6,480	13.669	38.300	70.881	-10.000	0.607
3,700	6,660	13.718	39.669	71.256	-8.589	0.507
3,800	6,840	13.764	41.043	71.622	-7.177	0.413
3,900	7,020	13.808	42.422	71.980	-5.766	0.323
4,000	7,200	13.850	43.805	72.331	-4.353	0.238
4,100	7,380	13.890	45.192	72.673	-2.938	0.157
4,200	7,560	13.927	46.583	73.008	-1.522	0.079
4,300	7,740	13.963	47.977	73.336	-0.105	0.005
4,400	7,920	13.997	49.375	73.658	1.311	-0.065
4,500	8,100	14.030	50.777	73.973	2.729	-0.133
4,600	8,280	14.061	52.181	74.281	4.154	-0.197
4,700	8,460	14.091	53.589	74.584	5.576	-0.259
4,800	8,640	14.120	55.000	74.881	6.998	-0.319
4,900	8,820	14.148	56.413	75.172	8.422	-0.376
5,000	9,000	14.174	57.829	75.459	9.844	-0.430
5,100	9,180	14.201	59.248	75.740	11.275	-0.483
5,200	9,360	14.228	60.669	76.016	12.700	-0.534
5,300	9,540	14.254	62.093	76.287	14.135	-0.583
5,400	9,720	14.279	63.520	76.653	15.560	-0.630
5,500	9,900	14.303	64.949	76.816	16.995	-0.675
5,600	10,080	14.328	66.381	77.074	18.426	-0.719
5,700	10,260	14.351	67.815	77.327	19.862	-0.762
5,800	10,440	14.375	69.251	77.577	21.299	-0.803
5,900	10,620	14.398	70.690	77.823	22.736	-0.842
6,000	10,800	14.422	72.131	78.065	24.174	-0.880

K	°R	$\frac{\text{cal}}{\text{gmole} \cdot \text{K}}$	$\frac{\text{kcal}}{\text{gmole}}$	$\frac{\text{cal}}{\text{gmole} \cdot \text{K}}$	$\frac{\text{kcal}}{\text{gmole}}$	—
---	----	--	------------------------------------	--	------------------------------------	---

Note that the tables have been adapted from the Chemkin [53] and JANAF [54] databases.  
1 cal/gmole K = 4.1842 kJ/kgmol K



## B.6– Nitrogen (N<sub>2</sub>)

Nitrogen (N <sub>2</sub> )		September 30, 1965				
MW = 28.0134						
$\bar{h}_f^0 = 0.000$ kcal/gmole						
$T$		$\bar{c}_p^0$	$\bar{h}(T) - \bar{h}(T_0)$	$\bar{s}^0(T)$	$\Delta G^0(T)$	$\log K_p$
0	0	0.000	-2.072	0.000	0.000	0.000
100	180	6.956	-1.379	38.170	0.000	0.000
200	360	6.957	-0.683	42.992	0.000	0.000
298	536	6.961	0.000	45.770	0.000	0.000
300	540	6.961	0.013	45.813	0.000	0.000
400	720	6.990	0.710	47.818	0.000	0.000
500	900	7.069	1.413	49.386	0.000	0.000
600	1,080	7.196	2.125	50.685	0.000	0.000
700	1,260	7.350	2.853	51.806	0.000	0.000
800	1,440	7.512	3.596	52.798	0.000	0.000
900	1,620	7.670	4.355	53.692	0.000	0.000
1,000	1,800	7.815	5.129	54.507	0.000	0.000
1,100	1,980	7.945	5.917	55.258	0.000	0.000
1,200	2,160	8.061	6.718	55.955	0.000	0.000
1,300	2,340	8.162	7.529	56.604	0.000	0.000
1,400	2,520	8.252	8.350	57.212	0.000	0.000
1,500	2,700	8.330	9.179	57.784	0.000	0.000
1,600	2,880	8.398	10.015	58.324	0.000	0.000
1,700	3,060	8.458	10.858	58.835	0.000	0.000
1,800	3,240	8.512	11.707	59.320	0.000	0.000
1,900	3,420	8.559	12.560	59.782	0.000	0.000
2,000	3,600	8.601	13.418	60.222	0.000	0.000
2,100	3,780	8.638	14.280	60.642	0.000	0.000
2,200	3,960	8.672	15.146	61.045	0.000	0.000
2,300	4,140	8.703	16.015	61.431	0.000	0.000
2,400	4,320	8.731	16.886	61.802	0.000	0.000
2,500	4,500	8.756	17.761	62.159	0.000	0.000
2,600	4,680	8.779	18.638	62.503	0.000	0.000
2,700	4,860	8.800	19.517	62.835	0.000	0.000
2,800	5,040	8.820	20.398	63.155	0.000	0.000
2,900	5,220	8.838	21.280	63.465	0.000	0.000

K	°R	$\frac{\text{cal}}{\text{gmole} \cdot \text{K}}$	$\frac{\text{kcal}}{\text{gmole}}$	$\frac{\text{cal}}{\text{gmole} \cdot \text{K}}$	$\frac{\text{kcal}}{\text{gmole}}$	—
---	----	--	------------------------------------	--	------------------------------------	---

Note that the tables have been adapted from the Chemkin [53] and JANAF [54] databases.  
1 cal/gmole K = 4.1842 kJ/kgmol K





Nitrogen (N<sub>2</sub>)

$MW = 28.0134$

$\bar{h}_f^0 = 0.000 \text{ kcal/gmole}$

$T$		$\bar{c}_p^0$	$\bar{h}(T) - \bar{h}(T_0)$	$\bar{s}^0(T)$	$\Delta G^0(T)$	$\log K_p$
3,000	5,400	8.855	22.165	63.765	0.000	0.000
3,100	5,580	8.871	23.051	64.055	0.000	0.000
3,200	5,760	8.886	23.939	64.337	0.000	0.000
3,300	5,940	8.900	24.829	64.611	0.000	0.000
3,400	6,120	8.914	25.719	64.877	0.000	0.000
3,500	6,300	8.927	26.611	65.135	0.000	0.000
3,600	6,480	8.939	27.505	65.387	0.000	0.000
3,700	6,660	8.950	28.399	65.632	0.000	0.000
3,800	6,840	8.962	29.295	65.871	0.000	0.000
3,900	7,020	8.972	30.191	66.104	0.000	0.000
4,000	7,200	8.983	31.089	66.331	0.000	0.000
4,100	7,380	8.993	31.988	66.553	0.000	0.000
4,200	7,560	9.002	32.888	66.770	0.000	0.000
4,300	7,740	9.012	33.788	66.982	0.000	0.000
4,400	7,920	9.021	34.690	67.189	0.000	0.000
4,500	8,100	9.030	35.593	67.392	0.000	0.000
4,600	8,280	9.039	36.496	67.591	0.000	0.000
4,700	8,460	9.048	37.400	67.785	0.000	0.000
4,800	8,640	9.057	38.306	67.976	0.000	0.000
4,900	8,820	9.066	39.212	68.162	0.000	0.000
5,000	9,000	9.074	40.119	68.346	0.000	0.000
5,100	9,180	9.083	41.027	68.525	0.000	0.000
5,200	9,360	9.091	41.935	68.702	0.000	0.000
5,300	9,540	9.100	42.845	68.875	0.000	0.000
5,400	9,720	9.109	43.755	69.045	0.000	0.000
5,500	9,900	9.118	44.667	69.213	0.000	0.000
5,600	10,080	9.127	45.579	69.377	0.000	0.000
5,700	10,260	9.136	46.492	69.539	0.000	0.000
5,800	10,440	9.145	47.406	69.698	0.000	0.000
5,900	10,620	9.155	48.321	69.854	0.000	0.000
6,000	10,800	9.165	49.237	70.008	0.000	0.000

K	<sup>o</sup> R	$\frac{\text{cal}}{\text{gmole} \cdot \text{K}}$	$\frac{\text{kcal}}{\text{gmole}}$	$\frac{\text{cal}}{\text{gmole} \cdot \text{K}}$	$\frac{\text{kcal}}{\text{gmole}}$	—
---	----------------	--	------------------------------------	--	------------------------------------	---

Note that the tables have been adapted from the Chemkin [53] and JANAF [54] databases.  
1 cal/gmole K = 4.1842 kJ/kgmol K

## B.7– Nitric oxide (NO)

Nitric Oxide (NO) <span style="float: right;">June 30, 1963</span>						
$MW = 30.008$						
$\bar{h}_f^0 = 21.580 \text{ kcal/gmole}$						
$T$		$\bar{C}_p^0$	$\bar{h}(T) - \bar{h}(T_0)$	$\bar{s}^0(T)$	$\Delta G^0(T)$	$\log K_p$
0	0	0.000	-2.197	0.000	21.456	infinite
100	180	7.721	-1.451	42.286	21.256	-46.453
200	360	7.271	-0.705	47.477	20.984	-22.929
298	536	7.133	0.000	50.347	20.697	-15.171
300	540	7.132	0.013	50.392	20.692	-15.073
400	720	7.157	0.727	52.444	20.394	-11.142
500	900	7.287	1.448	54.053	20.095	-8.783
600	1,080	7.466	2.186	55.397	19.795	-7.210
700	1,260	7.655	2.942	56.562	19.494	-6.086
800	1,440	7.832	3.716	57.596	19.192	-5.243
900	1,620	7.988	4.507	58.528	18.890	-4.587
1,000	1,800	8.123	5.313	59.377	18.588	-4.062
1,100	1,980	8.238	6.131	60.157	18.285	-3.633
1,200	2,160	8.336	6.960	60.878	17.981	-3.275
1,300	2,340	8.419	7.798	61.548	17.678	-2.972
1,400	2,520	8.491	8.644	62.175	17.373	-2.712
1,500	2,700	8.552	9.496	62.763	17.069	-2.487
1,600	2,880	8.605	10.354	63.317	16.765	-2.290
1,700	3,060	8.651	11.217	63.840	16.461	-2.116
1,800	3,240	8.692	12.084	64.335	16.156	-1.962
1,900	3,420	8.727	12.955	64.806	15.853	-1.823
2,000	3,600	8.759	13.829	65.255	15.548	-1.699
2,100	3,780	8.788	14.706	65.683	15.244	-1.586
2,200	3,960	8.813	15.587	66.092	14.941	-1.484
2,300	4,140	8.837	16.469	66.484	14.637	-1.391
2,400	4,320	8.858	17.354	66.861	14.336	-1.305
2,500	4,500	8.877	18.241	67.223	14.033	-1.227
2,600	4,680	8.895	19.129	67.571	13.732	-1.164
2,700	4,860	8.912	20.020	67.908	13.432	-1.087
2,800	5,040	8.927	20.911	68.232	13.132	-1.025
2,900	5,220	8.941	21.805	68.545	12.834	-0.967

K	°R	$\frac{\text{cal}}{\text{gmole} \cdot \text{K}}$	$\frac{\text{kcal}}{\text{gmole}}$	$\frac{\text{cal}}{\text{gmole} \cdot \text{K}}$	$\frac{\text{kcal}}{\text{gmole}}$	—
---	----	--	------------------------------------	--	------------------------------------	---

Note that the tables have been adapted from the Chemkin [53] and JANAF [54] databases.  
 1 cal/gmole K = 4.1842 kJ/kgmol K





Nitric Oxide (NO)

$MW = 30.008$

$\bar{h}_f^0 = 21.580 \text{ kcal/gmole}$

$T$		$\bar{C}_p^0$	$\bar{h}(T) - \bar{h}(T_0)$	$\bar{s}^0(T)$	$\Delta G^0(T)$	$\log K_p$
3,000	5,400	8.955	22.700	68.849	12.535	-0.913
3,100	5,580	8.968	23.596	69.143	12.237	-0.863
3,200	5,760	8.980	24.493	69.427	11.940	-0.815
3,300	5,940	8.991	25.392	69.704	11.644	-0.771
3,400	6,120	9.002	26.291	69.973	11.349	-0.729
3,500	6,300	9.012	27.192	70.234	11.054	-0.690
3,600	6,480	9.022	28.094	70.488	10.762	-0.653
3,700	6,660	9.032	28.997	70.735	10.470	-0.618
3,800	6,840	9.041	29.900	70.976	10.179	-0.585
3,900	7,020	9.050	30.805	71.211	9.889	-0.554
4,000	7,200	9.058	31.710	71.440	9.598	-0.524
4,100	7,380	9.066	32.616	71.664	9.311	-0.496
4,200	7,560	9.074	33.523	71.882	9.024	-0.470
4,300	7,740	9.082	34.431	72.096	8.739	-0.444
4,400	7,920	9.090	35.340	72.305	8.452	-0.420
4,500	8,100	9.097	36.249	72.509	8.169	-0.397
4,600	8,280	9.105	37.159	72.709	7.888	-0.375
4,700	8,460	9.112	38.070	72.905	7.605	-0.354
4,800	8,640	9.119	38.982	73.097	7.324	-0.333
4,900	8,820	9.125	39.894	73.285	7.040	-0.314
5,000	9,000	9.132	40.807	73.470	6.763	-0.296
5,100	9,180	9.139	41.720	73.651	6.484	-0.278
5,200	9,360	9.145	42.634	73.828	6.207	-0.261
5,300	9,540	9.152	43.549	74.002	6.932	-0.245
5,400	9,720	9.158	44.465	74.173	5.654	-0.229
5,500	9,900	9.164	45.381	74.342	5.383	-0.214
5,600	10,080	9.170	46.298	74.507	5.107	-0.199
5,700	10,260	9.176	47.215	74.669	4.835	-0.185
5,800	10,440	9.182	48.133	74.829	4.566	-0.172
5,900	10,620	9.188	49.051	74.986	4.292	-0.159
6,000	10,800	9.194	49.970	75.140	4.024	-0.147

K	°R	$\frac{\text{cal}}{\text{gmole} \cdot \text{K}}$	$\frac{\text{kcal}}{\text{gmole}}$	$\frac{\text{cal}}{\text{gmole} \cdot \text{K}}$	$\frac{\text{kcal}}{\text{gmole}}$	—
---	----	--	------------------------------------	--	------------------------------------	---

Note that the tables have been adapted from the Chemkin [53] and JANAF [54] databases.  
1 cal/gmole K = 4.1842 kJ/kgmol K



## B.8– Oxygen diatomic (O<sub>2</sub>)

Oxygen, Diatomic (O<sub>2</sub>)

September 30, 1965

MW = 31.9988

$\bar{h}_f^0 = 0.000$  kcal/gmole

$T$		$\bar{c}_p^0$	$\bar{h}(T) - \bar{h}(T_0)$	$\bar{s}^0(T)$	$\Delta G^0(T)$	$\log K_p$
0	0	0.000	-2.075	0.000	0.000	0.000
100	180	6.958	-1.381	41.395	0.000	0.000
200	360	6.961	-0.685	46.218	0.000	0.000
298	536	7.020	0.000	49.004	0.000	0.000
300	540	7.023	0.013	49.047	0.000	0.000
400	720	7.196	0.724	51.091	0.000	0.000
500	900	7.431	1.455	52.722	0.000	0.000
600	1,080	7.670	2.210	54.098	0.000	0.000
700	1,260	7.883	2.988	55.297	0.000	0.000
800	1,440	8.063	3.786	56.361	0.000	0.000
900	1,620	8.212	4.600	57.320	0.000	0.000
1,000	1,800	8.336	5.427	58.192	0.000	0.000
1,100	1,980	8.439	6.266	58.991	0.000	0.000
1,200	2,160	8.527	7.114	59.729	0.000	0.000
1,300	2,340	8.604	7.971	60.415	0.000	0.000
1,400	2,520	8.674	8.835	61.055	0.000	0.000
1,500	2,700	8.738	9.706	61.656	0.000	0.000
1,600	2,880	8.800	10.583	62.222	0.000	0.000
1,700	3,060	8.858	11.465	62.757	0.000	0.000
1,800	3,240	8.916	12.354	63.265	0.000	0.000
1,900	3,420	8.973	13.249	63.749	0.000	0.000
2,000	3,600	9.029	14.149	64.210	0.000	0.000
2,100	3,780	9.084	15.054	64.652	0.000	0.000
2,200	3,960	9.139	15.966	65.076	0.000	0.000
2,300	4,140	9.194	16.882	65.483	0.000	0.000
2,400	4,320	9.248	17.804	65.876	0.000	0.000
2,500	4,500	9.301	18.732	66.254	0.000	0.000
2,600	4,680	9.354	19.664	66.620	0.000	0.000
2,700	4,860	9.405	20.602	66.974	0.000	0.000
2,800	5,040	9.455	21.545	67.317	0.000	0.000
2,900	5,220	9.503	22.493	67.650	0.000	0.000

K	°R	$\frac{\text{cal}}{\text{gmole} \cdot \text{K}}$	$\frac{\text{kcal}}{\text{gmole}}$	$\frac{\text{cal}}{\text{gmole} \cdot \text{K}}$	$\frac{\text{kcal}}{\text{gmole}}$	—
---	----	--	------------------------------------	--	------------------------------------	---

Note that the tables have been adapted from the Chemkin [53] and JANAF [54] databases.  
1 cal/gmole K = 4.1842 kJ/kgmol K



Oxygen, Diatomic (O<sub>2</sub>)

MW = 31.9988

$\bar{h}_f^0 = 0.000$  kcal/gmole

T		$\bar{C}_p^0$	$\bar{h}\langle T \rangle - \bar{h}\langle T_0 \rangle$	$\bar{s}^0\langle T \rangle$	$\Delta G^0\langle T \rangle$	log K <sub>p</sub>
3,000	5,400	9.551	23.446	67.973	0.000	0.000
3,100	5,580	9.596	24.403	68.287	0.000	0.000
3,200	5,760	9.640	25.365	68.592	0.000	0.000
3,300	5,940	9.682	26.331	68.889	0.000	0.000
3,400	6,120	9.723	27.302	69.179	0.000	0.000
3,500	6,300	9.762	28.276	69.461	0.000	0.000
3,600	6,480	9.799	29.254	69.737	0.000	0.000
3,700	6,660	9.835	30.236	70.006	0.000	0.000
3,800	6,840	9.869	31.221	70.269	0.000	0.000
3,900	7,020	9.901	32.209	70.525	0.000	0.000
4,000	7,200	9.932	33.201	70.776	0.000	0.000
4,100	7,380	9.961	34.196	71.022	0.000	0.000
4,200	7,560	9.988	35.193	71.262	0.000	0.000
4,300	7,740	10.015	36.193	71.498	0.000	0.000
4,400	7,920	10.039	37.196	71.728	0.000	0.000
4,500	8,100	10.062	38.201	71.954	0.000	0.000
4,600	8,280	10.084	39.208	72.176	0.000	0.000
4,700	8,460	10.104	40.218	72.393	0.000	0.000
4,800	8,640	10.123	41.229	72.606	0.000	0.000
4,900	8,820	10.140	42.242	72.814	0.000	0.000
5,000	9,000	10.156	43.257	73.019	0.000	0.000
5,100	9,180	10.172	44.274	73.221	0.000	0.000
5,200	9,360	10.187	45.292	73.418	0.000	0.000
5,300	9,540	10.200	46.311	73.613	0.000	0.000
5,400	9,720	10.213	47.332	73.803	0.000	0.000
5,500	9,900	10.225	48.353	73.991	0.000	0.000
5,600	10,080	10.237	49.377	74.175	0.000	0.000
5,700	10,260	10.247	50.401	74.356	0.000	0.000
5,800	10,440	10.258	51.426	74.535	0.000	0.000
5,900	10,620	10.267	52.452	74.710	0.000	0.000
6,000	10,800	10.276	53.479	74.883	0.000	0.000

K	°R	$\frac{\text{cal}}{\text{gmole} \cdot \text{K}}$	$\frac{\text{kcal}}{\text{gmole}}$	$\frac{\text{cal}}{\text{gmole} \cdot \text{K}}$	$\frac{\text{kcal}}{\text{gmole}}$	—
---	----	--	------------------------------------	--	------------------------------------	---

Note that the tables have been adapted from the Chemkin [53] and JANAF [54] databases.  
1 cal/gmole K = 4.1842 kJ/kgmol K